**Progress in Oceanography**
June 2022, Volume 204, Pages 102788 (13p.)
https://doi.org/10.1016/j.pocean.2022.102788
https://archimer.ifremer.fr/doc/00764/87634/



# Contrasted spatio-temporal changes in the demersal fish assemblages and the dominance of the and not fishing pressure, in the Bay of Biscay and Celtic Sea

Eme David [1, 2, *], Rufino Marta [3, 4], Trenkel Verena [1], Vermard Youen [1], Laffargue Pascal [1], Petitgas Pierre [1], Pellissier Loïc [5, 6], Albouy Camille [1]

[1] IFREMER - French Research Institute for Exploitation of the Sea, Unité Ecologie et Modèles pour l'Halieutique (EMH), Rue de l'Ile d'Yeu - BP 21105, 44311 Nantes cedex 3, France
[2] RiverLY Research Unit, National Research Institute for Agriculture Food and Environment, (INRAE), Villeurbanne, France
[3] IPMA- Portuguese Institute for the Sea and the Atmosphere, Division of Modelling and Management of Fisheries Resources, Av. Dr. Alfredo Magalhães Ramalho, 6, 1495-165 Lisboa
[4] CEAUL, Centre of Statistics and its Applications Faculty of Sciences, University of Lisbon, Portugal
[5] Landscape Ecology, Institute of Terrestrial Ecosystems, Department of Environmental Systems Science, ETH Zürich, Zürich, Switzerland
[6] Unit of Land Change Science, Swiss Federal Research Institute WSL, Birmensdorf, Switzerland

* Corresponding author : David Eme, email address : david.eme3@gmail.com

**Abstract :**

Climate change and resource exploitation represent strong selection pressure affecting the spatio-temporal dynamics of marine assemblages that ensure food provision for humans. However, such dynamics remain poorly documented, and their drivers unclear. Here, we investigate changes in fish assemblages of two key European fishing areas, the Bay of Biscay (BoB) and the Celtic Sea (CS), during the last two decades. We quantify the relative contribution of change in energy (i.e. temperature and trophic resources), habitat (depth, substrate, oxygen) and fishing pressure to explaining observed spatial and temporal variations in fish diversity. We used long-term scientific surveys to evaluate the spatio-temporal changes in species richness (SR), abundance and composition of demersal fish (Actinopterygii) assemblages at different spatial scales combined with a range of regression models and variance partitioning. Diversity patterns showed greater variability in space than in time: SR weakly changed over time, while compositional dissimilarity showed local patterns of taxonomic homogenization in the CS and differentiation in the southern BoB, where local assemblages were becoming more similar and dissimilar over time, respectively. Energy funnelled through small pelagic species as a potential trophic link affecting the dynamics of demersal assemblages was the most important driver, while habitat and fishing pressure had limited importance. Our study revealed contrasted dynamics of demersal fish assemblages at a regional scale that were best explained by the dynamics of small pelagic species. Direct effects of environmental forcing and fishing pressure were limited in both regions which have a long history of fishing and still remain relatively buffered from global warming effects. This research paved the way to combine methods inspired by biogeography with scientific monitoring surveys to detect spatio-temporal dynamics of fish assemblages and their drivers in marine ecosystems under multiple pressures.
**Graphical abstract**

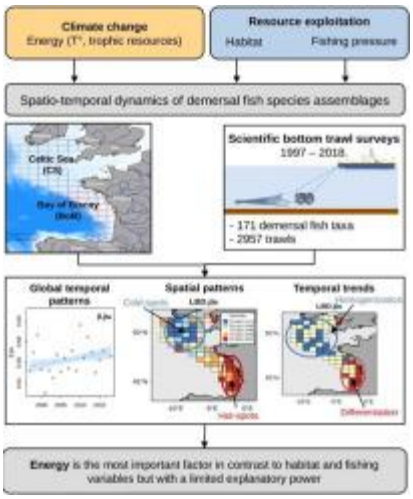


## Highlights

► The spatiotemporal dynamics of demersal fish communities were investigated in the Bay of Biscay (BoB) and Celtic Sea (CS). ► The role of two decades of changes in temperature, trophic resources, habitat and fishing pressure on community dynamics were assessed. ► Diversity patterns showed greater variability in space than in time and species richness and abundance weakly changed overall. ► Communities are becoming more spatially similar (homogeneous) in the CS and differentiated in the BoB. ► Such patterns are best explained by the dynamics of trophic resources mediated by small pelagic species rather than changes in temperature or fishing.

**Keywords** : Actinopterygii, Beta diversity, Energy, Habitat, Long-term ecological surveys, taxonomic homogenization.

**ACKNOWLEDGMENTS**

This work was supported by IFREMER, and the European Union's Horizon 2020 research and innovation programme for the CERES (Climate change and European aquatic RESources N° 678193), the PANDORA (Paradigm For Novel Dynamic Oceanic resources Assessment, No. 773713) and the APPEAL projects (ANR-10-IEED-0006-25). MM Rufino was funded by "Real-time monitoring of bivalve dredge fisheries" (MONTEREAL, Programme MAR2020). C Albouy was funded by an

"étoile montante" fellowship from the Pays de la Loire region (n° 2020_10792). This research is a product of the MAESTRO group funded by the synthesis center CESAB of the French Foundation for Research on Biodiversity (FRB; www.fondationbiodiversite.fr) and Filière France Pêche (FFP). We thank Pascal Lorance, Vincent Badts and Olivier Berthele for enlightening discussions and technical assistance.

## 1 INTRODUCTION

Understanding the spatio-temporal dynamics of species assemblages in the Anthropocene is essential to predict and mitigate ongoing and future changes (Blowes et al., 2019) to ensure the provision of ecosystem services (Tilman et al., 2017). Marine communities are prone to larger spatio-temporal dynamics and re-organisation than terrestrial communities (Dornelas et al., 2014) due to their greater sensitivity to environmental changes and faster rates of colonisation favoured by higher habitat connectivity (Pinsky et al., 2019). The pace of change of marine communities is not uniform across oceans and maximal in temperate regions, including the northeast Atlantic Ocean and European shelf seas (Antão et al., 2020). Long-term fishing pressure and (over-)exploitation of fish stocks represent additional drivers (Pauly et al., 2005). The exploitation of the northeast Atlantic and European shelf seas during the 19$^{th}$ and 20$^{th}$ centuries has negatively affected the abundance of many fish populations (Thurstan et al., 2010). Anthropogenic drivers are not acting independently, climate change interacting with fishing activities affects the recovery of depleted fish stocks (Planque et al., 2010) and these interactions are expected to intensify in the coming decades (Britten et al., 2017).

Decadal variations in the spatio-temporal dynamics of communities are ultimately driven by the presence of individuals of different species that depends on 1) stochastic variation in abundance, 2) tolerance of individuals in regards to the selective pressure of local environmental conditions, and 3) arrival or departure of individuals via dispersal (Vellend, 2010). Environmental forcings of the Anthropocene increase the selective pressure on populations and depending on a species' dispersal capacities, its distribution range can shift, shrink or extend (Dornelas et al., 2019). Key variables related to environmental forcing are associated with energy either directly through changes of ambient energy (i.e. kinetic energy, or solar energy) or indirectly through variations of productive energy (i.e. chemical energy, Evans et al., 2005; Koenigstein et al., 2016). Ambient energy corresponds to the amount of solar radiation received in the system which is often approximated by temperature (i.e. global warming), while productive energy corresponds to the conversion of solar energy into organic matter by photosynthetic organisms (i.e. plants, cyanobacteria, phytoplankton) which becomes available as trophic resources for heterotrophic organisms (see Evans et al., 2005 for a review). Productive energy in marine systems is often approximated by net primary productivity (Tittensor et al., 2010; Woolley et al., 2016). Ambient and productive energy represent two key factors of species niche through physiological tolerance and trophic requirements known to play a crucial role for metabolism, and geographic distribution (Brown et al., 2004; Evans et al., 2005; Valentine & Jablonsky, 2015; Tittensor & Worms, 2016). The species-energy hypothesis holds a central position to explain large biodiversity gradients through a wide range of mechanisms (Wright 1983; Evans et al., 2005; Clarke & Gaston, 2006). Species-energy relationships are mostly either positive or hump-

shaped (Bonn et al., 2004; Cusens et al., 2012). As such it implies that the number of individuals and species increase with energy up to a certain point before possibly decreasing (Cusens et al., 2012). Fishing pressure represents an additional selective force affecting species abundance in space and time (e.g. Lotze & Worm, 2009). Fishing might not be simply decreasing the abundance of caught species, but it can indirectly increase the abundance of non targeted species due to predation release or an increase in trophic resources (Moullec et al., 2017).

Environmental forcings and fishing can increase the spatio-temporal variability of fish assemblages, whose diversity dimensions can be differentially affected. Within communities, measures of α diversity (i.e. the mean species richness at local scale; Whittaker, 1972), including species richness (SR, i.e. the number of species) can increase, decrease or remain stable over time under environmental changes (e.g. Blowes et al., 2019; Antão et al., 2020). Variations of biodiversity over time can be scale-dependent, and differ in space, across taxa and ecosystems (Albouy et al., 2012; Dornelas et al., 2014; Magurran et al., 2019). Complementing α diversity, measures of β diversity (Anderson et al., 2011) can be used to quantify how the difference in species composition among spatial communities (dissimilarity) changes over time (Olden, 2006). The arrival of generalist species and the loss of locally endemic species may not change species richness (Dornelas et al., 2019) but leads communities to become more similar spatially, a phenomenon identified as taxonomic homogenization (as opposed to taxonomic differentiation, McKinney & Lockwood, 1999). β diversity can also quantify the variability in species composition within a community over time, the so-called temporal β diversity (e.g. Albouy et al., 2012; Magurran et al., 2019). These incidence-based indices can be less sensitive to environmental variations than abundance-based biodiversity indices (Santini et al., 2016). For example, exploitation of fish stocks (i.e. populations) can strongly affect abundance (Hutchings et al., 2010), while incidence-based indices will be affected only by local extinction (Burgess et al., 2013). Investigating the spatio-temporal dynamics of species assemblages and their potential drivers requires a holistic approach documenting simultaneously changes in α and β diversity within and among communities over time at different spatial scales (McGill et al., 2015) with both presence/absence and abundance-based biodiversity indices (Antão et al., 2020).

Increase in sea surface temperature is hypothesised to be the main driver of the distribution shift observed for major Northeast Atlantic commercial marine species (Baudron et al., 2020), the taxonomic homogenization of groundfish communities on the west coast of Scotland (Magurran et al., 2015), and the taxonomic differentiation of North Sea fish communities (McLean et al., 2019). In the Northeast Atlantic, the Bay of Biscay and the Celtic Sea are highly productive shelf seas (Moullec et al., 2017) with a long fishing history (Gascuel et al., 2016) and harbouring benthic

communities and habitats heavily degraded by bottom trawl fishing activities (Hily et al., 2008). Moreover, the combination of diversification of fish stock exploitation and the over-exploitation of several stocks has not yet led to a clear recovery in community biomass (Gascuel et al., 2016). Despite the effects of global warming being smaller in the Bay of Biscay and Celtic Sea in comparison to other regions (Chust et al., 2011), a forty-year time-series revealed an increase in temperature of the upper sea layer (200m) of the Bay of Biscay (Michel et al., 2009), which correlates with a northward shift of boreal species (Poulard & Blanchard, 2005) and an increase in the abundance of lusitanian species (e.g. Hermant et al., 2010) that is expected to further increase in the coming decades (LeMarchand et al., 2020). Global warming effects on biodiversity dynamics are not necessarily monotonic (Pecl et al., 2017) and subtle environmental forcings may have already triggered important community re-organisation (e.g. for species located at the limits of their distribution range) as suggested by several examples in the Bay of Biscay and the Celtic Sea (Poulard & Blanchard, 2005; Hermant et al., 2010; Iglesias & Lorance, 2016; Merillet et al., 2019). So far, scientific bottom trawl surveys in the Bay of Biscay and Celtic Sea have contributed *inter alia* to the annual assessment of commercial species (e.g. ICES, 2017), to study their habitat preferences (Persohn et al., 2009) and the dynamics of functional groups (Hosack & Trenkel, 2019). Studies were restricted to smaller areas or species pools (Poulard & Blanchard, 2005; Mérillet et al., 2019), or included disparate taxa groups (i.e. belonging to different phyla or subphyla) with variable taxonomic resolution (Poulard & Trenkel, 2007). However, these studies offered mixed results, and a holistic view of the spatio-temporal patterns of the demersal fish communities and their potential drivers is currently lacking despite the importance of the ecosystem services provided by the Bay of Biscay and Celtic Sea ecosystems.

In this study, we investigated the spatio-temporal changes of demersal marine ray-finned fishes in the Bay of Biscay and the Celtic Sea during the last two decades, and assessed the relative contribution of energy, habitat and fishing pressure as drivers of spatial and temporal biodiversity patterns. We used data from a standardised scientific survey carried out in the Bay of Biscay and the Celtic Sea from 1997 to 2018 to derive biodiversity indices to document changes in α and β diversity within and among communities over-time, considering incidence and abundance-based indices at regional and local scales. We hypothesised that the spatio-temporal dynamics of communities would be more evident using abundance-based indices than presence/absence indices because the effects of climate change in the study area remain currently more subtle than further north (Dye et al., 2013). Then, we selected a large set of environmental variables related to ambient (*e.g.* temperature) and productive energy (*e.g.* trophic resources), habitat, and fishing. We performed a variable selection procedure and used the best set of variables to assess the relative contribution of energy, habitat and fishing to spatio-temporal variability in biodiversity using a range of regression models. We hypothesised that fishing

pressure should have a higher contribution than energy because the diversification of fish stock exploitation following fishing regulations attributed to several over-exploited stocks (Gascuel et al., 2016) may have a greater impact on spatio-temporal dynamics of fish communities rather than climate change effects.

## 2 MATERIALS AND METHODS

### *2.1 Data acquisition and study area*

The biological data sets came from the French international bottom trawl survey (EVHOE) carried out annually during autumn to evaluate demersal fish resources in the Bay of Biscay (BoB) since 1987 and the Celtic Sea (CS) since 1997 (Fig. 1a). The BoB, which stretches from Spain to Armorica, is an intracontinental sea that is largely open to the Atlantic Ocean. The French part of the BoB continental shelf (80 000 km²) is narrow in the south and becomes broader in the north mainly influenced by the warm water of the Gulf Stream (Palter, 2015; Fig. 1A). The epicontinental CS is open to the Atlantic Ocean, stretching between Ireland, Wales, British Cornwall and Armorican Brittany. We compiled the presence/absence and abundance data for the period 1997-2018, the most homogenous time series in terms of research vessel, taxonomic identification and gear (GOV 36/47, the opening is 20 m horizontally at the wings and 4 m vertically). The time series is continuous, except for 2017 due to a technical problem, and the number of sampling stations varied between 119 and 158 per year (n= 2957 in total). Our data set included 180 fish (Actinopterygii) species or genera after grouping taxa that could not be unambiguously identified at the species level for the whole time series. For example, *Trachurus mediterraneus* and *Trachurus trachurus* were merged into *Trachurus sp*. We analysed taxonomic diversity for 171 benthic and demersal species/genera. We excluded from diversity calculations, nine of the most abundant small and medium-sized pelagic species (*Alosa alosa, Alosa fallax, Atherina presbyter, Engraulis encrasicolus, Sardina pilchardus, Scomber japonicus, Scomber scombrus, Sprattus sprattus, Trachurus sp.*) because the bottom trawl used in EVHOE has a 4 m vertical opening, which leads to low catchability and thus unreliable spatial patterns (Laffargue et al., 2021, but see Supplementary material S.2 Fig. S6, Fig. S7, Fig.S8, Fig. S9, for biodiversity patterns including these 9 species). However, we found that the overall temporal abundance trends estimated with the EVHOE data set for most of these pelagic species (see *Supplementary Material S2. Fig.S13*) were in good agreement with temporal biomass trends estimated by the dedicated PELGAS acoustic survey (Doray et al. 2018). Therefore, we used pelagic species richness and total pelagic abundance from EVHOE as explanatory variables (see "*Environmental variables and fishing pressure"*). We used the ICES statistical rectangle resolution (1° longitude x 0.5° latitude, ICES, 2019) to analyse spatial patterns (74 rectangles) and the full data set included 1242 ICES rectangles sampled from 1997 to 2018. ICES rectangles corresponded to the

highest spatial resolution available for fishing data. We controlled for the temporal imbalance in sampling effort (1 to 10 stations per rectangle per year) and the increasing number of stations over the years (i.e. increasing sampling effort over time, $r_{Spearman} = 0.55$, $p = 0.01$), which biases the temporal trends of biodiversity indices (e.g. creates an artificial increase in species richness). We used a sample-based rarefaction approach consisting of randomly sampling 1 station per ICES rectangle for each year and repeating this process 100 times to calculate average biodiversity indices. This approach is commonly undertaken in biodiversity studies to account for heterogeneous sampling efforts for both presence/absence and abundance data in an α and β diversity context (Dornelas et al., 2014; Magurran et al., 2015; Blowes et al., 2019; Antão et al., 2020).

### *2.2 Biodiversity indices*

We first computed species richness (SR), abundance and evenness (i.e. the uniformity in abundance among species within a sample). Abundance was log10 transformed to decrease the overdispersion caused by the most abundant species (Zuur et al., 2007). We used Hurlbert's evenness index (Hurlbert, 1971) ranging from 0 (uneven community dominated by one species) to 1 (even abundance among species). Using presence/absence community data matrices, we decomposed the overall β diversity between communities measured by the Jaccard index (β.jac, Jaccard, 1912) into its two additive components, turnover (β.jtu) and nestedness-resultant -hereafter called nestedness - (β.jne), that represent distinct mechanisms (Baselga, 2012). β.jtu measures the differences in composition caused by species replacement independently of the differences in species richness between sampling sites, while β.jne measures the differences in species composition caused by species loss or gain. We also used the β.ratio, defined as β.jtu/β.jac, to assess the relative importance of turnover *vs* nestedness. Overall, β diversity is dominated by turnover or nestedness for a β.ratio > 0.5 and <0.5, respectively. We also partitioned the abundance-based Ruzicka β diversity index (β.ruz, Ruzicka, 1958) into its two additive antithetic components, the balanced variation in abundance (β.ruz.bal) and abundance gradients (β.ruz.gra, Baselga, 2013). The balanced variation in abundance corresponds to the replacement of individuals of some species in one site (or at time t-1) by the same number of individuals by different species in another site (or at time t). The abundance gradient describes the loss/gain of individuals from one site to another (or between two time periods). We used the β.ruz.ratio (β.ruz.bal/β.ruz) to estimate the relative importance of the balanced variation in abundance compared to the abundance gradient. We then assessed how local β diversity (LBD) was structured in space, which was defined as the average β diversity between a focal ICES rectangle and neighbouring rectangles within a certain distance. High LBD values then indicate singular community composition in the focal rectangle in comparison to its neighbours. We tested 16 distance thresholds, 150 to 300 km in 10 km steps (Fig. S4), and retained the threshold that presented the largest number

of rectangles with a significant temporal trend for the β diversity indices to test at which spatial scale communities were susceptible to express taxonomic differentiation/homogenisation over time. Ten kilometre increments allowed a constant increase in the number of neighbours between 150 and 300 km because distances among rectangle centroids were not evenly spaced. We explored LBD variations through time. A temporal decrease (increase) of LBD indicates that the neighbouring communities are getting more similar (dissimilar). Therefore, the temporal variation of LBD was used as a proxy of taxonomic spatial homogenization (differentiation).

### *2.3 Environmental variables and fishing pressure*

For each year (1997-2018) and the 74 ICES rectangles, we selected 19 variables to test the relative influence of three main drivers on SR, abundance, evenness and the LBDs indices.

- Energy

To investigate the influence of ambient energy, we considered seafloor temperature (°C) and a variable that integrated temperature (°C) across the water column. For these two variables, we considered annual averages, monthly minima and as a surrogate for seasonality the standard deviation of monthly averages. To document the influence of productive energy, we considered the annual average of net primary productivity (NPP). We did not retain the seasonality of NPP as its standard deviation was highly correlated with the annual average ($r_{Pearson} = 0.97$). In addition, we considered species richness and the abundance (log10) of nine pelagic species as they represent potential key links in the food web (Cury et al., 2000).

- Habitat

We retained eight variables to document the contribution of habitats: rectangle surface area ($km^2$), distance to the nearest coast (km), average depth (m), diversity of seabed habitats based on substrate, minimum and average of mixed layer depth (m, MLD) as a surrogate for water column stratification intensity, minimum and standard deviation of monthly oxygen concentrations ($O_2.l^{-1}$). The later variables allowed us to assess the prevalence of oxygen minimum zones (OMZs) and the effect of oxygen seasonality. Additional details about environmental variables are provided in *Supplementary material S1.1*.

- Fishing pressure

Fishing pressure (in hours fished) was extracted from the STECF Fisheries Dependent Information Database (STECF 18-11, 2018) using the spatial effort information from 2000 to 2016. Due to inconsistencies in the French effort time series, effort estimates were extracted from Ifremer's database (Demanèche et al., 2013) using the STECF methodology. We calculated annual fishing effort summing across all gear types and estimated fishing diversity using the Shannon index (Shannon, 1948) based on the proportion of fishing hours for the 11 main types of fishing gears. This

fishing diversity index enabled us to assess the degree of heterogeneity in the fishing effort among the different fishing gears.

Mean spatial patterns of all variables and pairwise Spearman correlation coefficients are provided in *Supplementary material* (Fig. S1, S2). Several explanatory variables were log10 transformed to avoid excessive dispersion of model residuals and fulfil the normality assumption of residuals for the linear models (see paragraph 2.5 and see *Supplementary material S1.1).* All variables were normalised by subtracting the mean and dividing by the standard deviation. For consistency among explanatory variables, we considered a shorter time series from 2000 to 2016 (i.e. including 1014 rectangles over the years) when modelling the contribution of energy, habitat and fishing pressure to the variability of biodiversity indices. For each variable, we considered the linear and quadratic terms, to account for a certain degree of nonlinearity in the response curves in the models. We used elastic-net regularised generalised linear models (Elastic-net GLMs: Zou & Hastie, 2005) to select the most influential variables related to energy, habitat and fishing pressure separately for each of the 11 biodiversity metrics, before further modelling. This approach is useful when large numbers of potentially correlated variables with limited effect are available. Additional details about this approach are provided in *Supplementary material S1.2*.

### *2.4 Inferring spatio-temporal patterns*

*Regional scale*

At the regional scale (i.e. BoB and CS), we estimated the temporal change of average SR, abundance and evenness per rectangle and the average pairwise values among all ICES rectangles for β.jac, β.jtu, β.jne and β.ratio (see flowchart of the analytical steps in Fig. S5). We applied a generalised additive model (GAM) to better detect non linear temporal trends by using the general equation:

$Y = a + f(year) + \varepsilon$,

where $Y$ is the response variable (i.e. the different biodiversity indices), a is the intercept, $f(year)$ is a smooth function (thin plate regression spline) of the fixed effect "year" limited to a maximum of 3 basis dimensions to avoid overfitting and ε represents residuals. We considered a gaussian error and an identity link function for the average SR, abundance and evenness because we modelled the average values over the 100 resampled communities which are all positive continuous variables truncated at 0, and a Beta error distribution and a logit link function for the average values of β diversity indices because they take values between 0 and 1 (i.e. see Figure 1). The relatively short time series (maximum 21 years) leads to a small sample size and thus limits the statistical power to test for temporal trends (positive vs negative). Considering the strong relationships between p.value and sample size, we adapted the significance threshold to the sample size (Pérez & Pericchi, 2014,

Betensky 2019). Thus, we reported weak evidence (Muff et al., 2021) for a positive or a negative temporal trend (the p.value of the temporal slope < 0.1). In contrast, all temporal slopes associated with a p.value > 0.1 were considered as stable. Moreover, to assess general interdecadal trends we estimated the slope of generalised linear models (GLM) with year as explanatory variable and biodiversity indices as response variables, considering the same error distributions and link functions as for GAMs.

*Local scale*

We next explored the spatial and temporal patterns of biodiversity indices at the local scale (1° longitude x 0.5° latitude, ICES rectangle). For each rectangle we averaged across years SR, abundance, evenness and local β diversity indices (LBD.jac, LBD.jtu, LBD.jne, LBD.ruz, LBD.ruz.bal, LBD.ruz.gra, see Fig. S5). Then, to test for temporal trends, we estimated the slope of a GLM, which represents a summary statistic of the temporal trend with year as explanatory variable and biodiversity indices as response variable according to the following equation:

$Y = a + B * year + \varepsilon$,

where $Y$ are biodiversity indices, a is the intercept, B is the linear slope of the "year" effect and ε represents residuals. Gaussian errors and identity links were considered for SR, abundance and evenness and a Beta error with logit link function for LBD indices. To avoid boundary problems with the logit link (i.e. response values of 0 or 1), the response variable was transformed following the recommendation by Cribari-Neto & Zeileis (2010) as $(y * (n - 1) + 0.5)/n$, being n the sample size. To investigate temporal trends, 71 rectangles sampled at least five years were retained. We considered spatial differentiation and homogenisation of communities over time as soon as weak evidence (p.value of slope < 0.1, Muff et al., 2021) of either positive or negative temporal linear slopes respectively were reported for LBD indices . In addition, we also assessed the variability of species composition within a rectangle over time, the so called temporal β diversity (TBI; Albouy et al., 2012), using both Jaccard and Ruzicka indices and their respective components (see methodological details in *Supplementary material S1.3*., and Fig. S3 for the pairwise relationships among temporal trends for all biodiversity indices).

*Partitioning space and time variations*

For the full data set of 1242 rectangles sampled from 1997 to 2018, we used a variance partitioning approach based on the Moran Eigenvector Map (MEM) method (Dray et al., 2012) to test the relative importance of spatial and temporal variability of biodiversity patterns (Legendre et al., 2014; for more details see *Supplementary material S1.4*; Fig. S5).

### *2.5 Partitioning diversity variations among energy, habitat and fishing pressure*

We applied a steady-state linear mixed effects model (LMM) considering time (i.e. year ) as a random effect, to test the relative influence of energy, habitat and fishing pressure on SR, abundance, evenness and LBDs indices. Only the most influential variables previously retained with the Elastic-net GLMs (see paragraph 2.3) for the three groups of variables were included as fixed effects in the full LMM. We used average values of 100 resampled biodiversity indices (i.e. species richness is not an integer anymore but can be a decimal value) and we considered a large data set of 1014 rectangles sampled between 2000 and 2016. Therefore, the central limit theorem justifies the use of a gaussian error model, which we combined with an identity link for all biodiversity indices. Based on these full LMM, a variance partitioning approach (Legendre *&* Legendre, 1998) was performed to estimate the independent and shared contributions of the three groups of variables for each biodiversity index.

The general equation of the full LMM including the best set of variables related to energy, habitat and fishing was as follows:

$$Y_i = a + B_{energy} * x_{energy\ i} + B_{habitat} * x_{habitat\ i} + B_{fishing} * x_{fishing\ i} + Z_i * b_i + \varepsilon_i,$$

where $Y_i$ are the biodiversity index in year $i$, a is the intercept, $B_{energy}$, $B_{habitat}$ and $B_{fishing}$ are the slopes of the energy, habitat and fishing variables respectively, $Z_i$ is a design matrix (identity matrix for the random intercept model) associated with the random year effect $b_i$ and $\varepsilon_i$ represents model residuals. For each biodiversity index, the best set of explanatory variables for energy, habitat and fishing retained in the full LMM model for variance partitioning are available in *Supplementary material S4 Table S2*. We estimated the marginal $R^2$ (Nakagawa et al., 2017) as a proxy for the variance explained by fixed effects. To test for potential lack of fit of the LMMs due to complex nonlinear relationships, we conducted the same approach using generalised additive mixed models (GAMM) using the same general equation, except that we associated fixed effects with smoothing functions. Normality and homogeneity assumptions of the GAMM and LMM residuals were assessed for each model through visual inspection (histogram, qqplot, plot of the fitted vs residuals) and shapiro tests (Shapiro & Wilk, 1965). The list of R packages used for variance partitioning is available in *Supplementary material S1.5*.

### *2.6 Determining variables importance within energy, habitats and fishing pressure*

For each biodiversity index, we used a model selection approach to select the most parsimonious model and assess the relative importance of the main variables within the three groups of explanatory variables included in the LMMs presented in 2.5. First, we performed a multimodel inference approach based on information theory running all possible models (Grueber et al., 2011). We retained the most parsimonious model based on the Bayesian Information Criteria (BIC) among the best set of models that have less than 2 BIC units difference with the best model with the lowest BIC. Second,

we computed the semi-partial marginal $R^2$ as a proxy of explained variance for each variable retained in the most parsimonious model (Jaeger et al., 2017; Nakagawa et al., 2017). In addition, for the most parsimonious LMM we also considered alternative models to investigate the existence of temporal and/or spatial autocorrelation in residuals (Zuur et al., 2009, additional details are provided in *Supplementary material S1.6*). To assess the goodness-of-fit of these alternative models we used the Pseudo.$R^2$ (Efron, 1978) which is defined as the coefficient of determination of the linear relationships between the observed and fitted values.

### *2.7 Testing for temporal effects, time lag and environmental forcings*

For each biodiversity index, we also investigated the temporal variation of the environmental-biodiversity relationships by testing 1) the significance of temporal effects in the most parsimonious models presented in 2.6, 2) for time lag effects of 1 and 2 years between the biodiversity indices and explanatory variables and 3) the relationships between environmental forcing and temporal trends of biodiversity indices. All methodological details related to these three approaches are provided in *Supplementary material S1.7, S1.8 and S1.9 respectively* (see Fig. S5 for the flowchart of the analytical steps).

**Table 1**: Definition of acronyms

| **Acronym** | **Definition** |
|---|---|
| SR | Species richness |
| β.jac | Beta diversity estimated by the Jaccard index (accounting for presence/absence) |
| β.jtu | Beta diversity estimated by the Jaccard's turnover component |
| β.jne | Beta diversity estimated by the Jaccard's nestedness-resultant component |
| β.ruz | Beta diversity estimated by the Ruzicka index (accounting for abundance) |
| β.ruz.bal | Beta diversity estimated by the balanced variation in abundance component of the Ruzicka index |
| β.ruz.gra | Beta diversity estimated by the gradient in abundance component of the Ruzicka index |
| LBD | Local beta diversity |
| LBD.jac | Local beta diversity of the Jaccard index |
| LBD.jtu | Local beta diversity of the Jaccard's turnover component |
| LBD.jne | Local beta diversity of the Jaccard's nestedness-resultant component |
| LBD.ruz | Local beta diversity of the Ruzicka index |
| LBD.ruz.bal | Local beta diversity of the Ruzicka's balanced variation in abundance component |
| LBD.ruz.gra | Local beta diversity of the Ruzicka's gradient in abundance component |
| TBI | Temporal beta diversity indices; suffix specifies which index (Jaccard, or Ruzicka) and which component (jtu, jne, bal, gra) is used. |

| | |
|---|---|
| GLM | Generalised linear model |
| LMM | Linear mixed model |
| GAM | Generalised additive model |
| GAMM | Generalised additive mixed model |
| MEM | Moran Eigenvector Map |
| BIC | Bayesian Information Criteria |

## 3 RESULTS

### *3.1 Temporal patterns at regional scale*

At the regional scale, as expected, abundance-based biodiversity indices displayed clearer temporal changes than incidence-based indices. Species richness remained stable in the Bay of Biscay (BoB) and Celtic Sea (CS) between 1997-2018 (GAM, edf = 1.65, $p$ = 0.37, Fig. 1b), while overall abundance declined (GAM, edf = 1, $p$ = 0.01, GLM slope = -0.01, $p$ = 0.01). The incidence-based $\beta$ diversity was dominated by species turnover. While *β.jac* increased significantly over time (GAM, edf = 1, $p$ = 0.06, GLM slope = 0.004, $p$ = 0.05), none of its components, *β.jtu, β.jne* and *β.ratio,* had a significant time trend (Fig. 1b). In contrast, overall abundance-based $\beta$ diversity (*β.ruz)* as well as its two components and *β.ruz.ratio* showed clear significant time trends (Fig. 1b). *β.ruz* increased significantly since 2005 (GAM, edf = 1.87, $p$ = 0.01). This increase is mainly driven by balanced variation in abundance, i.e. compensation between species (*β.ruz.bal*: GAM, edf = 1.88, $p$ = 0.01; *β.ruz.ratio*: GAM, edf = 1.81, $p$ = 0.01). The abundance gradient component made a smaller contribution, remaining stable from 1997 to 2005 and decreasing thereafter (GAM, edf = 1.78, p = 0.02, Fig. 1b; see Fig. S6-S9 for patterns including small pelagic species).

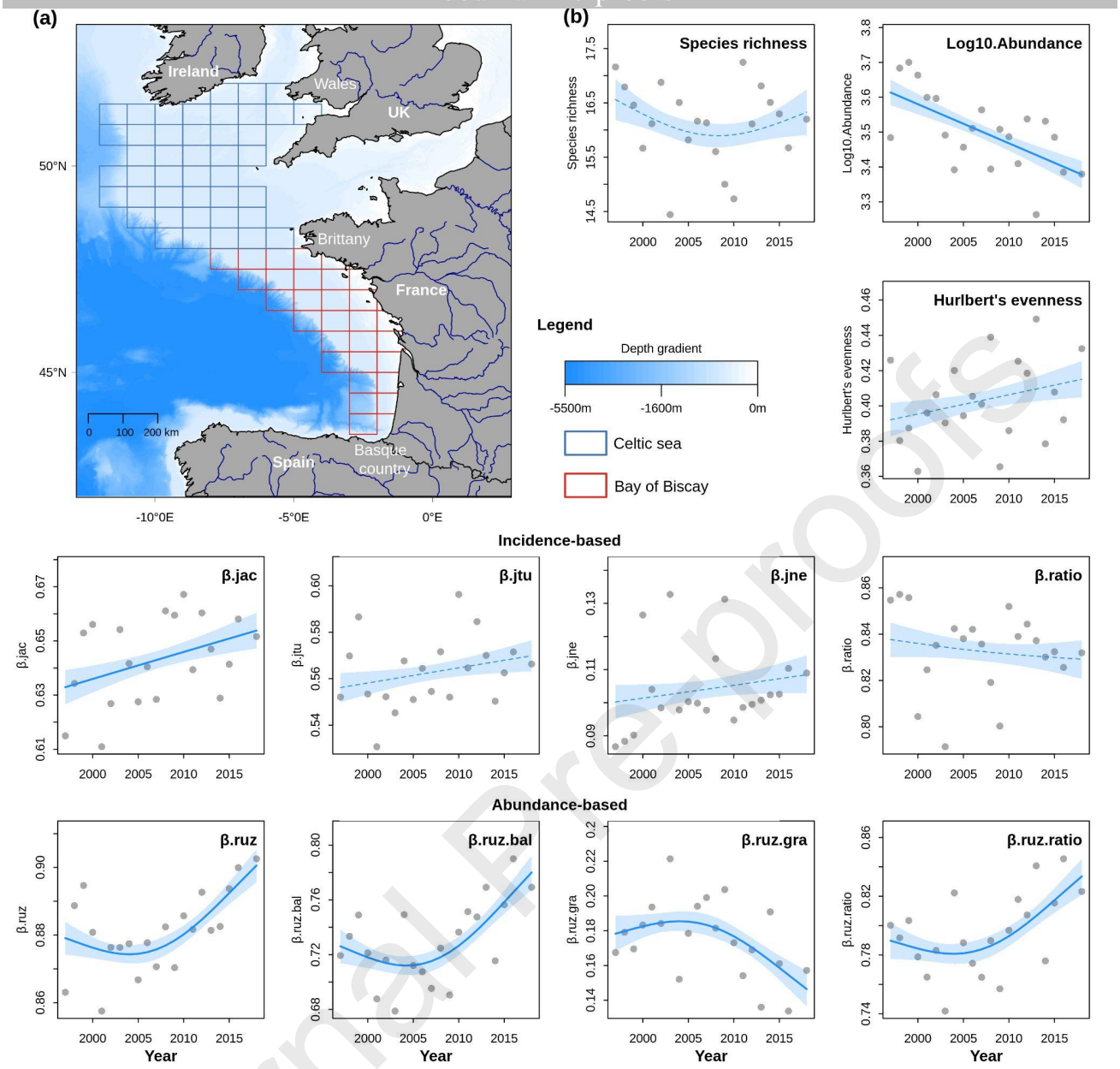


**Fig. 1: (a)** Map depicting the ICES rectangles of the Celtic Sea and the Bay of Biscay covered by the EVHOE bottom trawl survey from 1997 to 2018 sampling demersal fish assemblages (n=171 sp.). **(b)** Temporal trend average by ICES rectangle per year for species richness (SR), abundance (log10(abundance)), Hurlbert's evenness, and for all pairwise ICES rectangle comparisons for the Jaccard index (β.jac), its species turnover (β.jtu) and nestedness (β.jne) components, the ratio of species turnover over the Jaccard index (β.ratio), and abundance-based dissimilarity indices, including the Ruzicka index (β.ruz) and its balanced variation in abundance (β.ruz.bal), and abundance gradient (β.ruz.gra) components as well as the ratio β.ruz.bal/β.ruz (β.ruz.ratio). The continuous curves represent the fits of generalised additive models (GAM), with solid lines indicating a significant relationship, while dotted lines indicate a non-significant time trend (p.value > 0.1), and the light blue area one standard error around the fitted models.

### *3.2 Spatio-temporal patterns at local scale*

At the local scale, contrary to our expectation, geographic patterns were clearer for incidence-based than for abundance-based biodiversity indices and revealed a pattern of taxonomic homogenization in the CS and differentiation in the southern BoB. SR averaged over time showed two local "hot-spots" (SR = 17-19 species per ICES rectangle), one in the CS along the coasts of Ireland and the UK and the other one in the BoB along the coast of France, from Brittany to the Basque country (Fig. 2a). The average abundance pattern revealed a geographic division (t test = 5.2, $p < 0.001$) between the CS and the BoB showing higher (log10(abund), mean = 3.6, standard deviation +/- 0.13) and lower (log10(abund) mean = 3.42 +/- 0.16) abundances, respectively (Fig. 2a). The average pattern of evenness was driven by SR (Fig. 2a). At the local scale, in 75% of rectangles (n = 53), SR remained stable during the study period, while 18% (n = 13), mostly located on the outer-shelf and in coastal areas of the southern Bay of Biscay, lost species (Fig. 2b). The 7% of rectangles (n = 5) gaining species over time were located in the northern part of the Celtic Sea. Similarly, abundance in 73% of rectangles (n = 52) had a stable temporal trend, and 23% (n = 17) showed a significant loss of individuals. The latter rectangles were located both in the CS and the BoB, mostly near the coast (Fig. 2b). The pattern of temporal changes of evenness was inverted in comparison to abundance patterns ($r_{Spearman} = -0.49$, $p < 0.001$, Fig. 2b).

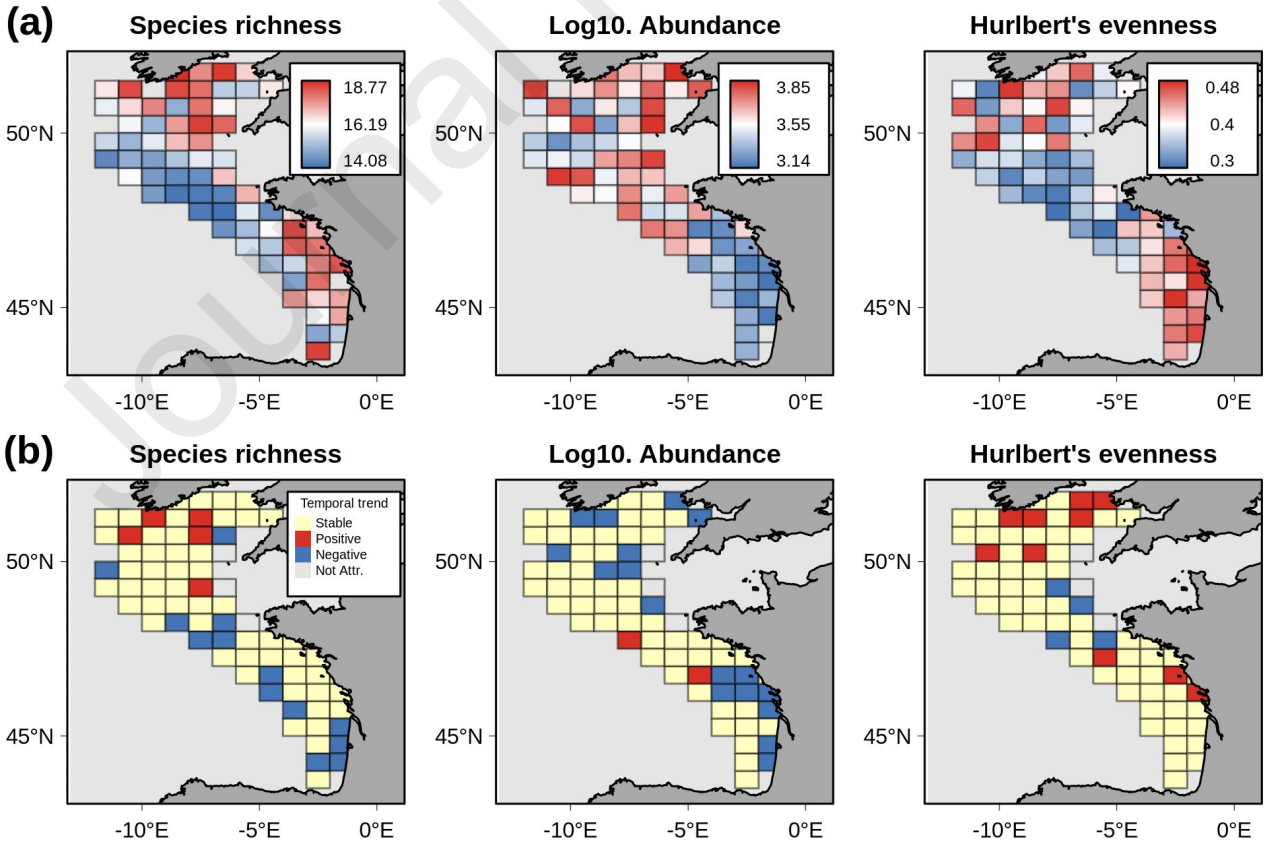

**Fig. 2:** Species richness, abundance (log10 transformed), and the Hurlbert's evenness patterns of the demersal fish assemblages of the Bay of Biscay and the Celtic Sea for the period 1997-2018**.** The row (a) represents the mean species richness (SR), the mean abundance (log10(abundance)) and the mean evenness (Hurlbert's index) over the period 1997-2018. The row (b) shows the trends of the temporal evolution of SR, abundance and Hurlbert's evenness. The beige colour indicates a stable trend (slope not significantly different from 0, with a p.value > 0.1), while positive and negative trends are in red and blue, respectively.

For incidence-based local $\beta$ diversity (LBDs), we retained 190 km as the spatial distance maximising the number of rectangles with a significant temporal trend of taxonomic differentiation/homogenisation to build local $\beta$ diversity indices (Fig. S4a). Average geographic patterns for LBDs indices were dominated by the turnover component ($\beta.jtu$) and showed strong north/south and coastal/offshore patterns (Fig. 3a). LBD.jac and LBD.jtu indicated similar spatial patterns ($r_{Spearman}$ = 0.78 - 0.98) with high values along the coast of the BoB and low values in the central CS (Fig. 3a). The nestedness component had a limited contribution to the jaccard index, and LBD.jne displayed a reversed pattern ($r_{Spearman}$ = -0.93, $p < 0.001$; Fig. 3a). The spatial pattern of temporal changes of LBD.jac revealed a significant decrease (27% of rectangles, n = 17) in compositional dissimilarity over time in the offshore part of the southern CS (Fig. 3b), while the coastal communities in the south of the Bay of Biscay and along the Welsh coast became more dissimilar (Fig. 3b). The LBD.jac pattern was mostly driven by species turnover (LBD.jtu) reinforcing a pattern of taxonomic homogenization (31% of rectangles, mean slope = -0.03 +/- 0.001) in the north (Fig. 3b) and taxonomic differentiation (15% of rectangles, mean slope = 0.04 +/- 0.014) mostly in the south (Fig. 3b).

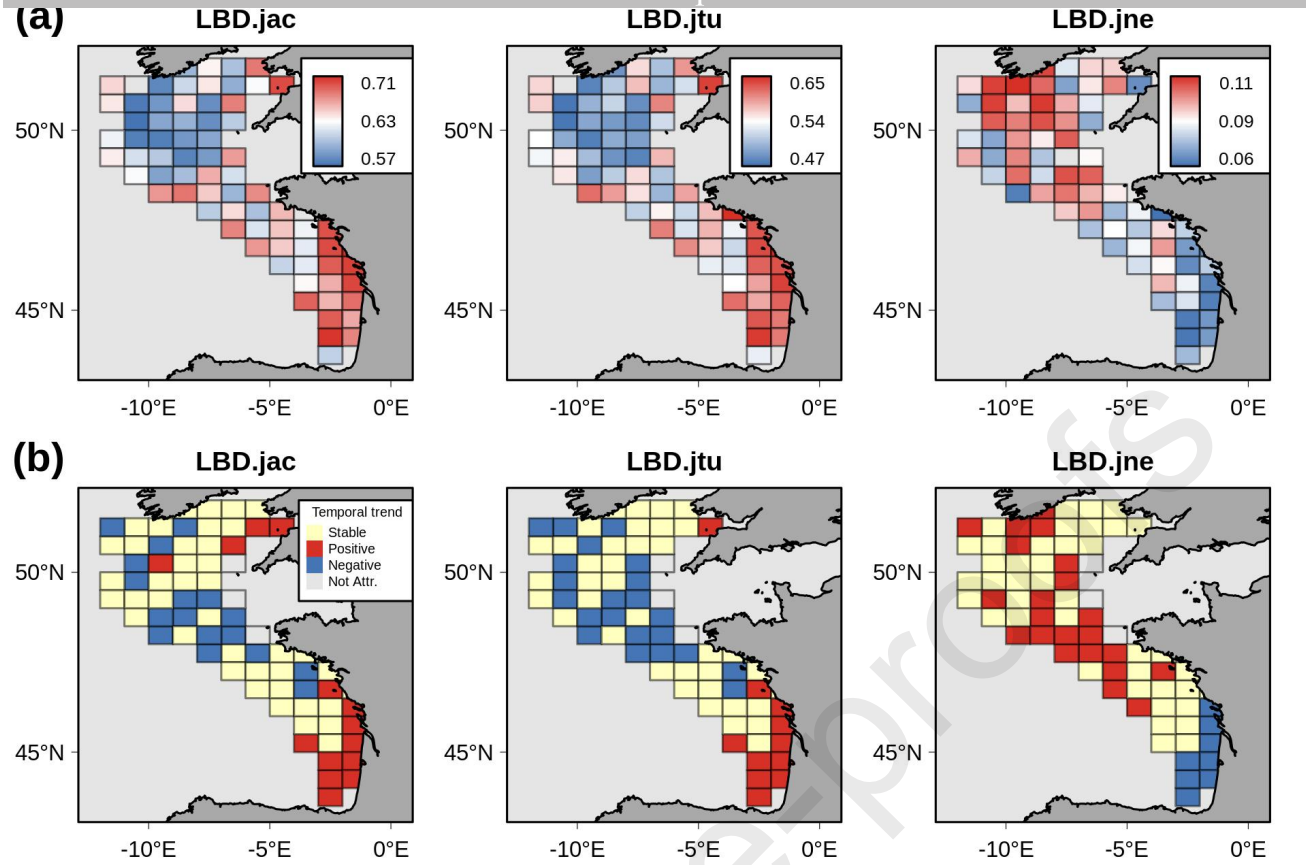


**Fig. 3:** Local β diversity of incidence-based indices of the demersal fish assemblages in the Bay of Biscay and Celtic Sea for the period 1997-2018. The first row (a) shows the mean local Jaccard index (LBD.jac), mean local species turnover (LBD.jtu), and mean local nestedness (LBD.jne) over the period 1997-2018. The second row (b) shows the trends of the temporal evolution of LBD.jac, LBD.jtu and LBD.jne. The beige colour indicates a stable trend (slope not significantly different from 0, with a p.value > 0.1), while positive and negative trends are in red and blue, respectively.

For abundance-based LBD indices, average geographic patterns were dominated by balanced variations in abundance (LBD.ruz.bal, $r_{Spearman} = 0.76$, $p < 0.001$) and showed a more patchy spatial pattern than incidence-based indices (Fig. 4a). A distance of 290 km maximising the number of rectangles with a significant temporal trend of taxonomic differentiation/homogenisation was retained to investigate abundance-based LBDs (Fig. S4b). Spatial patterns for the two components LBD.ruz and LBD.ruz.bal were similar ($r_{Spearman} = 0.76$), with higher values (0.73 - 0.8) in the northern part of the Celtic Sea and along the coast of the Bay of Biscay (Fig. 4a), while LBD.ruz.gra showed an inverted spatial pattern ($r_{Spearman} = -0.95$, $p < 0.001$; Fig. 4a, additional details in *Supplementary material S2.1*). The temporal trend of the spatial patterns for abundance-based LBD indices revealed an increase in LBD.ruz.bal (23% of rectangles, mean slope = 0.03 +-0.01) and a decrease in LBD.ruz.gra (18% of rectangles, mean slope = -0.02 +/- 0.01, Fig. 4.b) for both the entrance of the St George Channel in the Celtic Sea and the southern coast of the Bay of Biscay. The

temporal β diversity (TBI) patterns based on both incidence and abundance-based indices were consistent with the identified LDB patterns (see *Supplementary material S2.1* Fig. S3, S10a,b, S11a,b).

### *3.3 Partitioning space and time variations*

Overall, partitioning the variance between space and time revealed that the spatial dimension explained more than double of the variability (7.6 +/- 2.5%) than time (3.3 +/- 1.26%) for all biodiversity indices except LBD.jne (Table S1).

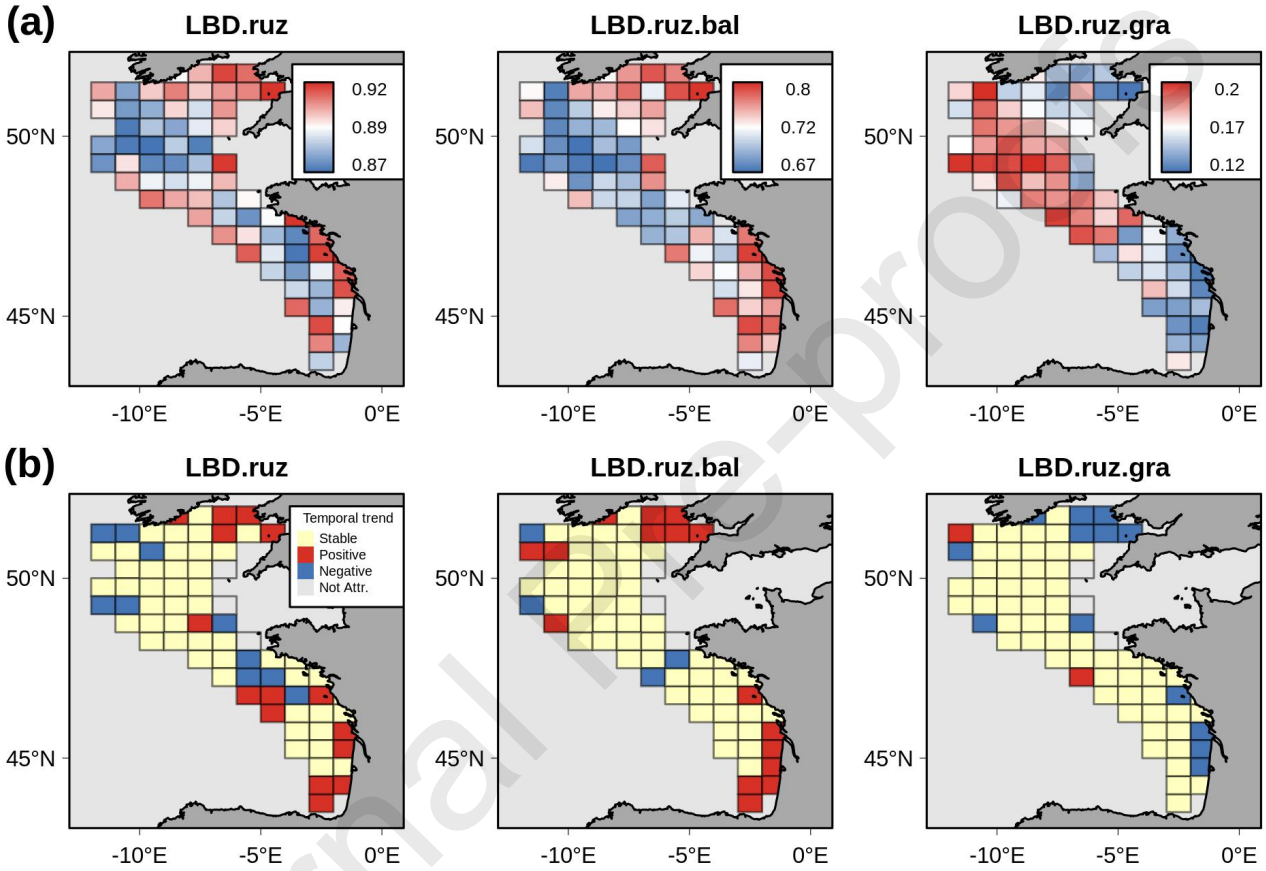


**Fig. 4:** Local β diversity of abundance-based indices of the demersal fish assemblages in the Bay of Biscay and the Celtic Sea for the period 1997-2018. The first row (a) shows the mean local Ruzicka index (LBD.ruz), mean local balance variation in abundance (LBD.ruz.bal), and mean local abundance gradient (LBD.ruz.gra) over the period 1997-2018. The second row (b) shows the trends of the temporal evolution of LBD.ruz, LBD.ruz.bal and LBD.ruz.gra. Only 71 ICES rectangles sampled at least 5 times were retained. The beige colour indicates a stable trend (slope not significantly different from 0, with a p.value > 0.1), while positive and negative trends are in red and blue, respectively.

### *3.4 Partitioning diversity variations among energy, habitat and fishing pressure*

Contrary to our expectation, we found that energy (temperature and trophic resources) had a greater

influence on spatio-temporal biodiversity variations than habitat or fishing. The steady-state LMMs based on the four best explanatory variables for energy, habitat and fishing pressure (see Table S2 for the selection of the explanatory variables for each biodiversity metric) explained on average a small proportion of variance (mean = 15.4 +/- 6.53%, Table 2). The explained variance (for the fixed effects) was smallest for the evenness model (4.4%), moderate for SR (12.5%), LBD.jne (11%) and all abundance-based LBD indices (11.7 - 16%) while variations in abundance (20.3%), LBD.jac (23.2%) and LBD.jtu (25%) were best explained (Table 2). Energy explained the highest proportion of variance (8.1 +/- 5.5%), followed by habitat (1.6 +/- 0.8%) and fishing pressure (0.9 +/- 0.8%, Table 2). The largest fraction of shared variance was attributed among the three categories (2.2 +/- 1.7%), followed by energy and habitat (1.1 +/- 0.6%; Table 2). The contribution of energy alone was particularly high for abundance (14.7%), LBD.jac (14.8%), and LBD.jtu (14.9%). Variance partitioning performed with GAMMs showed very consistent results with the results obtained using LMMs indicating that the relationships were well captured by simple linear and quadratic terms (i.e. second order polynomial; Table S3).

### *3.5 Importance of variables within energy, habitats and fishing pressure*

Model selection revealed that SR and the abundance of the nine small pelagic species (i.e. productive energy related to trophic resources) were two of the most important variables for explaining variability in biodiversity indices (Table S3-S11). Species richness of small pelagics had the highest or second highest semi-partial marginal $R^2$ for abundance (5.6%), LBD.jac (8%), LBD.jtu (10.5%) and LBD.jne (5.2%). It was positively related to evenness, LBD.jac, LBD.jtu, LBD.ruz and LBD.ruz.bal and negatively to abundance, LBD.jne and LBD.ruz.gra (Table S5-S12). The abundance of small pelagics achieved the highest or the second highest, though still small, semi-partial marginal $R^2$ for SR (5.5%), abundance (5.8%), LBD.jac (10.8%), LBD.jtu (9.7%), LBD.ruz (6.3%), and was negatively related to SR and positively related to abundance, LBD.jac, LBD.jtu, and LBD.ruz. Distance to the coast, minimum thickness of the mixed layer depth (MLD.min), and bathymetry were the most important habitat variables, though they only explained a low percentage of variation in diversity indices when they were retained (1.3 - 6%, Table S4-S12). Fishing pressure and its heterogeneity were retained for the SR models, while they had limited explanatory power for the different incidence and abundance-based LBD indices (0.8 - 4.5%) (Table S3, S7-S12). Overall, accounting for the remaining spatial or temporal autocorrelation in the model residuals did not affect the importance of the main variables described above but improved the explained variance of the models and even more so when both spatial and temporal autocorrelation were simultaneously accounted for (pseudo.$R^2$ = 58% +/- 25), in comparison to accounting only for spatial (53% +/- 8) or temporal correlations (50% +/- 14), (see Supplementary material S4. *Table S4-S12* for model outputs).

Only marginal improvements were obtained by testing for temporal effect by including time as fixed effect, or lagged variables, or testing for relationships between environmental forcings and temporal trends of biodiversity indices (more detailed results are available in Supplementary material in Table S4-S12 for temporal effect, for lag effect see results in paragraph S2.2 and Table S13-S22, for environmental forcing see results in paragraph S2.3, Fig. S12 and Table S23-S24).

**Table 2**: Variance partitioning based on linear mixed models (LMM) including time (i.e. Year effect) as a random intercept, for species richness (SR), abundance, Hurlbert's evenness (evenness), and all local β diversity indices (LBD, see text for the meaning of LBD indices), considering contemporaneous explanatory variables, for the demersal fish assemblages of the Bay of Biscay and the Celtic Sea. E: energy, H: habitat, F: fishing pressure. Values correspond to the percentage of explained variance. In abbreviations, energy E, habitat H, and fishing pressure F.

| **Biodiversity index** | **Explained**(%) | **E** (%) | **H**(%) | **F** (%) | **Shared.E.F.** | **Shared.E.H.** | **Shared.H.F.** | **Shared.E.H.F** |
|---|---|---|---|---|---|---|---|---|
| SR | 12.5 | 6.5 | 3 | 0.7 | 0.3 | 2 | 0.5 | 0[a] |
| Abundance | 20.3 | 14.7 | 2.1 | 0.3 | 0.2 | 0.7 | 1.2 | 1.2 |
| Evenness | 4.4 | 1.7 | 1.1 | 0.6 | 0[a] | 0.3 | 0.5 | 0.4 |
| LBD.jac | 23.2 | 14.8 | 1.1 | 1 | 1.6 | 1.1 | 0.4 | 3.3 |
| LBD.jtu | 25 | 14.9 | 1.8 | 1.2 | 1.6 | 1.1 | 0.7 | 3.8 |
| LBD.jne | 11 | 5.9 | 0.6 | 0.9 | 0.7 | 0.4 | 0.8 | 1.7 |
| LBD.ruz | 14.3 | 8.4 | 1.4 | 0.2 | 0.3 | 1.5 | 0.3 | 2.1 |
| LBD.ruz.bal | 16 | 4.2 | 2.8 | 0.4 | 0.4 | 1.6 | 1.8 | 4.7 |
| LBD.ruz.gra | 11.7 | 1.7 | 1 | 2.7 | 0.2 | 1.6 | 1.4 | 3.1 |

[a] Negative values were converted to 0 (Legendre and Legendre, 1998), as such the sum of the variance of the individual categories might not add-up to the total explained variance.

## 4 DISCUSSION

In this study, we investigated the spatio-temporal changes of demersal marine ray-finned fishes in the Bay of Biscay and in the Celtic Sea and assessed the relative contribution of energy, habitat and fishing pressure, during the last two decades by using long-term scientific surveys. We found that species richness weakly changed over time, while compositional dissimilarity showed contrasted patterns of taxonomic homogenization in the Celtic Sea and differentiation in the southern Bay of Biscay, where local assemblages were becoming more similar and dissimilar over time, respectively. In agreement with our first expectation, the temporal trends of the abundance-based indices showed stronger relationships than incidence-based indices at regional scale while the latter indices provided clearer patterns at local scale. In contrast to our second expectation, we showed that the contrasted spatio-temporal changes of demersal fish assemblages were best explained by productive energy

funnelled through the dynamics of small pelagic species, whereas effects of environmental forcing and most notably fishing pressure were limited.

### *4.1 Incidence-based biodiversity patterns*

One of the striking results of this study was the different temporal dynamics of communities situated in the offshore regions of the Celtic Sea (CS) and the southern coast of the French part of the Bay of Biscay (BoB). Indeed, our investigation at the local scale of β diversity (up to 200 km) showed spatially contrasting patterns of either taxonomic homogenization or differentiation among communities that compensated each other at the regional scale. Contrary to our expectation, these patterns of homogenization and differentiation were better detected by incidence-based indices at the local scale and indicated that variations of species assemblages over time can display different signals when analysed at different spatial scales (Chase et al., 2019). In the Celtic Sea, SR was stable or increased over time while local β diversity (LBD) driven by species turnover decreased, indicating that local communities were becoming more homogenous. A similar pattern of taxonomic homogenization for the last three decades has been found for demersal fish communities off the west coast of Scotland (Magurran et al., 2015). The stability of SR suggests that taxonomic homogenization on the west coast of Scotland is mostly due to community re-organisation of existing species. However, in our results the only locations (7% of rectangles) significantly gaining species (*Agonus cataphractus, Pleuronectes platessa, Trisopterus esmarkii, Callionymus reticulatus*) were located in the CS suggesting that taxonomic homogenization is the result to both spatial re-organisation of the communities, with species getting less spatially segregated (more dispersal), and the arrival of new taxa within multiple communities (Olden 2006). In contrast, on the south coast of the BoB, communities tended to lose species while the temporal increase of the local β diversity was mostly influenced by species turnover. Taken together, these results showed spatial differentiation of communities and confirmed that temporal dynamics of assemblages can drastically vary over short spatial distances (Leprieur et al., 2008).

Another striking result is that the southern BoB is losing species over time, despite southern newcomers having been detected (Iglésias & Lorance 2016). In this region the species turnover increased in recent years among local communities (LBD.jtu), potentially due to an increase in patchiness of species populations. The loss of species was counterintuitive, as we expected that species range shifts and arrival of southerly species would increase species richness (Dornelas et al., 2019) if the tempo of immigration is higher than extirpation (Chase et al., 2019). Several species were becoming rarer, such as *Trisopterus minutus, Hippoglossoides platessoides, Melanogrammus aeglefinus, Merlangius merlangus* or *Lophius piscatorius,* while others were becoming more frequent

(e.g. *Scomber colias, Sponayltosoma cantharus, Trigla lyra, Boops boops, Trachinus araco, Dicentrarchus labrax, Liza ramada)*. Additional results showed that at regional scale, incidence-based biodiversity indices had weak temporal variation when averaged over space, and species richness remained stable. These results confirmed that global species range shifts of marine species do not necessarily translate into species richness variation over time (Dornelas et al., 2014) or into taxonomic homogenization of communities (McKinney & Lockwood, 1997).

### *4.2 Abundance-based biodiversity indices*

Temporal trends of abundance-based diversity patterns revealed contrasted pictures at regional and local scale. At regional scale, in agreement with our expectation, abundance-based indices provided clear temporal trends. Abundance of the demersal communities decreased over the time series and abundance-based dissimilarity measures indicated a differentiation among communities, which was mostly driven by the balanced variation of abundance. This implies that abundant species in one community were replaced by other species in other communities and this mechanism of replacement increased over the years. The balanced variation in abundance has been previously investigated through the compensation mechanism explained by the replacement of the most sensitive species to a disturbance (such as fishing) by less sensitive species (Rochet et al., 2013). In a spatial context, an increasing compensation mechanism may be related to increasing variation in abundance among species present in different locations. Over large spatial and temporal scales, such patterns might be caused by fishing and predator-prey interactions that generate fluctuating abundance among prey and predators such as suggested between hake and horse mackerel in the BoB (Moullec et al., 2017).

On the other hand, at local scale, abundance-based patterns were more patchy than incidence-based patterns and we did not detect clear ecosystem dynamics as expected. Higher abundances were detected in the CS compared to the BoB (for similar results see Moullec et al., 2017), abundances remained stable over time for most rectangles (73%) and a majority of species (72%) showed stable abundances over the study period (see Table S25). We noticed that our simple estimate of the general temporal trend of the abundance can differ from the more detailed trends reported by ICES for several commercial stocks on larger spatial scales than considered here using additional data sets (e.g. *Lophius budegassa* and *L. piscatorius, ICES, 2020*). However, despite EVHOE surveys might have different catchability for part of the population (adults or juveniles) of certain species, our results, based on abundance, are in line with published results showing that overall fish biomass of most European seas has not yet recovered during the last two decades (Gascuel et al., 2016). Over time, the balanced variation in abundance among communities increased in coastal rectangles of the southern BoB and along the Welsh coast of the CS, showing an increasing exchange of individuals belonging to different species among communities. However, it remains unclear how much of this

increase is also driven by the influence of species turnover on the balanced variation in abundance as the two components are not independent (Baselga, 2013). Disentangling the contributions of balanced variations in abundance and abundance gradients to species turnover and nestedness is beyond the scope of this study but merits further research. Finally, not only incidence but also abundance-based indices revealed greater spatial than temporal variation of community dynamics, which confirmed previous findings for the Celtic Sea (Mérillet et al., 2019) and the Bay of Biscay (Poulard et al., 2003). Overall, the local patterns may have suffered from high variability in the sampling process (see section 4.4), which is unlikely to be improved if bottom trawl remains the main sampling technique as it is influenced by meteorological conditions while sampling (Poulard & Trenkel, 2007).

### *4.3 Evidence for trophic drivers of regional and local-scale biodiversity patterns*

Observed spatial patterns of community re-organisations were mainly explained by variables describing energy (14.9% Table 2) rather than habitat and fishing. These results contradict our second expectation, even though the variance explained by these models remained low (25% Table 2). Accounting for the remaining temporal and spatial autocorrelation improved the predictive power of all models (Table S4-S14) which suggests that we may be currently missing covariates, or that fine scale variability has not yet been captured. Considering the huge source of uncertainty (see section 4.4 for details) associated with long-term ecological surveys (Cauvy-Fraunié, et al., 2020), what looks at first as a deceptive model fit, could yet provide first insights into the main drivers.

We found that among energy variables, both diversity and abundance of the small pelagics were the most important variables, while temperature and primary production had limited explanatory power. These results suggest that productive energy, especially the bentho-pelagos trophic link (Cury et al., 2000) could be an important driver of the studied demersal community dynamics. The increasing diversity of small pelagic species and their abundance favoured the differentiation among demersal communities, while the abundance of small pelagics was positively related to the abundance of demersal species. These results may be related to positive predator-prey interactions allowing demersal predators to increase in abundance following increasing pelagic abundance (Moullec et al., 2017). These predator-prey interactions might be partly driven by the strong recovery of *Engraulis encrasicolus* since 2005 (Fig. S13) and the high biomass of pelagic species in general in the BoB supported by high pelagic primary production (Cresson et al., 2020). If pelagic species constitute a large proportion of trophic resources consumed by the demersal community, variation in pelagic species abundance could significantly affect the variations in the abundance of demersal species as well. An indirect relationship driven by the productivity of benthic communities (Lassalle et al., 2011) is also possible but could not be tested here. Our results do not confirm the role of rising temperatures as the main driver of taxonomic re-organisation as suggested for ecosystems elsewhere (Magurran et

al., 2015; McLean et al., 2019). However, our analysis of environmental forcing on temporal variations of LBD.jtu revealed that decreasing temperature seasonality favoured taxonomic differentiation (southern BoB), while increasing temperature seasonality favoured taxonomic homogenization (CS; Fig. S13 and additional results in *Supplementary material S2.3*). Nevertheless, because the temporal trends in temperature seasonality remained non-significant, such results might be too preliminary to be attributed to global change yet (see Fig. S14).

Concerning habitat, we confirmed that bathymetry, water stratification (mixed layer depth), and distance to the coast were important drivers of the spatial distribution of marine biodiversity, specifically the importance of shallow coastal habitat with a thin mixed layer depth (Ray, 1991; Poulard et al., 2003; Leathwick et al., 2006; Tittensor et al., 2010; Seitz et al., 2014).

The limited contribution of fishing pressure might be explained by the long fishing history that may have selected the most resilient species and shaped adaptable communities (Blanchard et al., 2004; McLean et al., 2019). Indeed, the BoB and the CS have been impacted by fishing for over a century (Quéro & Cendrero, 1996; Thurstan et al., 2010; Moullec et al., 2017) and this constant pressure on species communities may have been detectable at the beginning of the exploitation (Pauly, 1995; Lotze & Worm, 2009) but difficulties to pinpoint fishing as the main driver based on recent (i.e. two decades) scientific surveys is common for areas with a long fishing history (Farriols et al., 2017; Mérillet et al., 2019). Indeed, BoB ecosystem components in the early 1990s were considered widely impacted by fishing and locally by other human activities (Lorance et al., 2009; Gascuel et al., 2016).

Overall, the negligible effect of the tested time lags for environmental variables suggests a rapid biological response of communities to the environment, as previously shown for small pelagic species (Huret et al., 2018). One exception though was the two year lag for the minimum thickness of the mixed layer depth (MLD.min) for LBD indices suggesting a multiannual effect of water stratification on the change in species abundance among communities (LBD.ruz.bal), though the causal mechanism remains unknown.

### *4.4 Some limitations of long-term ecological surveys*

Long-term ecological surveys (LTES) are key to document temporal dynamics (Kuebbing et al., 2018), but their drawbacks should also be considered. First, variations in sampling effort over time or space are likely especially for LTES carried out over large spatial or temporal scales such as fish stock surveys (Trenkel & Cotter, 2009). For the EVHOE time series, it was crucial to use a sample-based rarefaction approach with resampling (e.g. Dornelas et al., 2014; Magurran et al., 2015; Blowes et al., 2019; Antão et al., 2020), to avoid temporal sampling bias that might lead to an artificial increase in species richness. Second, variations in species identification due to inherent progress in taxonomy, and/or knowledge differences among scientific staff represent another source of bias that

must be accounted for. Here, we homogenised the species list over the time series by lumping taxa that could have been misidentified during the early years of the survey. As a consequence, all detected patterns are expected to be robust and may have been even stronger if a greater precision in species identification would have been available from the start of the time series. Finally, the accumulation of sources of uncertainty in LTES often leads to weak signal to noise ratios (Cauvy-Fraunier et al., 2020). For example, the EVHOE survey is carried out during a transitional period, shifting from autumn to winter conditions with storms and high wind stress. These climatic conditions can affect the variation in catchability among species (Poulard & Trenkel, 2007) and thus impact species composition and abundance of the catch. Changes in gear catchability creating a biased representation of communities and species abundance is a frequent concern of bottom trawl surveys such as EVHOE (Poulard & Trenkel, 2007). Further, trawl selectivity is size-dependent (Krag et al., 2014). However, the main advantage of these surveys is that sampling is standardised and constant throughout the time series. Indeed, the sampling period (October-December), gear (GOV 36/47), tow duration (30 minutes) and trawl speed (7.4 $km.h^{-1}$) remained the same during the whole campaign and over the years (Laffargue et al., 2021). Hence, we believe that the identified strong multi-annual trends convey a genuine biological signal of change. The EVHOE data set has already been used (e.g. Merillet et al., 2019), as have other similar surveys, to derive indicators of diversity (including abundance), and ecological status (e.g. Rufino et al., 2018, Mahé et al., 2018). Despite those different sources of uncertainty and bias, the different conservative solutions applied in this study enabled us to detect spatio-temporal variations of community composition and reassert the crucial role of standardised LTES to understand community dynamics in a fast-evolving environment.

### 4.5 Conclusion

A suite of complementary biodiversity indices based on scientific surveys allowed us to capture spatio-temporal community dynamics at different spatial scales. The stability of species richness, and the increasing composition dissimilarities at regional scale for abundance-based indices, hid a spatially contrasted pattern of taxonomic homogenization and differentiation for communities within the Celtic Sea and the southern Bay of Biscay, respectively. Abundance-based indices showed stronger temporal patterns at regional scale and confirmed higher abundance in the Celtic Sea than in the Bay of Biscay. However, at a local scale, abundance-based indices might be powerful to detect early changes in community dynamics only if new sampling approaches (e.g. environmental DNA; Stoeckle et al., 2020) can control and reduce the variability in the sampling process. Our modelling approach revealed greater spatial than temporal variation and a larger contribution of energy, followed by habitat, while fishing pressure had a very limited contribution. Furthermore, we showed

that the benthо-pelagos trophic link (Moullec et al., 2017; Cresson et al., 2020) had a greater influence on community dynamics of demersal species than changes in sea temperature (Magurran et al., 2015). By applying methods inspired by biogeography and community ecology to a scientific survey data set, our study paved the way to better disentangle and explain the subtle dynamics of communities and their drivers for ecosystems providing crucial services.

## DATA AVAILABILITY STATEMENT

The original biological data as DATRAS files are available at: https://www.ices.dk/data/data-portals/Pages/DATRAS.aspx

The curated data set used in this study will be available in DRYAD upon acceptance and is currently available at: https://drive.google.com/drive/folders/14aK1ADQiwGalsNdx9owca15qALK-toLx?usp=sharing

## DECLARATION OF COMPETING INTERESTS

The authors declare that they have no conflict of interest.

## REFERENCES

Albouy, C., Guilhaumon, F., Araújo, M.B., Mouillot, D. & Leprieur, F. (2012). Combining projected changes in species richness and composition reveals climate change impacts on coastal Mediterranean fish assemblages. *Global Change Biology,* **18**, 2995–3003. https://doi.org/10.1111/j.1365-2486.2012.02772.x

Antão, L.H., Bates, A.E., Blowes, S.A., Waldock, C., Supp, S.R., Magurran, A.E., Dornelas, M. & Schipper, A.M. (2020). Temperature-related biodiversity change across temperate marine and terrestrial systems. *Nature Ecology and Evolution*, **4**, 927–933. https://doi.org/10.1038/s41559-020-1185-7

Baselga, A. (2017). Partitioning abundance-based multiple-site dissimilarity into components: balanced variation in abundance and abundance gradients. *Methods in Ecology and Evolution,* **8**, 799–808. https://doi.org/https://doi.org/10.1111/2041-210X.12693

Baselga, A. (2013). Separating the two components of abundance-based dissimilarity: balanced changes in abundance vs. abundance gradients. *Methods in Ecology and Evolution,* **4**, 552–557. https://doi.org/https://doi.org/10.1111/2041-210X.12029

Baselga, A. (2012). The relationship between species replacement, dissimilarity derived from nestedness, and nestedness. *Global Ecology and Biogeography*, **21**, 1223–1232. https://doi.org/10.1111/j.1466-8238.2011.00756.x

Baudron, A.R., Brunel, T., Blanchet, M.-A., Hidalgo, M., Chust, G., Brown, E.J., Kleisner, K.M., Millar, C., MacKenzie, B.R., Nikolioudakis, N., Fernandes, J.A. & Fernandes, P.G. (2020). Changing fish distributions challenge the effective management of European fisheries. *Ecography*, **43**, 494–505. https://doi.org/https://doi.org/10.1111/ecog.04864

Bauman, D., Drouet, T., Fortin, M.-J. & Dray, S. (2018). Optimizing the choice of a spatial weighting matrix in eigenvector-based methods. *Ecology,* **99**, 2159–2166. https://doi.org/https://doi.org/10.1002/ecy.2469

Blanchard, F., LeLoc'h, F., Hily, C. & Boucher, J. (2004). Fishing effects on diversity, size and community structure of the benthic invertebrate and fish megafauna on the Bay of Biscay coast of France. *Marine Ecology Progress Series*, **280**: 249–260

Blowes, S.A., Supp, S.R., Antão, L.H., Bates, A., Bruelheide, H., Chase, J.M., Moyes, F., Magurran, A., McGill, B., Myers-Smith, I.H., Winter, M., Bjorkman, A.D., Bowler, D.E., Byrnes, J.E.K., Gonzalez, A., Hines, J., Isbell, F., Jones, H.P., Navarro, L.M., Thompson, P.L., Vellend, M., Waldock, C., Dornelas, M. (2019). The geography of biodiversity change in marine and terrestrial assemblages. *Science,* **366**, 339 – 345. https://doi.org/10.1126/science.aaw1620

Bonn, A., Storch, D. & Gaston, K.J., (2004). Structure of the species-energy relationship. *Proceedings of the Royal Society B Biological Science* **271**, 1685–1691. https://doi.org/10.1098/rspb.2004.2745

Britten, G.L., Dowd, M., Kanary, L. & Worm, B. (2017). Extended fisheries recovery timelines in a changing environment. *Nature Communication,* **8**, 15325. https://doi.org/10.1038/ncomms15325

Brown, J.H., Gillooly, J.F., Allen, A.P., Savage, V.M. & West, G.B., (2004). Toward a Metabolic theory of ecology. *Ecology,* **85**, 1771–1789.

Burgess, M.G., Polasky, S. & Tilman, D. (2013). Predicting overfishing and extinction threats in multispecies fisheries. *Proceedings of the National Academy of Sciences*, **110**, 15943 – 15948. https://doi.org/10.1073/pnas.1314472110

Cauvy-Fraunié, S., Trenkel, V.M., Daufresne, M., Maire, A., Capra, H., Olivier, J.-M., Lobry, J., Cazelles, B. & Lamouroux, N. (2019). Interpretation of interannual variability in long-term aquatic ecological surveys. *Canadian Journal of Fisheries and Aquatic Sciences*, **77**, 894–903. https://doi.org/10.1139/cjfas-2019-0146

Chase, J.M., McGill, B.J., Thompson, P.L., Antão, L.H., Bates, A.E., Blowes, S.A., Dornelas, M., Gonzalez, A., Magurran, A.E., Supp, S.R., Winter, M., Bjorkman, A.D., Bruelheide, H., Byrnes, J.E.K., Cabral, J.S., Elahi, R., Gomez, C., Guzman, H.M., Isbell, F., Myers-Smith, I.H., Jones, H.P., Hines, J., Vellend, M., Waldock, C. & O'Connor, M. (2019). Species richness change across spatial scales. *Oikos*, **128**, 1079–1091. https://doi.org/https://doi.org/10.1111/oik.05968

Chust, G., Borja, Á., Caballero, A., Irigoien, X., Sáenz, J., Moncho, R., Marcos, M., Liria, P., Hidalgo, J., Valle, M. & Valencia, V. (2011). Climate change impacts on coastal and pelagic

environments in the southeastern Bay of Biscay. *Climate Research*, **48**, 307–332.

Clarke, A., Gaston, K.J., 2006. Climate, energy and diversity. *Proceedings of the Royal Society B Biological Science,* **273**, 2257–2266. https://doi.org/10.1098/rspb.2006.3545

Cresson, P., Chouvelon, T., Bustamante, P., Bănaru, D., Baudrier, J., Le Loc'h, F., Mauffret, A., Mialet, B., Spitz, J., Wessel, N., Briand, M.J., Denamiel, M., Doray, M., Guillou, G., Jadaud, A., Lazard, C., Prieur, S., Rouquette, M., Saraux, C., Serre, S., Timmerman, C.-A., Verin, Y. & Harmelin-Vivien, M. (2020). Primary production and depth drive different trophic structure and functioning of fish assemblages in French marine ecosystems. *Progress in Oceanography,* **186**, 102343. https://doi.org/https://doi.org/10.1016/j.pocean.2020.102343

Cribari-Neto, F. & Zeileis, A. (2010). Beta Regression in R. J. Stat. Software, Artic. **34**, 1–24. https://doi.org/10.18637/jss.v034.i02

Cury, P., Bakun, A., Crawford, R., Jarre, A., Quiñones, R., Shannon, L. & Verheye, H.M. (2000). Small pelagics in upwelling systems: patterns of interaction and structural changes in "wasp-waist" ecosystems. *ICES Journal of Marine Science*, **57**, 603–618.

Cusens, J., Wright, S.D., McBride, P.D. & Gillman, L.N. (2012). What is the form of the productivity–animal-species-richness relationship? A critical review and meta-analysis. *Ecology,* **93**, 2241–2252. https://doi.org/https://doi.org/10.1890/11-1861.1

Demanèche, S., Bégot, E., Goüello, A., Campéas, A., Habasque, J., Merrien, C., Leblond, E., Berthou, P., , Harscoat, V., Fritsch, N., Leneveu, C., & Laurans, M. (2013). Projet SACROIS «IFREMER/DPMA» V 3.2.5 – 11/2013, France: Ifremer.

Doray, M., Petitgas, P., Romagnan, J.B., Huret, M., Duhamel, E., Dupuy, C., Spitz, J., Authier, M., Sanchez, F., Berger, L., Dorémus, G., Bourriau, P., Grellier, P. & Massé, J. (2018). The PELGAS survey: Ship-based integrated monitoring of the Bay of Biscay pelagic ecosystem. *Progress in Oceanography,* **166**, 15–29. https://doi.org/https://doi.org/10.1016/j.pocean.2017.09.015

Dornelas, M., Gotelli, N.J., McGill, B., Shimadzu, H., Moyes, F., Sievers, C. & Magurran, A.E. (2014). Assemblage Time Series Reveal Biodiversity Change but Not Systematic Loss. *Science,* **344**, 296 – 299. https://doi.org/10.1126/science.1248484

Dornelas, M., Gotelli, N.J., Shimadzu, H., Moyes, F., Magurran, A.E. & McGill, B.J. (2019). A balance of winners and losers in the Anthropocene. *Ecology Letters,* **22**, 847–854. https://doi.org/https://doi.org/10.1111/ele.13242

Dray, S., Pélissier, R., Couteron, P., Fortin, M.-J., Legendre, P., Peres-Neto, P.R., Bellier, E.,

Blvand, K., Blanchet, F.G., De Cáceres, M., Dufour, A.-B., Heegaard, E., Jombart, T., Muñoz, F., Oksanen, J., Thioulouse, J. & Wagner, H.H. (2012). Community ecology in the age of multivariate multiscale spatial analysis. *Ecological Monographs,* **82**, 257–275. https://doi.org/https://doi.org/10.1890/11-1183.1

Dye, S., Hughes, S.L., Tinker, J., Berry, D.I., Holliday, N.P., Kent, E.C., Kennington, K., Inall, M., Smythe, T., Nolan, G., Lyons, K., Andres, O. & Beszczynska-Möller, A. (2013). Impacts of climate change on temperature (air and sea), in: Buckley, P.J., Baxter, J.M., Wallace, C.J. (Eds.), Marine Climate Change Impacts Partnership Science Review 2013. MCCIP Secretariat.

Efron, B. (1978). Regression and ANOVA with zero-one data: Measures of residual variation. *Journal of the American Statistical Association*, **73**, 113-121.

Evans, K.L., Warren, P.H. & Gaston, K.J. (2005). Species–energy relationships at the macroecological scale: a review of the mechanisms. *Biological Reviews,* **80**, 1–25. https://doi.org/10.1017/S1464793104006517

Ferrari, S. & Cribari-Neto, F. (2004). Beta Regression for Modelling Rates and Proportions. *Journal of Apply Statistic*, **31**, 799–815. https://doi.org/10.1080/0266476042000214501

Farriols, M.T., Ordines, F., Somerfield, P.J., Pasqual, C., Hidalgo, M., Guijarro, B., Massutí, E., 2017. Bottom trawl impacts on Mediterranean demersal fish diversity: Not so obvious or are we too late? *Continental Shelf Research,* **137**, 84–102. https://doi.org/https://doi.org/10.1016/j.csr.2016.11.011

Gascuel, D., Coll, M., Fox, C., Guénette, S., Guitton, J., Kenny, A., Knittweis, L., Nielsen, J.R., Piet, G., Raid, T., Travers-Trolet, M. & Shephard, S. (2016). Fishing impact and environmental status in European seas: a diagnosis from stock assessments and ecosystem indicators. *Fish and Fisheries,* **17**, 31–55. https://doi.org/https://doi.org/10.1111/faf.12090

Grueber, C.E., Nakagawa, S., Laws, R.J., Jamieson, I.G., 2011. Multimodel inference in ecology and evolution: Challenges and solutions. *Journal of Evolutionary Biology,* **24**, 699–711. https://doi.org/10.1111/j.1420-9101.2010.02210.x

Hermant, M., Lobry, J., Bonhommeau, S., Poulard, J.-C. & Le Pape, O. (2010). Impact of warming on abundance and occurrence of flatfish populations in the Bay of Biscay (France). *Journal of Sea Research*, **64**, 45–53. https://doi.org/https://doi.org/10.1016/j.seares.2009.07.001

Hily, C., Le Loc'h, F., Grall, J. & Glémarec, M. (2008). Soft bottom macrobenthic communities of

North Biscay revisited: Long-term evolution under fisheries-climate forcing. *Estuarine, Coastal and Shelf Science*, **78**, 413–425. https://doi.org/https://doi.org/10.1016/j.ecss.2008.01.004

Hosack, G.R. & Trenkel, V.M. (2019). Functional group based marine ecosystem assessment for the Bay of Biscay via elasticity analysis. *PeerJ,* **7**, e7422. https://doi.org/10.7717/peerj.7422

Huret, M., Bourriau, P., Doray, M., Gohin, F. & Petitgas, P. (2018). Survey timing vs. ecosystem scheduling: Degree-days to underpin observed interannual variability in marine ecosystems. *Progress in Oceanography*, **166**, 30–40. https://doi.org/https://doi.org/10.1016/j.pocean.2017.07.007

Hurlbert, S. H. (1971). The nonconcept of species diversity: a critique and alternative parameters. *Ecology*, **52**, 577–586

Hutchings, J.A., Minto, C., Ricard, D., Baum, J.K. & Jensen, O.P. (2010). Trends in the abundance of marine fishes. *Canadian Journal of Fisheries and Aquatic Sciences*, **67**, 1205–1210. https://doi.org/10.1139/F10-081

ICES, (2017). Report of the Working Group for the Bay of Biscay and Iberian waters Ecoregion (WGBIE), 4-11 May 2017, Cadiz, Spain. ICES CM 2017/ACOM:12. 552pp
ICES, (2019). Maps and spatial information. https://www.ices.dk/data/maps/Pages/default.aspx

ICES (2020). Working Group for the Bay of Biscay and the Iberian Waters Ecoregion (WGBIE). ICES Scientific Reports 2:49: 845 pp.

Iglésias, S.P. & Lorance, P. (2016). First record of Pagellus bellottii (Teleostei: Sparidae) in the Bay of Biscay, France. *Marine Biodiversity Records*, **9**, 16. https://doi.org/10.1186/s41200-016-0007-8

Jaccard, P. (1912). The distribution of the flora in the alpine zone. *New Phytologist*, **11**, 37–50.

Jaeger, B.C., Edwards, L.J., Das, K., Sen, P.K., 2017. An R2 statistic for fixed effects in the generalized linear mixed model. *Journal of Applied Statistics,* **44**, 1086–1105. https://doi.org/10.1080/02664763.2016.1193725

Koenigstein, S., Mark, F.C., Gößling-Reisemann, S., Reuter, H. & Poertner, H.-O. (2016). Modelling climate change impacts on marine fish populations: process-based integration of ocean warming, acidification and other environmental drivers. *Fish & Fisheries* **17**, 972–1004. https://doi.org/https://doi.org/10.1111/faf.12155

Krag, L.A., Herrmann, B., Karlsen, J.D., 2014. Inferring Fish Escape Behaviour in Trawls Based on Catch Comparison Data: Model Development and Evaluation Based on Data from Skagerrak,

Denmark. *PLoS One,* **9**, e88819. https://doi.org/10.1371/journal.pone.0088819

Kuebbing, S.E., Reimer, A.P., Rosenthal, S.A., Feinberg, G., Leiserowitz, A., Lau, J.A. & Bradford, M.A. (2018). Long-term research in ecology and evolution: a survey of challenges and opportunities. *Ecological Monographs*, **88**, 245–258. https://doi.org/https://doi.org/10.1002/ecm.1289

Laffargue, P., Delaunay, D., Badts, V., Berthele, O., Cornou, A-S., & Garren, F. (2021). Fish and cephalopods monitoring on the Bay of Biscay and the Celtic Sea continental shelves. *Earth System Science Data Discussion*, [preprint] https://doi.org/10.5194/essd-2021-146, in review, 2021.

Lassalle, G., Lobry, J., Le Loc'h, F., Bustamante, P., Certain, G., Delmas, D., Dupuy, C., Hily, C., Labry, C., Le Pape, O., Marquis, E., Petitgas, P., Pusineri, C., Ridoux, V., Spitz, J. & Niquil, N. (2011). Lower trophic levels and detrital biomass control the Bay of Biscay continental shelf food web: Implications for ecosystem management. *Progress in Oceanography*, **91**, 561–575. https://doi.org/https://doi.org/10.1016/j.pocean.2011.09.002

Leathwick, J.R., Elith, J., Francis, M.P., Hastie, T. & Taylor, P. (2006). Variation in demersal fish species richness in the oceans surrounding New Zealand : an analysis using boosted regression trees. *Marine Ecology Progress Series,* **321**, 267–281.

Legendre, P. & Gauthier, O. (2014). Statistical methods for temporal and space–time analysis of community composition data. *Proceedings of the Royal Society B Biological Science*, **281**, 20132728. https://doi.org/10.1098/rspb.2013.2728

Legendre, P. &, Legendre, L. (1998). Numerical Ecology, 2nd Edition. Elsevier, Amsterdam.

Leprieur, F., Beauchard, O., Hugueny, B., Grenouillet, G. & Brosse, S. (2008). Null model of biotic homogenization: a test with the European freshwater fish fauna. *Diversity and Distribution*, **14**, 291–300. https://doi.org/10.1111/j.1472-4642.2007.00409.x

Lorance, P., Bertrand, J.A., Brind'Amour, A., Rochet, M.-J. & Trenkel, V.M. (2009). Assessment of impacts from human activities on ecosystem components in the Bay of Biscay in the early 1990s. *Aquatic Living Resources,* **22**, 409–431.

Lotze, H.K. & Worm, B. (2009). Historical baselines for large marine animals. *Trends in Ecology and Evolution*, **24**, 254–262. https://doi.org/10.1016/j.tree.2008.12.004

Le Marchand, M., Hattab, T., Niquil, N., Albouy, C., LeLoc'h, F., & Ben Rais Lasram, F. (2020). Climate change in the Bay of Biscay: Changes in spatial biodiversity patterns could be driven by the arrivals of southern species. *Marine Ecology Progress Series,* **647**, 17–31.

https://doi.org/10.3354/meps13401

Magurran, A.E., Dornelas, M., Moyes, F., Gotelli, N.J. & McGill, B. (2015). Rapid biotic homogenization of marine fish assemblages. *Nature Communication*, **6**, 8405. https://doi.org/10.1038/ncomms9405

Magurran, A.E., Dornelas, M., Moyes, F. & Henderson, P.A. (2019). Temporal β diversity—A macroecological perspective. *Global Ecology and Biogeography*, **28**, 1949–1960. https://doi.org/10.1111/geb.13026

Mahé, K., Bellamy, E., Delpech, J.P., Lazard, C., Salaun, M., Vérin, Y., Coppin, F., Travers-Trolet, M., 2018. Evidence of a relationship between weight and total length of marine fish in the North-eastern Atlantic Ocean: physiological, spatial and temporal variations. *Journal of the Marine Biological Association of the United Kingdom,* **98**, 617–625. https://doi.org/DOI: 10.1017/S0025315416001752

McGill, B.J., Dornelas, M., Gotelli, N.J. & Magurran, A.E. (2015). Fifteen forms of biodiversity trend in the Anthropocene. *Trends in Ecology and Evolution*, **30**, 104–113. https://doi.org/10.1016/j.tree.2014.11.006

McKinney, M.L. & Lockwood, J.L. (1999). Biotic homogenization: a few winners replacing many losers in the next mass extinction. *Trends in Ecology and Evolution*, **14**, 450–453. https://doi.org/https://doi.org/10.1016/S0169-5347(99)01679-1

McLean, M., Mouillot, D., Lindegren, M., Villéger, S., Engelhard, G., Murgier, J. & Auber, A. (2019). Fish communities diverge in species but converge in traits over three decades of warming. *Global Change Biology*, **25**, 3972–3984. https://doi.org/10.1111/gcb.14785

Mérillet, L., Kopp, D., Robert, M., Mouchet, M. & Pavoine, S. (2020). Environment outweighs the effects of fishing in regulating demersal community structure in an exploited marine ecosystem. *Global Change Biology*, **26**, 2106–2119. https://doi.org/10.1111/gcb.14969

Michel, S., Vandermeirsch, F. & Lorance, P. (2009). Evolution of upper layer temperature in the Bay of Biscay during the last 40 years. *Aquatic Living Resources*, **22**, 447–461.

Moullec, F., Gascuel, D., Bentorcha, K., Guénette, S. & Robert, M. (2017). Trophic models: What do we learn about Celtic Sea and Bay of Biscay ecosystems? *Journal of Marine System*, **172**, 104–117. https://doi.org/https://doi.org/10.1016/j.jmarsys.2017.03.008

Muff, S., Nilsen, E.B., O'Hara, R.B. & Nater, C.R. (2021). Rewriting results sections in the

language of evidence. *Trends in Ecology and Evolution*, [in press] https://doi.org/10.1016/j.tree.2021.10.009

Nakagawa, S., Johnson, P.C.D. & Schielzeth, H. (2017). The coefficient of determination R(2) and intra-class correlation coefficient from generalized linear mixed-effects models revisited and expanded. *Journal of the Royal Society Interface*, **14**. https://doi.org/10.1098/rsif.2017.0213

Olden, J.D. (2006). Biotic homogenization: a new research agenda for conservation biogeography. *Journal of Biogeography*, **33**, 2027–2039. https://doi.org/https://doi.org/10.1111/j.1365-2699.2006.01572.x

Palter, J.B. (2015). The role of the Gulf Stream in European climate. *Annual review of marine science*, **7**, 113–137. https://doi.org/10.1146/annurev-marine-010814-015656

Pauly, D. (1995). Anecdotes and the shifting baseline syndrome of fisheries. *Trends in Ecology and Evolution*, **10**, 430. https://doi.org/10.1016/s0169-5347(00)89171-5

Pauly, D., Watson, R. & Alder, J. (2005). Global trends in world fisheries: impacts on marine ecosystems and food security. *Philosophical transactions of the Royal Society of London. Series B, Biological sciences,* **360**, 5–12. https://doi.org/10.1098/rstb.2004.1574

Pecl, G.T., Araújo, M.B., Bell, J.D., Blanchard, J., Bonebrake, T.C., Chen, I.-C., Clark, T.D., Colwell, R.K., Danielsen, F., Evengård, B., Falconi, L., Ferrier, S., Frusher, S., Garcia, R.A., Griffis, R.B., Hobday, A.J., Janion-Scheepers, C., Jarzyna, M.A., Jennings, S., Lenoir, J., Linnetved, H.I., Martin, V.Y., McCormack, P.C., McDonald, J., Mitchell, N.J., Mustonen, T., Pandolfi, J.M., Pettorelli, N., Popova, E., Robinson, S.A., Scheffers, B.R., Shaw, J.D., Sorte, C.J.B., Strugnell, J.M., Sunday, J.M., Tuanmu, M.-N., Vergés, A., Villanueva, C., Wernberg, T., Wapstra, E. & Williams, S.E. (2017). Biodiversity redistribution under climate change: Impacts on ecosystems and human well-being. *Science,* **355**, https://doi.org/10.1126/science.aai9214

Pérez, M.-E. & Pericchi, L.R. (2014). Changing Statistical Significance with the Amount of Information: The Adaptive α Significance Level. *Statistical and Probability Letter,* **85**, 20–24. https://doi.org/10.1016/j.spl.2013.10.018

Pershon C., Lorance, P. & Trenkel, V.M. (2009). Habitat preferences of selected demersal fish species in the Bay of Biscay and Celtic Sea, North-East Atlantic. *Fisheries Oceanography*, **18**, 268–285. https://doi.org/https://doi.org/10.1111/j.1365-2419.2009.00515.x

Planque, B., Fromentin, J.-M., Cury, P., Drinkwater, K.F., Jennings, S., Perry, R.I. & Kifani, S. (2010). How does fishing alter marine populations and ecosystems sensitivity to climate? *Journal of*

*Marine System*, **79**, 403–417. https://doi.org/10.1016/j.jmarsys.2008.12.018

Poulard, J.-C. & Blanchard, F. (2005). The impact of climate change on the fish community structure of the eastern continental shelf of the Bay of Biscay. *ICES Journal of Marine Science*, **62**, 1436–1443. https://doi.org/10.1016/j.icesjms.2005.04.017

Poulard, J.-C. & Trenkel, V.M. (2007). Do survey design and wind conditions influence survey indices? *Canadian journal of fisheries and aquatic sciences*, **64**, 1551–1562. https://doi.org/10.1139/f07-123

Poulard, J.C., Blanchard, F., Boucher, J. & Souissi, S. (2003). Variability in the demersal fish assemblages of the Bay of Biscay during the 1990s. *ICES Journal of Marine Science*, **219**, 411-414.

Quéro, J.-C., Cendrero, O., 1996. Incidence de la pêche sur la biodiversité ichtyologique marine du bassin d'Arcachon et du plateau continental sud Gascogne. *Cybium,* **20**, 323–356.

Ray, G.C., 1991. Coastal-Zone Biodiversity Patterns. *Bioscience,* **41**, 490–498. https://doi.org/10.2307/1311807

Rochet, M.-J., Collie, J.S. & Trenkel, V. (2013). How Do Fishing and Environmental Effects Propagate Among and Within Functional Groups? *Bulletin of Marine Science*, **89**, 285–315. https://doi.org/10.5343/bms.2011.1138

Rufino, M.M., Bez, N., Brind'Amour, A., 2018. Integrating spatial indicators in the surveillance of exploited marine ecosystems. PLoS One, **13**, e0207538. https://doi.org/10.1371/journal.pone.0207538

Ruzicka, M. (1958). Anwendung mathematisch-statistiker Methoden in Geobotanik (Synthetische Bearbeitung von Aufnahmen). *Biologia*,**13**, 647–661.

Santini, L., Belmaker, J., Costello, M.J., Pereira, H.M., Rossberg, A.G., Schipper, A.M., Ceauşu, S., Dornelas, M., Hilbers, J.P., Hortal, J., Huijbregts, M.A.J., Navarro, L.M., Schiffers, K.H., Visconti, P. & Rondinini, C. (2017). Assessing the suitability of diversity metrics to detect biodiversity change. *Biological Conservation*, **213**, 341–350. https://doi.org/https://doi.org/10.1016/j.biocon.2016.08.024

Scientific, Technical and Economic Committee for Fisheries (STECF) 2018. Fisheries Dependent Information – New FDI (STECF-18-11). Publications Office of the European Union, Luxembourg, ISBN 978-92-79-79394-3, doi:10.2760/696153, JRC114717

Seitz, R.D., Wennhage, H., Bergström, U., Lipcius, R.N., Ysebaert, T., (2014). Ecological value of

coastal habitats for commercially and ecologically important species. *ICES Journal of Marine Science,* **71**, 648–665. https://doi.org/10.1093/icesjms/fst152

Shannon, C.E. (1948). A mathematical theory of communication. Bell System Technical Journal, **27**, 379– 423

Shapiro, S.S. & Wilk, M.B. (1965). An analysis of variance test for normality (complete samples). *Biometrika*, **52**, 591–611.

Stoeckle, M.Y., Adolf, J., Charlop-Powers, Z., Dunton, K.J., Hinks, G. & VanMorter, S.M. (2020). Trawl and eDNA assessment of marine fish diversity, seasonality, and relative abundance in coastal New Jersey, USA. *ICES Journal of Marine Science*, **78**, 293 - 304. https://doi.org/10.1093/icesjms/fsaa225

Thurstan, R.H., Brockington, S. & Roberts, C.M. (2010). The effects of 118 years of industrial fishing on UK bottom trawl fisheries. *Nature Communication*, **1**, 15. https://doi.org/10.1038/ncomms1013

Tilman, D., Clark, M., Williams, D.R., Kimmel, K., Polasky, S. & Packer, C. (2017). Future threats to biodiversity and pathways to their prevention. *Nature,* **546**, 73–81. https://doi.org/10.1038/nature22900

Tittensor, D.P. & Worm, B. (2016). A neutral-metabolic theory of latitudinal biodiversity. *Global Ecology and Biogeography,* **25**, 630–641. https://doi.org/https://doi.org/10.1111/geb.12451

Tittensor, D.P., Mora, C., Jetz, W., Lotze, H.K., Ricard, D., Berghe, E. Vanden & Worm, B. (2010). Global patterns and predictors of marine biodiversity across taxa. *Nature,* **466**, 1098–1101. https://doi.org/10.1038/nature09329

Trenkel, V.M. & Cotter, J. (2009). Choosing survey time series for populations as part of an ecosystem approach to fishery management. *Aquatic Living Resources*, **22**, 121–126.

Valentine, J.W. & Jablonski, D. (2015). A twofold role for global energy gradients in marine biodiversity trends. *Journal of Biogeography,* **42**, 997–1005. https://doi.org/https://doi.org/10.1111/jbi.1251

Vellend, M., 2010. Conceptual synthesis in community ecology. *The Quarterly review of biology*, **85**, 183–206.

Whittaker, R. H. (1972). Evolution and Measurement of Species Diversity. *Taxon*, **21**, 213-251.

Woolley, S.N.C., Tittensor, D.P., Dunstan, P.K., Guillera-Arroita, G., Lahoz-Monfort, J.J., Wintle, B.A., Worm, B. & O'Hara, T.D. (2016). Deep-sea diversity patterns are shaped by energy availability. *Nature,* **533**, 393–396. https://doi.org/10.1038/nature17937
Wright, D. H. (1983). Species-energy theory: an extension of the species-area theory. *Oikos*, **41**, 496-506.

Zou, H. & Hastie, T. (2005). Regularization and variable selection via the elastic net. *Journal of the Royal Statistical Society Series B*, **67**, 301–320. https://doi.org/https://doi.org/10.1111/j.1467-9868.2005.00503.x

Zuur, A.F., Ieno, E.N. & Smith, G.M. (2007). Analysing ecological data. Springer-Verlag, New York

Zuur, A.F., Ieno, E.N., Walker, N., Saveliev, A.A. & Smith, G.M. (2009). Mixed Effects Models and Extensions in Ecology with R. Springer-Verlag, New York

**CrediT authorship contribution statement**

**David Eme**: Data Curation, Conceptualization, Methodology, Investigation, Formal analysis, Writing - Original Draft, Writing - Review and Editing, Visualisation, Project administration, Funding acquisition.

**Marta Rufino**: Data Curation, Conceptualization, Methodology, Writing - Review and Editing, Project administration.

**Verena Trenkel:** Data Curation, Writing - Review and Editing

**Youen Vermard:** Data Curation, Resources, Writing - Review and Editing

**Pascal Laffargue:** Data Curation, Resources, Writing - Review and Editing

**Pierre Petitgas:** Funding acquisition, Writing - Review and Editing

**Loïc Pellissier:** Methodology, Writing - Review and Editing

**Camille Albouy**: Data Curation, Conceptualization, Methodology, Visualisation, Resources, Writing - Review and Editing, Project administration, Funding acquisition.

**SUPPLEMENTARY MATERIAL**

"Contrasted spatio-temporal changes in the demersal fish assemblages and the dominance of the environment *vs* fishing pressure, in the Bay of Biscay and the Celtic Sea."

David Eme, Marta M. Rufino,Verena M. Trenkel, Youen Vermard, Pascal Laffargue, Pierre Petitgas, Loïc Pellissier and Camille Albouy

Submitted to *Progress in Oceanography*

## S1. Supplementary material and methods

### *1) Additional information about the environmental variables*

We selected the average bathymetry within a ICES rectangle to describe the topography, as other potential descriptors of the topographic heterogeneity such as the standard deviation of the bathymetry, slope, roughness, Terrain roughness index (TRI), were all highly correlated with the average bathymetry ($r_{Pearson}$ = 0.91-0.95). We did not retain any salinity measures as they were all strongly correlated with the oxygen concentration (i.e. O2) ($r_{Pearson}$= 0.82 - 0.9) or net primary productivity (NPP), ($r_{Pearson}$ = 0.81-0.86). Both mean and max O2 were highly correlated with the minimum O2 and were discarded, ($r_{Pearson}$ = 0.90 and 0.96). The average bathymetry within an ICES rectangle was computed from a high resolution (0.004°) bathymetric raster provided by The General bathymetric Chart of the Oceans (GEBCO, https://download.gebco.net/). To test the influence of the heterogeneity of benthic habitat we computed a Shannon index from 10 seabed substrate habitats provided by the European Marine Observation Data Network (EMODnet) Seabed Habitats project (EUSeaMap 2019 updated 1st July 2019, http://www.emodnet-seabedhabitats.eu/). All the monthly average data for the bottom sea-floor temperature, sea temperature, Oxygen concentration, net primary productivity (NPP), salinity and thickness of the mixed layer depth (MLD) were obtained from the Copernicus European programme (available at: http://marine.copernicus.eu/services-portfolio/access-to-products/) from January 1997 to December 2018 at 0.028° resolution and at 10 depth strata (0, 20, 50, 110, 220, 330, 450, 565, 630, 770 m). We stopped at 770m because none of the trawls conducted during the EVHOE survey was performed deeper. All monthly variables but bottom seafloor temperature, were averaged over the maximum depth of the corresponding ICES rectangle, to integrate the values over the water column. To improve the normality assumption of residuals of the linear models and decrease the dispersion of residuals (i.e. decrease heteroscedasticity), we log10 transformed several explanatory variables such as the average bathymetry, the average NPP, the minimal MLD, the standard deviation of O2, the standard deviation of the bottom temperature, and the fishing pressure (Zuur et al., 2007). All variables were normalized by subtracting the mean and dividing by the standard deviation.

### *2) Variables selection before further modelling*

We used elastic-net regularized generalised linear models to select the most influential variables related to energy, habitat and fishing pressure separately for each of the 11 biodiversity metrics. Elastic-net regularisation methods are efficient to select variables when the number of predictors is bigger than the number of observations and when many predictors have a limited contribution and are correlated (Zou & Hastie, 2005). In this study, model predictors refers to all linear and quadratic terms associated with the explanatory variables included in a model. Elastic-net regularization generalised linear models (Elastic-net GLMs) are algorithmically suitable to perform fast variable

selection on large data sets (Friedman et al., 2010). The elastic-net penalty controls the stringency of the model selection and is a compromise between the lasso penalty (α = 1) which performs a stringent selection especially when variables are highly correlated, and the ridge regression (α = 0) which uses a continuous shrinkage method to optimise the estimate of all predictors in the model (Zou & Hastie, 2005). To estimate the best optimal elastic-net penalty, we performed 10 cross-validation for each α value (from 0.1 to 1 by 0.1 steps). The α providing the lowest cross-validated error (cvm), was retained as well as the penalty term of the predictors (ƛ) associated witht the optimal α. A final Elastic-net GLM was fitted with the selected α and ƛ values, and the coefficients of the model parameters were retained. For each of the seventeen years (2000 - 2016), this whole procedure was repeated 10 times and we reported the number of times the coefficient was non null to rank the variables retained the most often over the years. For energy and habitat, we selected the four best predictors retained over the years. For fishing pressure, all four predictors were retained, however for the three groups of variables, we filtered the predictors present in less than 20% of the iterations over the years. For all biodiversity metrics, we considered a gaussian error model and an identity link because we used the average biodiversity metric estimated over the 100 community data matrices, providing continuous values, and also because the Beta error model was not yet available with the elastic net regularization procedure to the best of our knowledge.

***3) Inferring spatio-temporal patterns***

To assess the temporal $\beta$ diversity (TBI) within a rectangle, we considered the multi-site version of the incidence and abundance-based $\beta$ diversity indices (Baselga, 2017). Then, to test for temporal change of the variability in species composition within a rectangle, we estimated the TBI of the different indices for pairs of consecutive years. Then, to test the temporal trend, we used the slope of a GLM with year as the explanatory variable and TBI indices as the response variable considering a Beta distribution and a logistic link.

The pairwise and multisite $\beta$ diversity indices were computed using the betapart R package (Baselga et al., 2018), while the GAM, and Beta regression models were fitted using mgcv (Woods, 2004) and betareg (Cribari-Neto & Zeileis, 2010) R packages.

***4) Partitioning the spatial and temporal variation***

We used a variance partitioning approach based on the Moran Eigenvector Maps (MEMs) method (Legendre et al., 2014) to test the relative importance of the spatial and temporal variability of the biodiversity patterns. MEMs corresponds to an eigenvector decomposition of spatial or temporal weighting matrix (SWM) which describes the spatial or temporal relations among a set of sampling units that can be included as multiscale (spatial or temporal) predictors in univariate or multivariate models (Dray et al., 2006, 2012; Bauman et al., 2018). SWM is the product of a connectivity matrix (defined the neighbors) and a weighting matrix (defined the strength of the relation) and the selection among the many SWMs possible is best performed using a data-driven approach (Dray et al., 2006; Bauman et al., 2018). To select the optimal set of spatial MEMs supporting significant correlation

with each biodiversity metric, we followed the approach of Bauman et al. (2018) to account for the influence of different spatial weighting matrices (SWM). We tested the influence of different graph-based (Delaunay triangulation, Gabriel graph, and relative neighbor graph) and distance-based connectivity matrices (Minimal distance connecting all rectangles, 100, 150, 200 km) and different spatial weighting schemes (linear: Flin = 1-(d/dmax) and concave-down: Fcon-dow = 1-(d/dmax)*α with α = 2). A first global test of goodness of fit (i.e. $R^2$) including all MEMs for each SWM was performed with a p.value correction (Sidak correction) for multiple testing to only retain the significant SWMs. Then, for the remaining SWMs, a forward selection was performed with a double stopping criterion (Blanchet et al., 2008) to retain the best subset of MEMs. Finally, the SWM providing the best subset of MEMs yielding the highest adjusted $R^2$ was retained (Bauman et al., 2018). In the selection procedure, 199 permutations were performed to compute the p.values. Before analyses, the geographic coordinates of the centroid of the ICES rectangle were slightly jittered (10 meters difference in average) to remove spatial duplicates caused by the temporal replication of the sampling scheme. The temporal MEMs were defined using distance-based MEMs (Dray et al., 2006), considering a truncation of the temporal distance of 2 years (the largest distance between two consecutive years). The selection of the best subset of temporal MEMs was also performed with the double stopping criterion (Blanchet et al., 2008) and the p.values were computed using 199 permutations. Then, we partitioned the variance with a linear model using the adjusted $R^2$ considering each biodiversity metric as response variable and the best set of spatial and temporal MEMs to estimate the unique and shared fractions of explained variance attributed to space and time (Legendre & Legendre, 1998; Legendre et al., 2014). The general equation of the full model including both the best set of spatial and temporal MEMs was as follows:

$$Y = a + B_{spatialMEMs} * x_{spatialMEMs} + B_{temporalMEMs} * x_{temporalMEMs} + \varepsilon,$$

where the term $Y$ is the response variable (i.e. the different biodiversity indices), a is the intercept, $B_{spatialMEMs}$, and $B_{temporalMEMs}$ are the parameters (i.e. slope) of the variables attributed to the spatial MEMs, and the temporal MEMs, respectively, and ε represents the model residuals. The MEMs selection and variance partitioning were performed with adespatial (Dray et al., 2019) and vegan (Oksanen et al., 2019) R packages, respectively.

***5) Partitioning the variance among energy, habitat and fishing pressure***

We fitted linear mixed models (LMMs) and generalised additive mixed models (GAMMs) with R packages lme4 (Bates et al., 2015) and mgcv (Wood, 2004) respectively, we used the R package MuMIn (Bartoń, 2019) to estimate the marginal $R^2$, and we performed the variance partitioning following a simple set of equations as described in Legendre & Legendre (1998).

***6) Variables importance within energy, habitats and fishing pressure and accounting for temporal and spatial autocorrelation in the model residuals***

For each biodiversity index, we used a model selection approach to select the most parsimonious model and assess the relative importance of the main variables within the three groups of explanatory

variables included in the linear mixed models (LMMs) presented in 2.5 (main manuscript). First, we performed a multimodel inference approach based on information theory running all possible models (Grueber et al. 2011). We retained the most parsimonious model based on the Bayesian Information Criteria (BIC) among the best set of models that have less than 2 BIC units difference with the best model (i.e. the model with the lowest BIC). Second, we computed the semi-partial marginal $R^2$ as a proxy of explained variance for each variable retained in the most parsimonious model (Jaeger et al. 2017; Nakagawa et al. 2017). We used the R packages MuMIn (Bartoń, 2019) and r2glmm (Jaeger, 2017) for multi-model inference and to compute the semi-partial $R^2$ respectively.

To account for the temporal and spatial autocorrelation in the residuals for the most parsimonious linear mixed models (LMM), we considered the following three step approach. First, we included an auto-regressive correlation structure in the residuals of order 1 (*corAR1* in nlme R package, or *ar1* in glmmTMB R package) based on the year effect accounting for the temporal autocorrelation (see Zuur et al., 2009 pages 149-150). The auto-regressive correlation structure is expressed as follows:

$cor(\varepsilon_s, \varepsilon_t) = \rho^{|s-t|}$,

where $\varepsilon_s$ and $\varepsilon_t$ are the model residuals at time $s$ and $t$ respectively, and $\rho$ is the auto-correlation parameter estimated from the data.

Second, we tested the presence of spatial autocorrelation in the residuals of the different models for each year separately using the Moran.I statistic considering the inverse great circle distance as a spatial weight and 199 monte carlo permutations. Then, we included an exponential correlation (i.e. *corExp* in the nlme R package or *exp* in the glmmTMB R package, see Zuur et al., 2009, page 167-168) structure using "year" as a grouping variable to account for slight differences in the spatial distribution of ICES rectangles over the years (Zuur et al., 2009).

The equation of the shape of the exponential correlation function is as follows:

$\gamma(s_i, \rho_i) = 1 - e^{(si/\rho i)}$,

with $s_i$ is the distance and $\rho_i$ the range for the year $i$ (year is considered as a discrete variable here), and $\gamma(s_i, \rho_i)$ is the variogram representing the shape of the spatial correlation structure of the model residuals. In other words, for a given year, the correlation between two observations is $e^{(-s/\rho)}$.

Third, both temporal and spatial autocorrelation structures were simultaneously included in the most parsimonious models. To assess the general goodness of fit of the most parsimonious models including a correlation structure in the residuals we used the Pseudo.$R^2$ (Efron, 1978) which is defined as the coefficient of determination of the linear relationships between the observed and the fitted values of the model.

We performed LMM models including both temporal and spatial autocorrelation structures, and Moran.I with, lme4 (Bates et al., 2015), glmmTMB (Brooks et al., 2017), nlme (Pinheiro et al., 2019) and spdep (Bivan et al., 2013) R packages.

### 7) Testing for temporal effect in the most parsimonious LMM model

To test for a temporal effect and its interaction with explanatory variables we included the continuous variable "time" (year) as a fixed effect and tested for two-way interactions between each variable

retained previously in the most parsimonious model and time in a linear model (LM). We performed multimodel inferences to retain the most parsimonious model according to the BIC and we assessed the relative importance of each variable using partial $R^2$. We also tested the robustness of parameters estimates and their significance to the remaining temporal and spatial non-independence in the residuals (see paragraph S1.6 above in *Supplementary material*).

***8) Testing a lag effect***

Lag effects can appear when the response variable lagged behind the explanatory variable, and the explanatory variable from a previous time period offers a better fit to the response variable than the contemporary explanatory variable (Huret et al., 2018). We developed the following three steps model selection procedure to test for this lag effect. First, for each biodiversity index and explanatory variable separately, we performed a suite of generalised additive mixed models (GAMMs, max of 3 basis dimensions for smooth terms). We constructed 3 models considering the absence of lag, a one year, and a two years lag. As in the previous steady-state model, "year" was considered as a random effect, and we accounted for spatial autocorrelation in the residuals, by including an exponential correlation structure using "year" as a grouping variable. Then, we performed a model selection based on the Akaike information criterion corrected for small sample size (AICc) to select the best model with lag effect (i.e. we compared the AICc of the models without lag, with 1 and 2 years lag). A lag was retained only if its associated model got the lowest AICc, the adjusted $R^2$ of the lag variable was higher than 2% and the increase in explained deviance in comparison to the contemporaneous model (i.e. absence of lag) was higher than 2%. We performed the model selection for the lag models considering the time series between 2000 and 2016 for the response variables. We tested for lag effects only for the dynamic environmental variables (e.g. bottom sea-floor temperature, sea temperature, oxygen concentration, NPP, salinity MLD, SR and abundance of the nine species of small and medium size pelagic fishes), and not for the static variables such as bathymetry, and distance to the coast. However we did not test for a lag effect for the fishing pressure variables because the missing values before 2000 trimmed too much the time series. Second, after the best variables were considered for a lag effect, we performed the variable selection using the GLM Elastic net procedure considering the linear and quadratic terms. Three, we performed the whole steady-state (see paragraph 2.5) and temporal modeling (see Supplementary Material S1.7) including the variance partitioning (see 2.5) and the model selection (see 2.6) to compare the results of the models with and without lag.

***9) Testing for the relationships between environmental forcing and the temporal trend of biodiversity metrics***

We explored the relationships between the temporal trend of the biodiversity metrics and the temporal dynamic of the explanatory variables by applying a four steps procedure. First, for each of the 71 ICES rectangles visited at least 5 times during the time series, we computed the slope of the linear model as a proxy of the temporal trend using each dynamic environmental variable as response variable and year as explanatory variable. Second, we described the relationship between the previous

estimated slope of the biodiversity metrics (see and the temporal trend of each explanatory variable using GAMM (max of 3 basis dimensions for smooth terms), and including an exponential correlation structure to account for potential spatial autocorrelation. Third, for each biodiversity metric we retained the explanatory variables with a significant smoothing parameter ( $\alpha = 0.05$) and an adjusted $R^2$ above 0.05. Fourth, we considered generalised least squares (GLS) models including the linear and quadratic term of the best explanatory variables previously retained and we accounted for the spatial autocorrelation using an exponential structure in the residuals (Zuur et al., 2009). Finally, we used multimodel inferences to run all possible GLS models and retained the best set of models according to AICc (delta AICc <2 with the best model). This model subset allowed us to measure the relative importance of each predictor as the sum of AICc weights of models in which the predictor occurred and to perform a multi-model averaging approach to get the estimate and significance of the predictors retained (Burnham & Anderson, 2002).

GAMM, multimodel inferences and GLS models were performed with mgcv (Wood, 2004), MuMIn (Bartoń, 2019) and nlme (Pinheiro et al., 2019) R packages, respectively.

## S2. Supplementary results

### *1) Results about the spatio-temporal patterns at local scale*

The temporal change of TBI.jac was also driven by species turnover (TBI.jtu, $r_{Spearman} = 0.96$, $p < 0.001$), and showed an even clearer decrease of community dissimilarities over time for 39% (n = 28, mean slope = -0.05, sd = 0.02) of rectangles located in the Celtic Sea and the northern and central Bay of Biscay (Fig. S10B). The increase over time of TBI.jac and TBI.jtu in the southern and coastal Bay of Biscay (8-10% of rectangles) confirmed the temporal differentiation of fish communities at the local scale (Fig. S10B). The spatial patterns of the abundance-based temporal beta diversity (TBI) indices were also in agreement with the abundance-based LBD patterns especially for balance variation in abundance ($r_{Spearman} = 0.41$, $p < 0.001$), the abundance gradient and the ratio ($r_{Spearman} = 0.56$, $p < 0.001$, Fig. S11A). On the contrary, the temporal evolution of the TBI.ruz decreased significantly in dissimilarities within communities over time for 35% of rectangles (n = 25, mean slope = -0.05, sd = 0.02) spread over the whole area (Fig. S11B). This pattern was driven mostly by the balance variation of abundance ($r_{Spearman} = 0.81$, $p < 0.001$).

Spatial patterns for the two components LBD.ruz and LBD.ruz.bal were similar ($r_{Spearman} = 0.76$), with higher values (0.73 - 0.8) in the northern part of the Celtic Sea and along the coast of the Bay of Biscay (Fig. 4A). Lower values (0.67 - 0.71) were located in the offshore regions of the Celtic Sea, and the Bay of Biscay to some extent. However, the offshore area between the south of the Celtic Sea and the north of the Bay of Biscay showed an increase in LBD.ruz (0.89 - 0.92) caused by higher abundance gradients (LBD.ruz.gra, Fig. 4A). The local gradient in abundance (LBD.ruz.gra) had overall values systematically lower than LBD.ruz.bal (paired t.test t = 97.02, $p < 0.001$, LBD.ruz.bal mean = 0.72, sd = 0.029, LBD.ruz.gra mean = 0.17, sd = 0.021), and showed an inverted spatial

pattern ($r_{Spearman}$ = -0.95, p < 0 .001; Fig. 4A).

***2) Results related to the lag effect.***

Individual tests for time lag effect for each dynamic environmental variable showed that significant improvements were detected for all biodiversity metrics except abundance and evenness (Table S13). For SR, one year and two years lag for the minimal bottom temperature and oxygen seasonality (e.g. O2.sd) respectively, offered small (2%) but significant improvement and were retained in the multivariate models. For LBD metrics, the most significant improvement in the explained variance, up to almost 5% for LBD.ruz.gra, was attributed to the two years lag for the minimal mixed layer depth (MLD.min, Table S13). Other variables such as a two year lag for the minimal oxygen concentration, and one year lag for the annual average thickness of the mixed layer depth were also retained for LBD.jne and LBD.ruz.gra (Table S13). After another variable selection step including the best lag variables for SR, and all LBD.metrics (see Table S14 for the best explanatory variables retained for each biodiversity metric), the variance partitioning revealed slight improvements (1+/-1.1% for the overall variance) in comparison to the contemporaneous variables. Most notables improvements were attributed to LBD.jac (2.3% overal) and LBD.ruz.bal (2.2% overal), that were mostly attributed to the habitat category (2.2% for LBD.jac and 2.1% for LBD.ruz.bal, see Table S15). The overall picture of the variance partitioning and the contribution of the independent variables did not change significantly in comparison to the models including contemporaneous variables only (see Table S16-S22 for the model outputs for the different biodiversity metrics).

***3) Results related to environmental forcing.***

The selection procedure revealed that the temporal trend of at least one dynamic environmental variable (from 1 to 5), was significantly related to the temporal trend for SR, Abundance, LBD.jtu, LBD.ruz, LBD.ruz.bal and LBD.ruz.gra, however the goodness of fit remained low to moderate (best adjusted.$R^2$ = 0.206, Table S23). The multi-model inference based on GLS confirmed the importance of the four main relationships worth mentioning (Table S24, Fig. S12). The temporal trend of the species abundance was negatively related to the temporal trend of the annual average of net primary productivity, and positively related to the minimum oxygen concentration. The temporal trend of LBD.jtu showed a negative relationship with the temporal trend of the temperature seasonality and the temporal trend of LBD.ruz.gra was negatively related to the species richness of small pelagic species (Fig. S12, S14). All relationships were robust to spatial autocorrelation and collinearity associated with the additional variables retained for the modelling (Table S23, S24).

## S3. Supplementary figures:

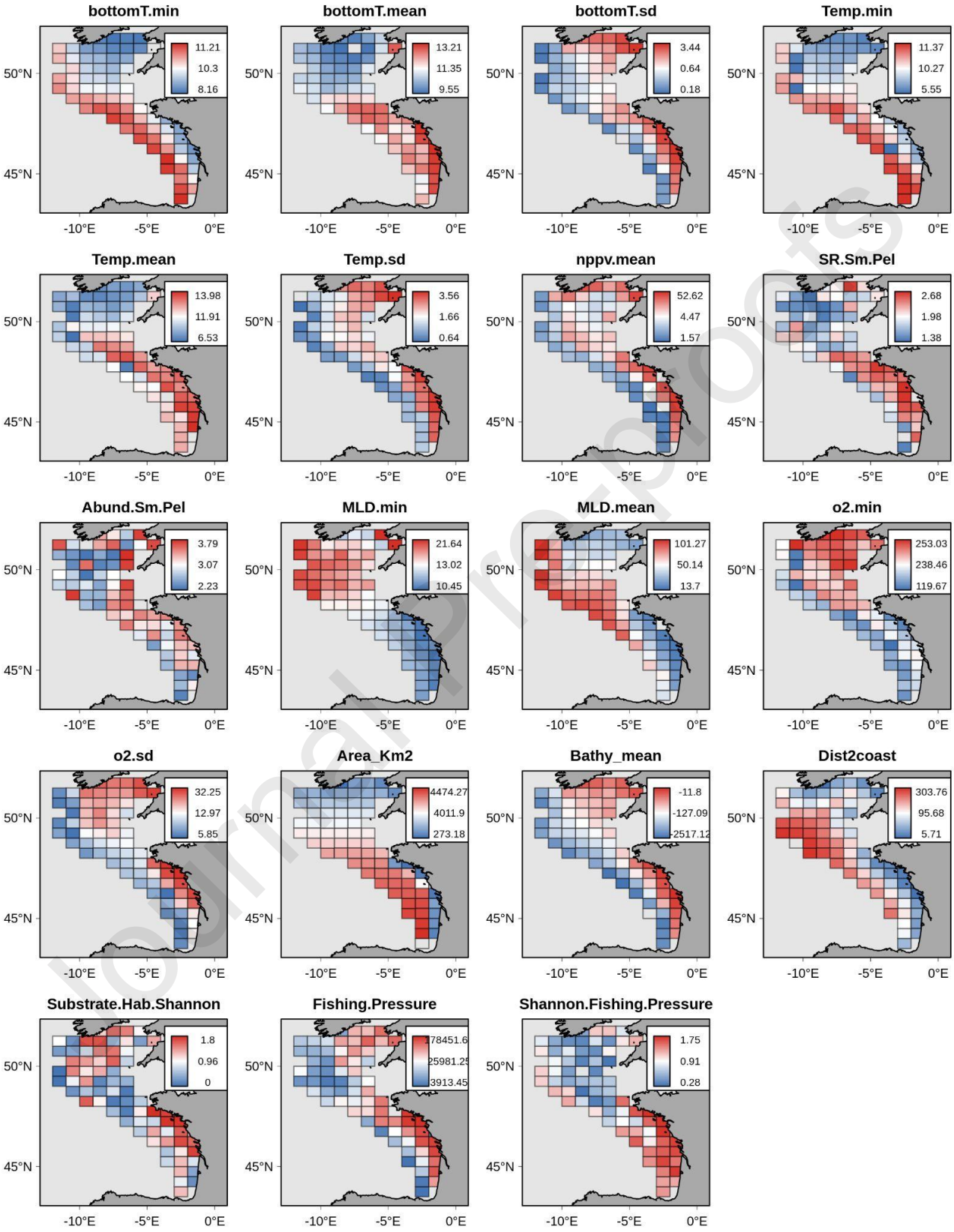


**Fig. S1:** Map of the average value over the time series (1997-2018) at the scale of the ICES rectangle for 19 environmental variables. bottomT.min: minimal annual bottom sea floor temperature, bottomT.mean: annual average of the bottom sea floor temperature, bottomT.sd: seasonality of the

bottom sea floor temperature, Temp.min: minimal annual temperature integrated over depth, Temp.mean: average annual temperature integrated over depth, Temp.sd: seasonality of the temperature integrated over depth, nppv.mean: annual average of the net primary productivity, SR.Sm.Pel: species richness of the small pelagic species, Abund.Sm.Pel: Abundance of the small pelagic species, MLD.min: minimal annual thickness of the mixed layer depth, MLD.mean: average annual thickness of the mixed layer depth, o2.min: minimal annual oxygen concentration, o2.sd: seasonality of the oxygen concentration, Area_Km2: aera of the ICES rectangle, Bathy: average bathymetry of the ICES rectangle, Dist2coast: distance to the nearest coast, Substrate.Hab.Shannon: habitat diversity based on the Shannon index of 11 substrat classes, Fishing.Pressure: sum of the fishing effort, Shannon.Fishing.Pressure: diversity of the fishing pressure based on the Shannon index of the fishing effort of the different fishing gears.

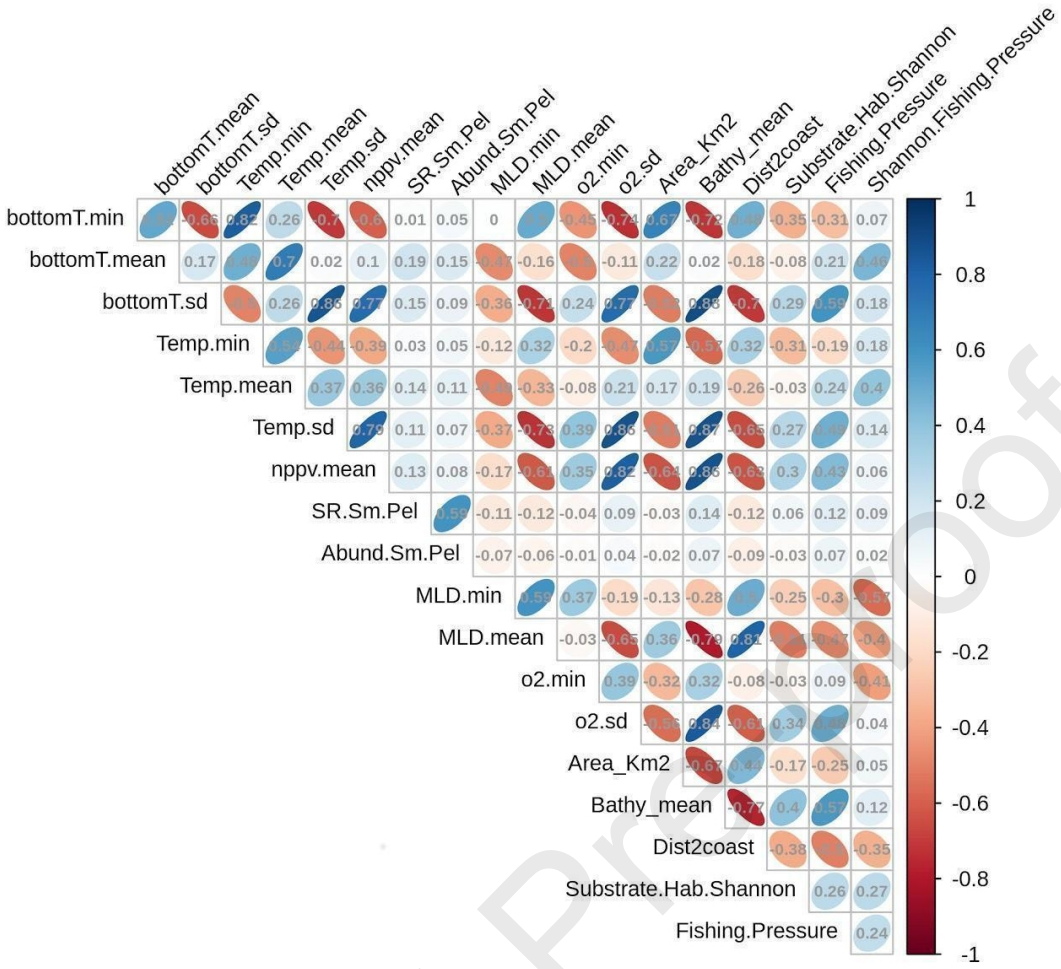


**Fig. S2:** Spearman correlation coefficients among all 19 environmental variables, belonging to energy, habitat and fishing pressure categories. bottomT.min: minimal annual bottom sea floor temperature, bottomT.mean: annual average of the bottom sea floor temperature, bottomT.sd: seasonality of the bottom sea floor temperature, Temp.min: minimal annual temperature integrated over depth, Temp.mean: average annual temperature integrated over depth, Temp.sd: seasonality of the temperature integrated over depth, nppv.mean: annual average of the net primary productivity, SR.Sm.Pel: species richness of the small pelagic species, Abund.Sm.Pel: Abundance of the small pelagic species, MLD.min: minimal annual thickness of the mixed layer depth, MLD.mean: average annual thickness of the mixed layer depth, o2.min: minimal annual oxygen concentration, o2.sd: seasonality of the oxygen concentration, Area_Km2: aera of the ICES rectangle, Bathy: average bathymetry of the ICES rectangle, Dist2coast: distance to the nearest coast, Substrate.Hab.Shannon: habitat diversity based on the Shannon index of 11 substrat classes, Fishing.Pressure: sum of the fishing effort, Shannon.Fishing.Pressure: diversity of the fishing pressure based on the Shannon index of the fishing effort of the different fishing gears.

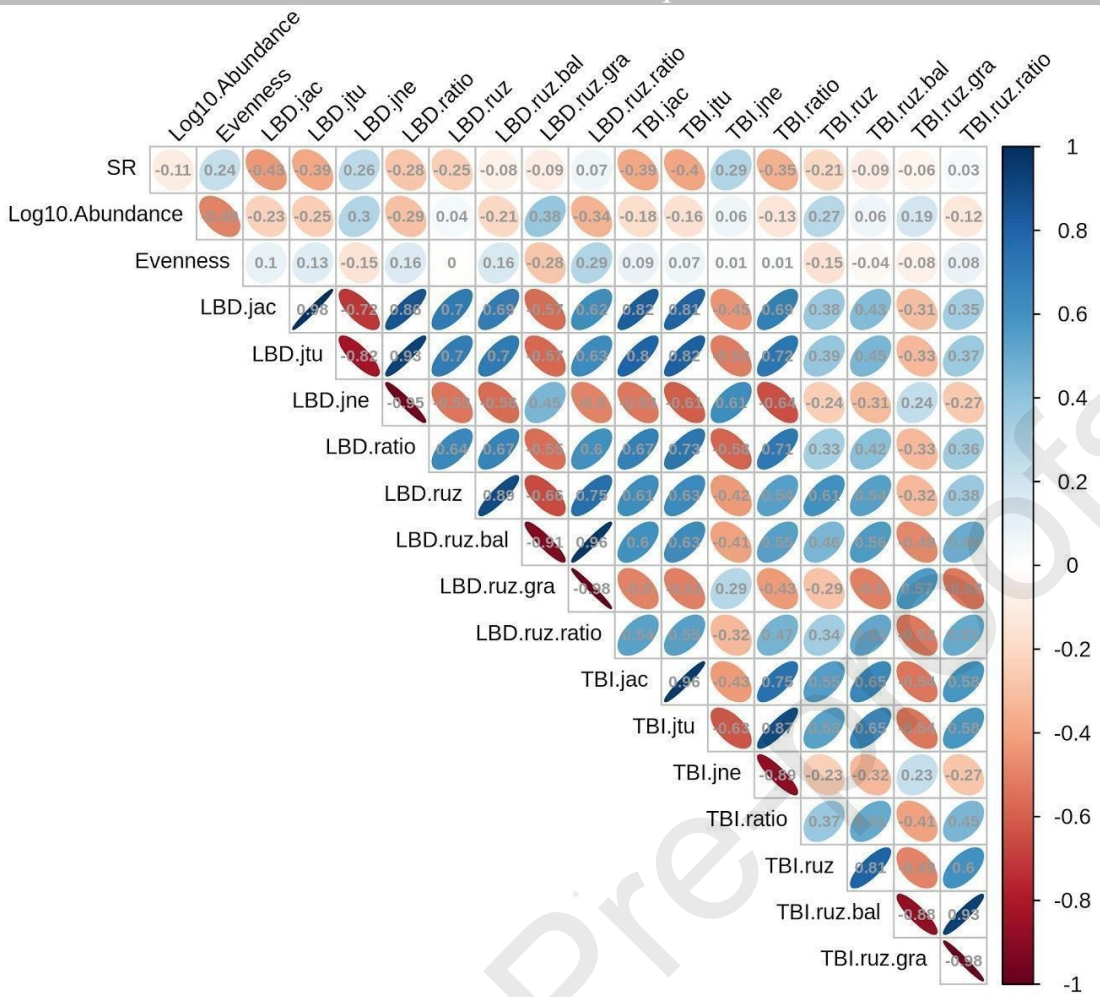


**Fig. S3:** Spearman correlation coefficient among the temporal evolution of all biodiversity metrics. See Fig. S2 for the definition of the variables.

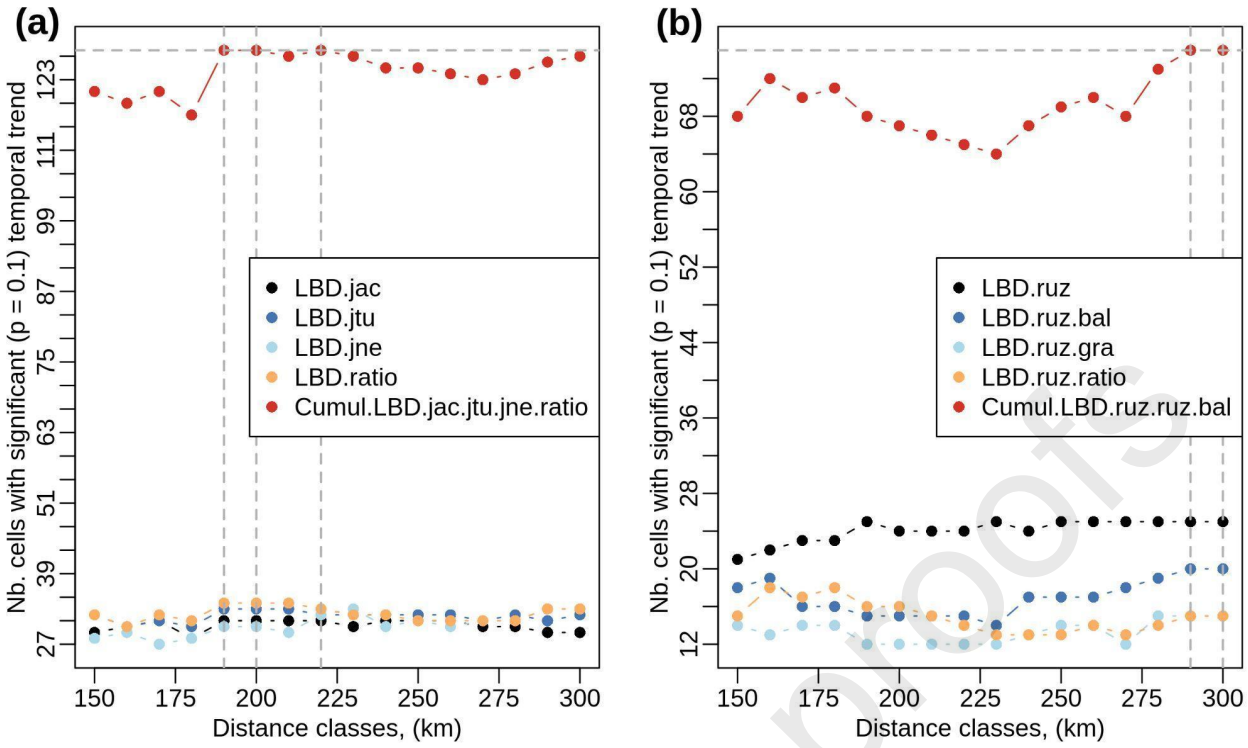


**Fig. S4:** Selection of the best geographic distance used to computed the local beta diversity (LBD) maximising the the number of ICES rectangles (i.e. cells) showing a significant temporal evolution (differentiation and homogenisation), for all incidence-based LBD (**a**) and abundance-based LBD indices (**b**). We estimated the LBD indices as the average beta diversity indices between a focal ICES rectangle and its neighbors defined within a distance radius (16 distance classes were considered from 150 to 300 km every 10 km). The smallest distance classes maximizing the number of rectangles with a significant temporal evolution (differentiation or homogenisation) was retained. Differentiation and homogenisation were considered for positive and negative slopes of a linear model respectively, that were significantly different from 0 (the p.value of the slope < 0.1), otherwise temporal trends were considered stable.

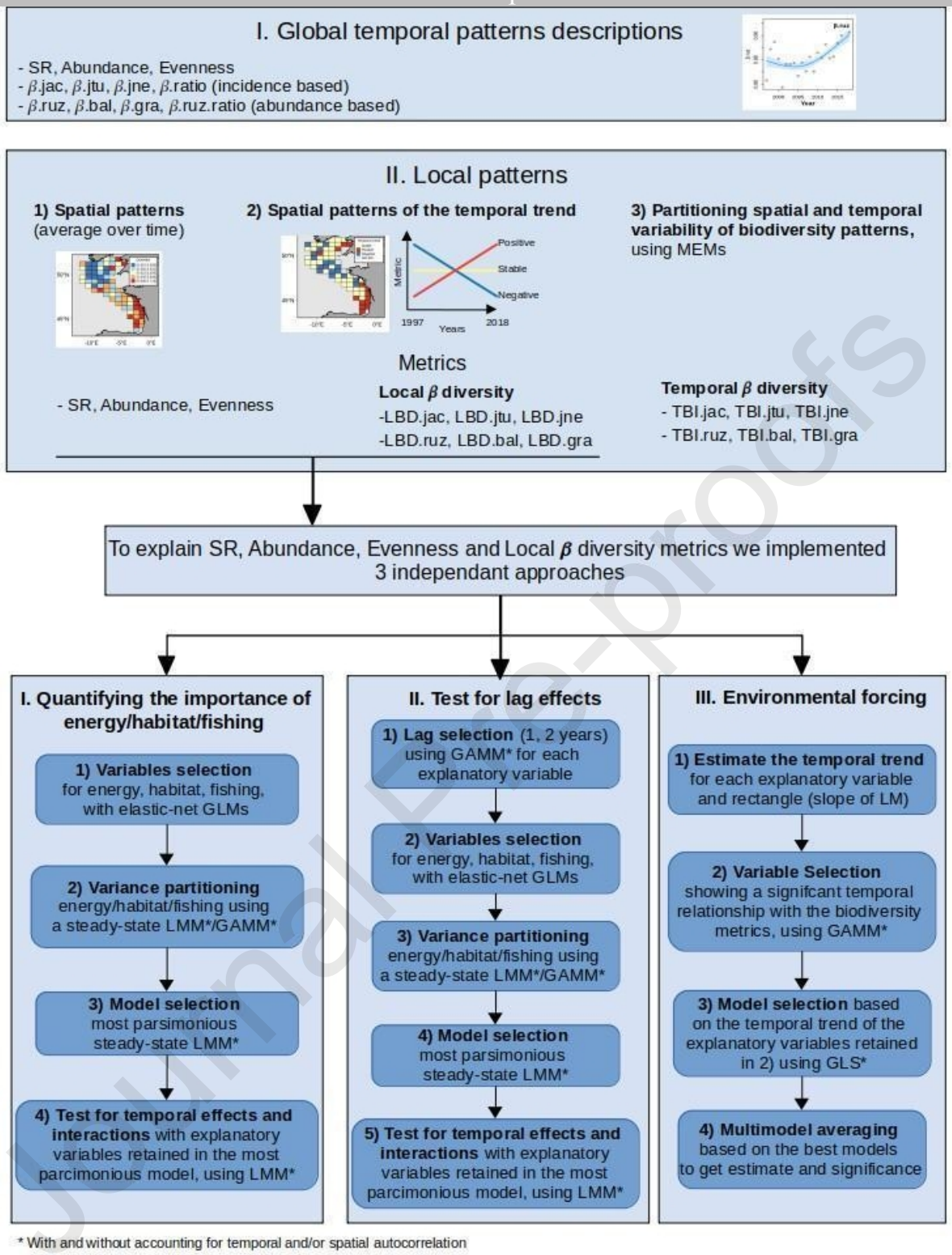


**Fig. S5:** Flowchart of the analytical steps related to the presentation of the biodiversity patterns and the modelling.

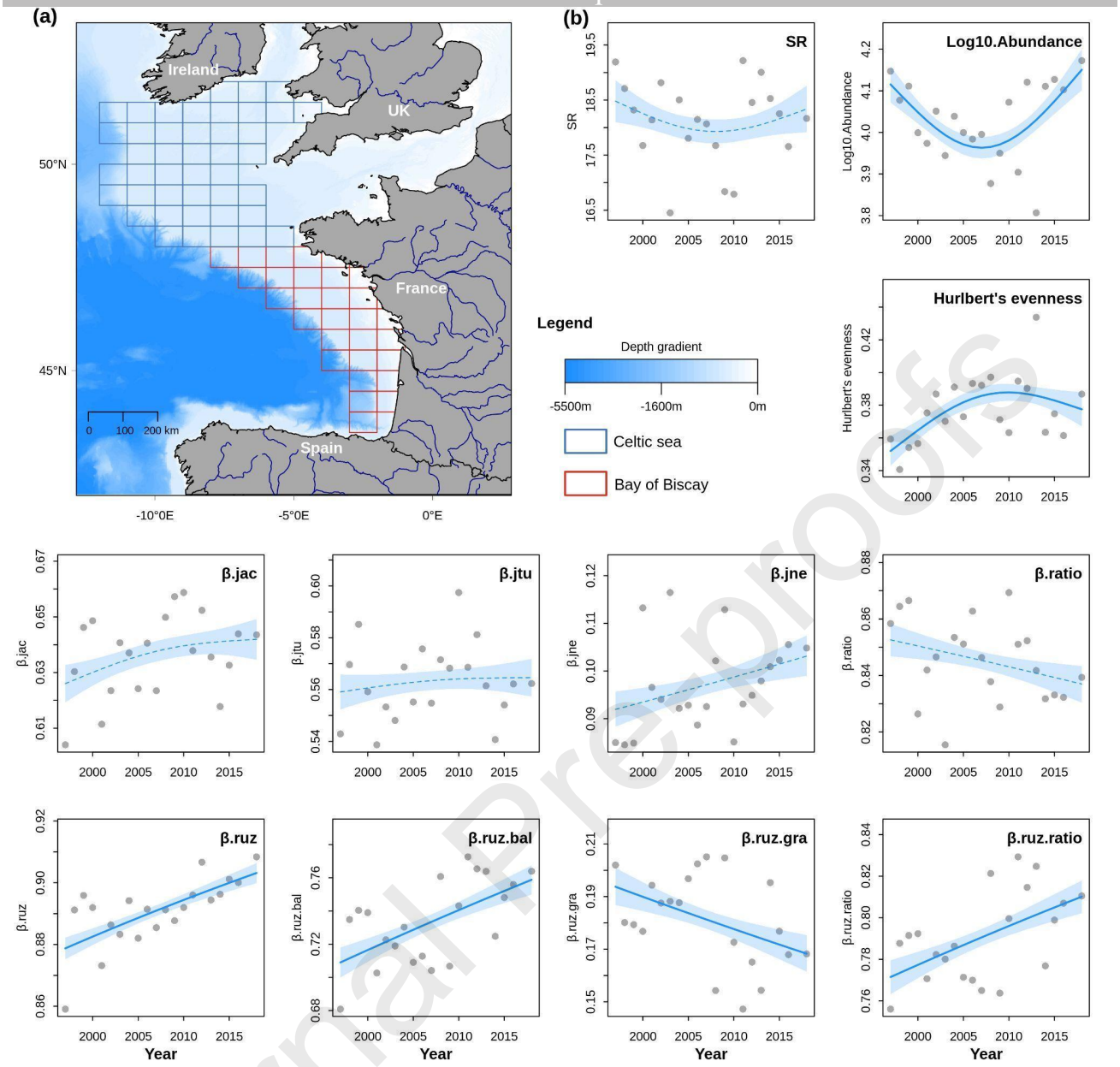


**Fig. S6**: **a)** Map depicting the ICES rectangles of the Celtic Sea and the Bay of Biscay sampled by the EVHOE bottom trawl survey from 1997 to 2018 including small pelagic species. **b)** Temporal trend average by ICES rectangle per year for SR, abundance (log10(abundance)), Hurlbert's evenness, or among all pairwise ICES rectangle comparisons for the Jaccard index (β.jac), its species turnover (β.jtu) and nestedness (β.jne) components, the ratio of species turnover over the Jaccard index (β.ratio), and the abundance-based dissimilarity index, including the Ruzicka index (β.ruz) and its balance variation in abundance (β.ruz.bal), and abundance gradient (β.ruz.gra) components as well as the ratio (β.ruz.ratio) of β.ruz.bal/β.ruz. The blue curves represent the fit of generalised additive models (GAM), with solid lines indicating a significant relationship, while the dotted lines indicate a non-significant trend (with a p.value > 0.1), and the light blue area the standard error around the fit of the model.

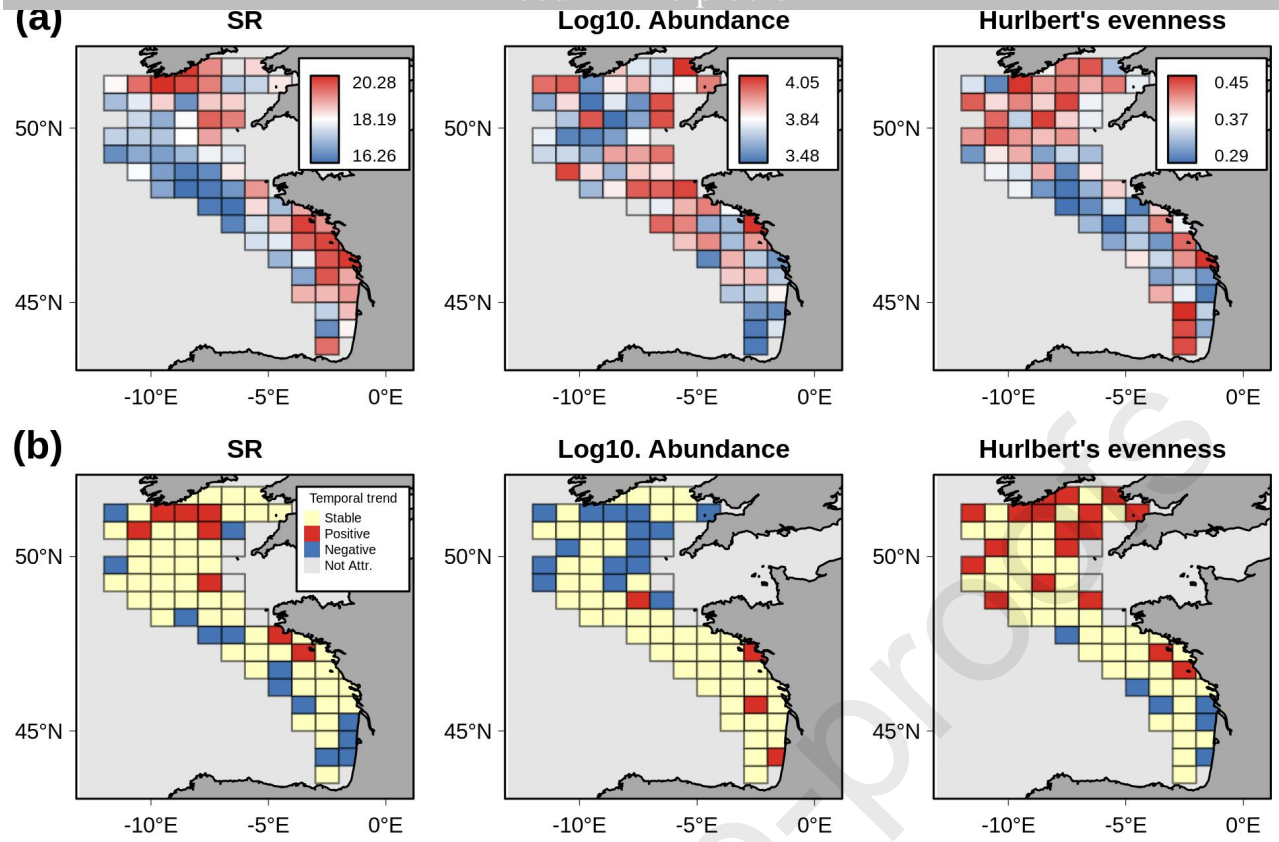


**Fig. S7:** Species richness, abundance (log10 transformation), and the Hurlbert's evenness patterns of the demersal fish assemblages of the Bay of Biscay and the Celtic Sea for the period 1997-2018 including small pelagic species. The Line (a) represents the mean species richness (SR), the mean abundance (log10(abundance)) and the mean evenness (Hurlbert's index) over the period 1997-2018. The line (b) showsthe temporal evolution of SR, abundance and Hurlbert's evenness. for the 71 retained ICES rectangles sampled at least 5 times. The beige colour indicates a stable trend (slope not significantly different from 0, with a p.value > 0.1), while positive and negative trends are in red and blue, respectively.

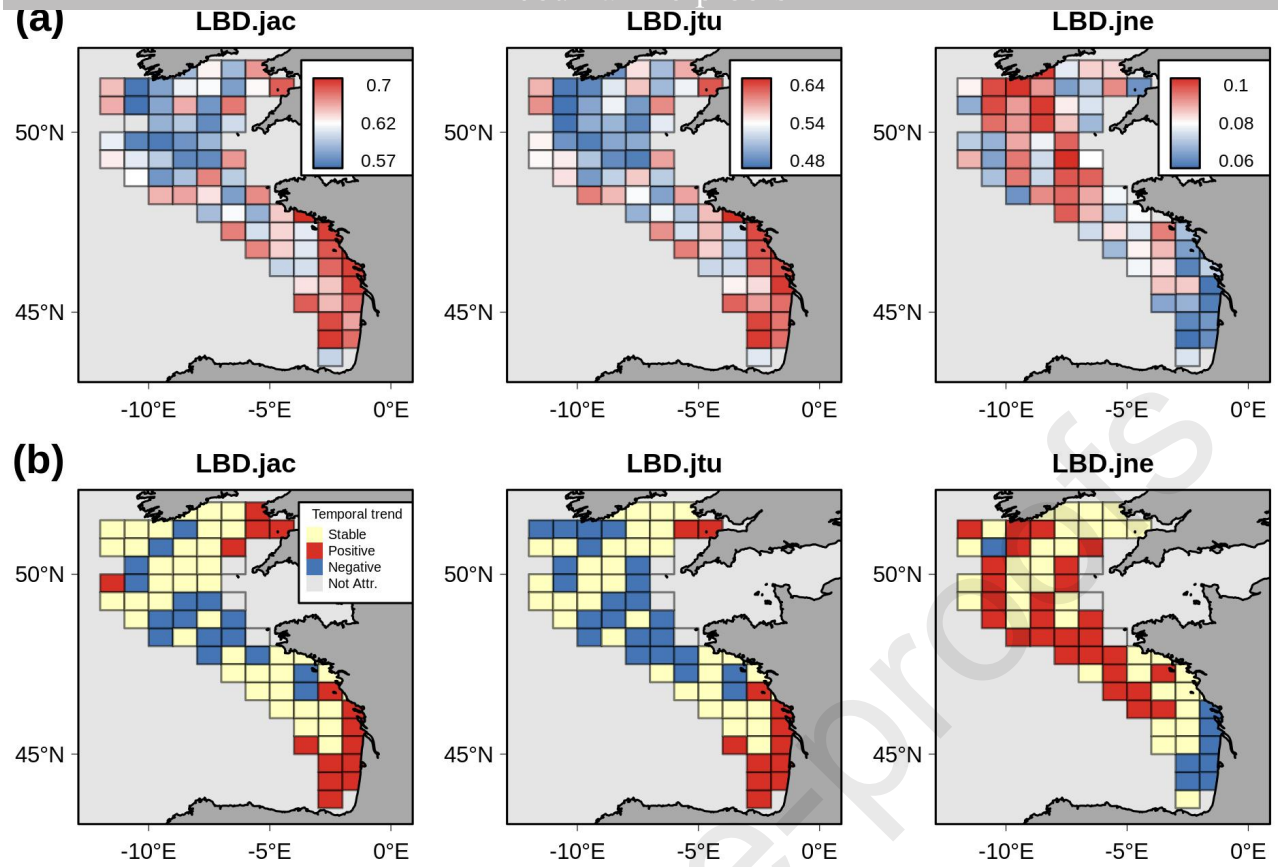


**Fig. S8:** Local beta diversity of incidence-based index of the demersal fish assemblages of the Bay of Biscay and the Celtic sea for the period 1997-2018 including small pelagic species. The line (a) represents the mean local Jaccard index (LBD.jac), mean local species turnover (LBD.jtu), and mean local nestedness (LBD.jne) over the period 1997-2018. The line (b) shows the trends of the temporal evolution of LBD.jac, LBD.jtu, and LBD.jne when 71 ICES rectangles sampled at least 5 times were retained. We computed the local beta diversity indices by averaging the dissimilarities among the focal rectangle and all its neighbours in a radius of 220km which was the distance maximising the number of rectangles with a significant temporal trend. The beige colour indicates a stable trend (slope not significantly different from 0, with a p.value > 0.1), while positive and negative trends are in red and blue, respectively.

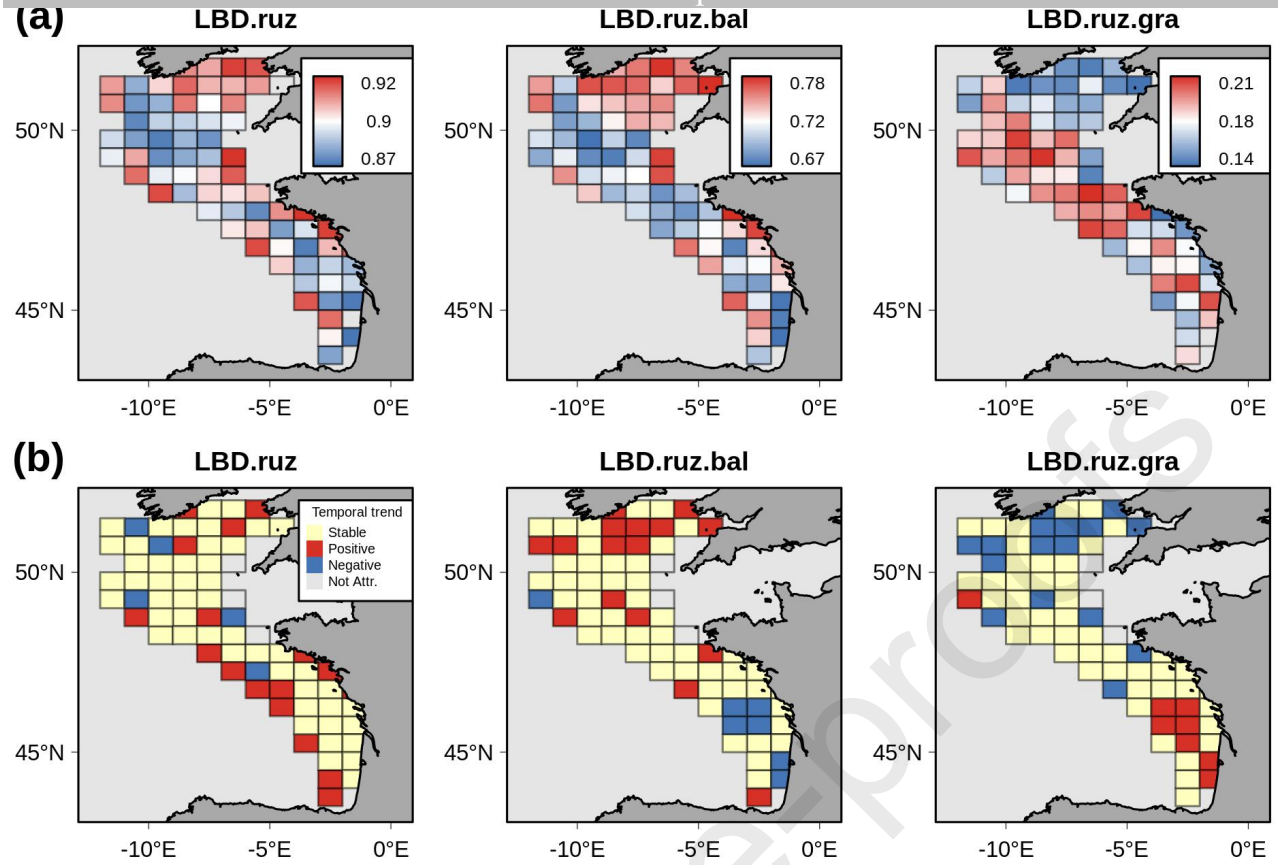


**Fig S9:** Local β diversity of abundance-based index of the demersal fish assemblages of the Bay of Biscay and the Celtic Sea for the period 1997-2018 including small pelagic species. The line (a) represents the mean local Ruzicka index (LBD.ruz), mean local balance variation in abundance (LBD.ruz.bal), and mean local abundance gradient (LBD.ruz.gra) over the period 1997-2018. The line (b) shows the trends of the temporal evolution of LBD.ruz, LBD.ruz.bal, and LBD.ruz.gra, only 71 ICES rectangles sampled at least 5 times were retained. We computed the local beta diversity indices by averaging the dissimilarities among the focal rectangle and all its neighbours in a radius of 290km which was the distance maximising the number of rectangles with a significant temporal trend. The beige colour indicates a stable trend (slope not significantly different from 0, with a p.value > 0.1), while positive and negative trends are in red and blue, respectively.

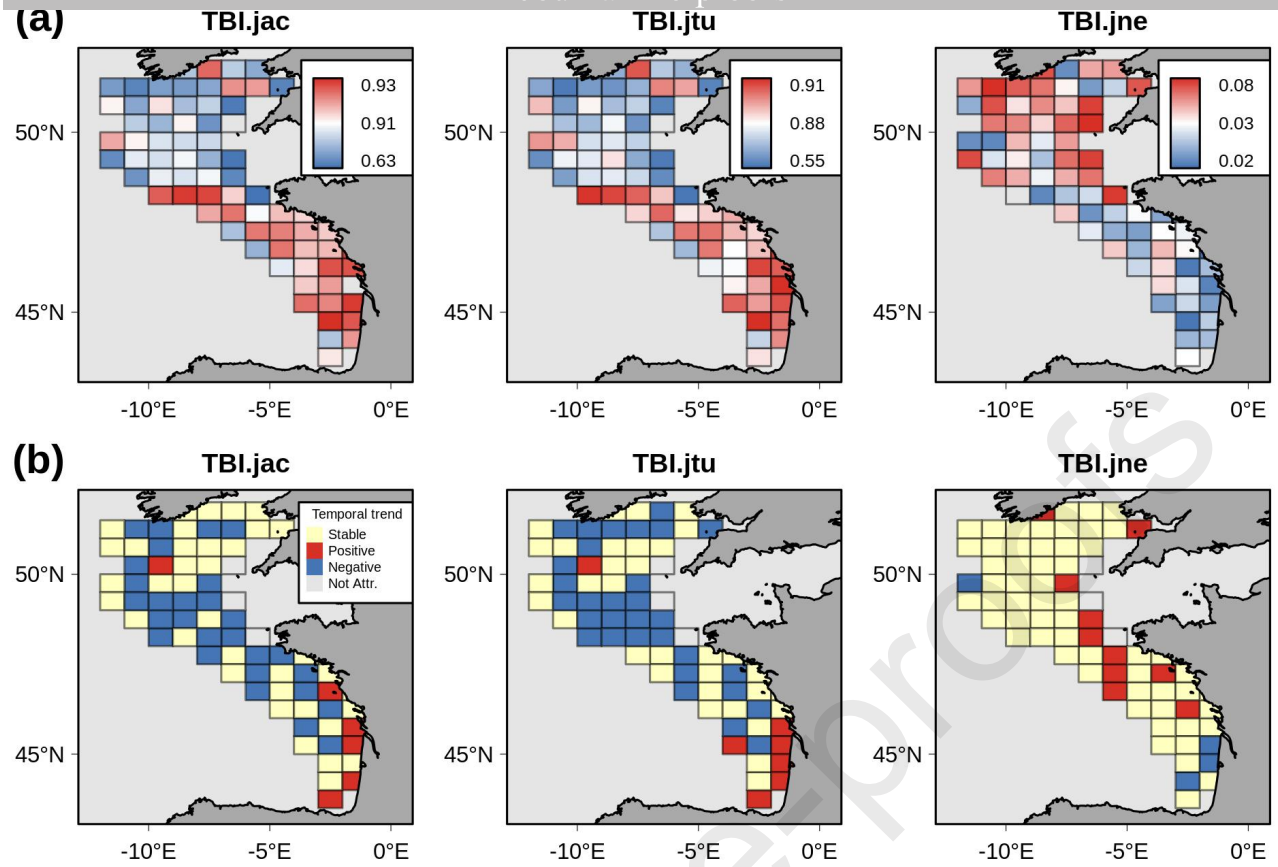


**Fig. S10:** Temporal beta diversity (TBI) patterns of the demersal fish assemblages of the Bay of Biscay and the Celtic Sea for the period 1997-2018 for incidence-based beta diversity indices. The line (a) represents the multisite (i.e. multiple years for the same ICES rectangle) Jaccard index (TBI.jac), species turnover (TBI.jtu), species nestedness (TBI.jne) over the period 1997-2018. The line (b) shows the trends of the temporal evolution of TBI.jac, TBI.jtu, and TBI.jne, only 71 ICES rectangles sampled at least 5 times were retained. The temporal evolution was measured as the slope of the linear model considering the pairwise TBI between adjacent periods(i.e. 1997-1998, 1998-1999) for a focal ICES rectangle. The beige colour indicates a stable trend (slope not significantly different from 0, with a p.value > 0.1), while positive and negative trends are in red and blue, respectively.

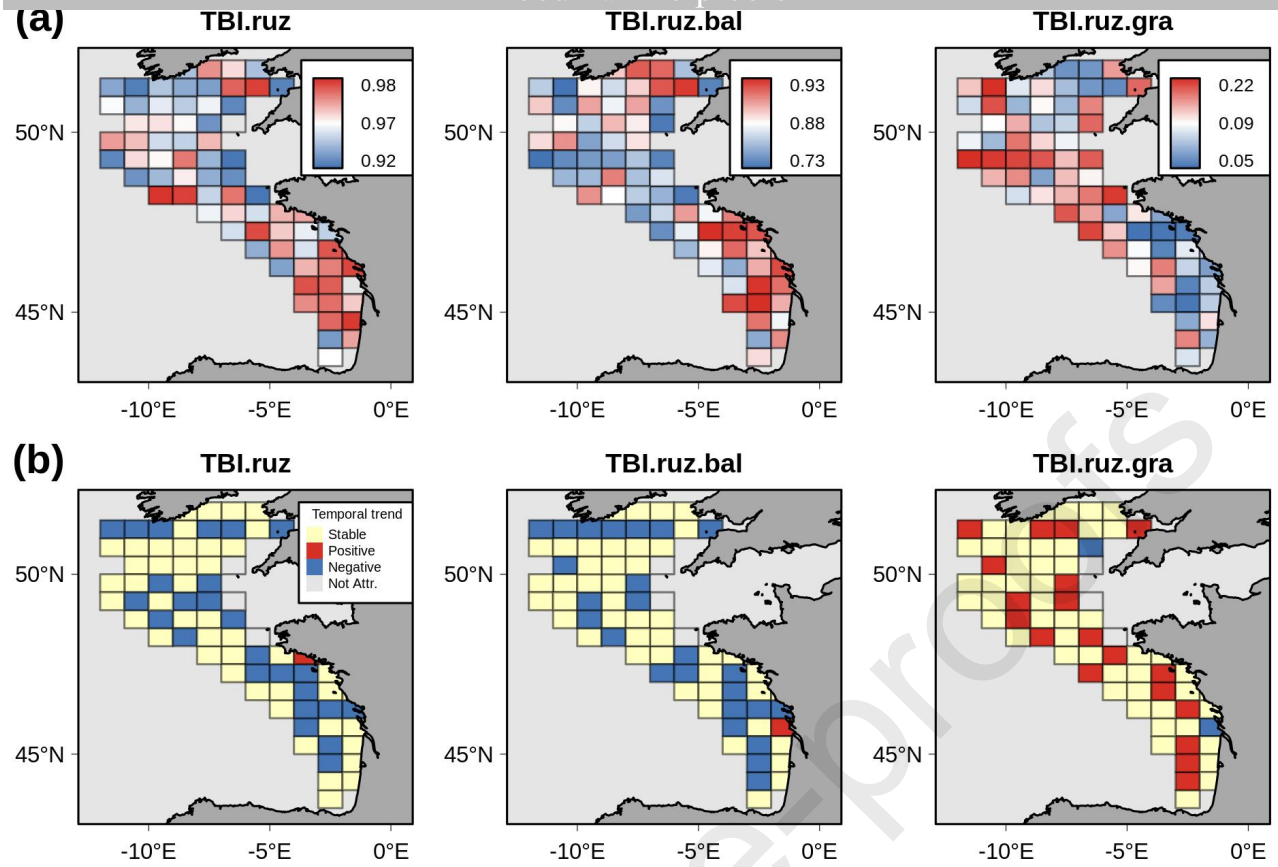


**Fig. S11:** Temporal beta diversity (TBI) patterns of the demersal fish assemblages of the Bay of Biscay and the Celtic Sea for the period 1997-2018 for abundance-based beta diversity indices. The line (a) represents the multisite (i.e. multiple years for the same ICES rectangle) Ruzicka index (TBI.ruz), the balance variation in abundance (TBI.ruz.bal) and the abundance gradient (TBI.ruz.gra) over the period 1997-2018. The line (b) shows the temporal evolution of TBI.ruz, TBI.ruz.bal, and TBI.ruz.gra, for the 71 selected ICES rectangles sampled at least 5 times. The temporal evolution was measured as the slope of the linear model considering the pairwise TBI between adjacent time periods (i.e. 1997-1998, 1998-1999) for a focal ICES rectangle. The beige colour indicates a stable trend (slope not significantly different from 0, with a p.value > 0.1), while positive and negative trends are in red and blue, respectively.

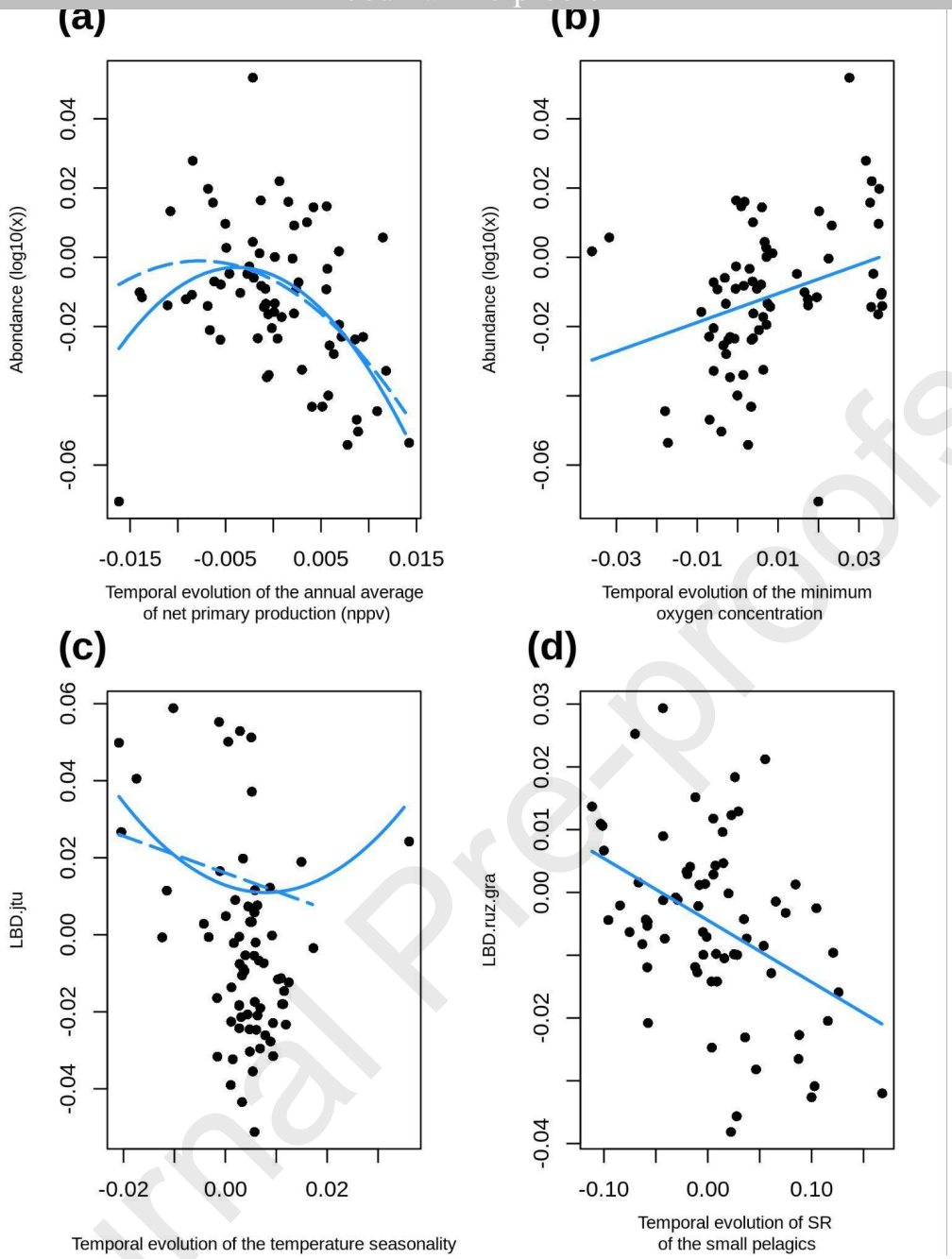


**Fig. S12:** Four of the main relationships between the temporal evolution of biodiversity metric and the temporal evolution of environmental variables. We present the relations between abundance and the annual average of the net primary productivity (a), abundance and the minimum oxygen concentration (b), LBD.jtu and temperature seasonality (c) and LBD.ruz.gra (local beta diversity of the gradient of abundance component) and the species richness of the small pelagic species. We used the slope of a linear model between a response variable and time as a proxy of temporal evolution. The relationships were fitted with generalised least square (GLS) models taking into account spatial autocorrelation using an exponential structure in the residuals. We retained linear and quadratic terms for (a) and (c), while only a linear term was retained for (b) and (d). Continuous lines represented the fit with all the 71 ICES rectangles while the dotted line represented the fit after removing one outlier ICES rectangle (n=70). All relationships were significant and the pseudo $R^2$ were 0.24, 0.16, 0.24, 0.21 for (a, b, c) and (d), respectively.

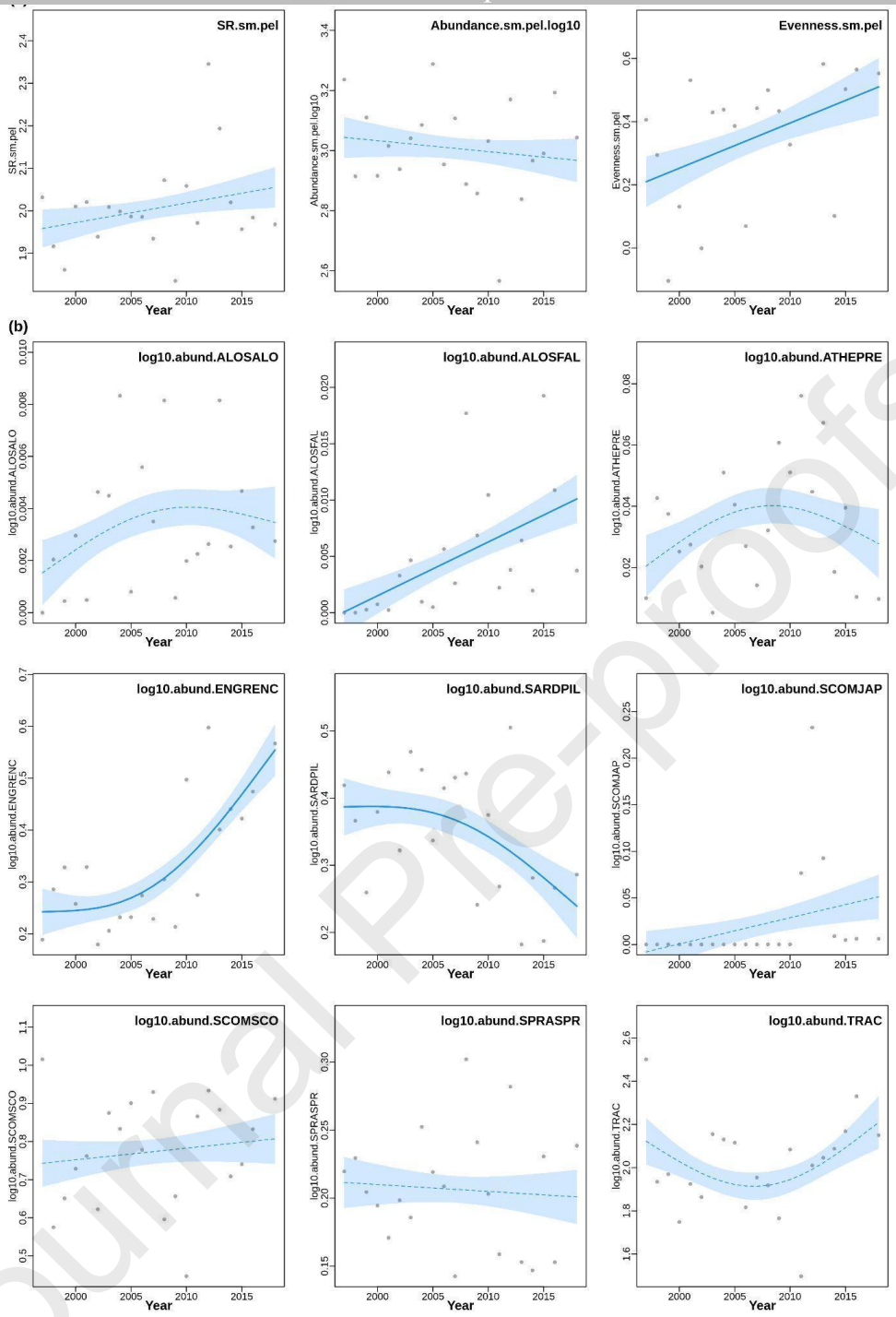


**Fig. S13:** (a) Temporal trends average by ICES rectangle per year for SR, abundance (log10(abundance)), Hurlbert's evenness for the 9 species of small pelagics of the Bay of Biscay and the Celtic Sea, and (b) the temporal trend of the abundance (log10) for each of the 9 species. ALOSALO: *Alosa alosa*, ALOSAFAL: *Alosa fallax*, ATHERPRE: *Atherina presbyter*, ENGRENC: *Engraulis encrasicolus*, SARDPIL: *Sardina pilchardus*, SCOMJAP: *Scomber japonicus*, SCOMSCO: *Scomber scrombrus*, SPRASPR: *Sprattus sprattus*, TRAC: *Tachurus sp.*. The blue curves represent the fit of generalised additive models (GAM), with solid lines indicating a significant relationship, while the dotted lines indicate a non-significant trend (with a p.value > 0.1), and the light blue area the standard error around the fit of the model.

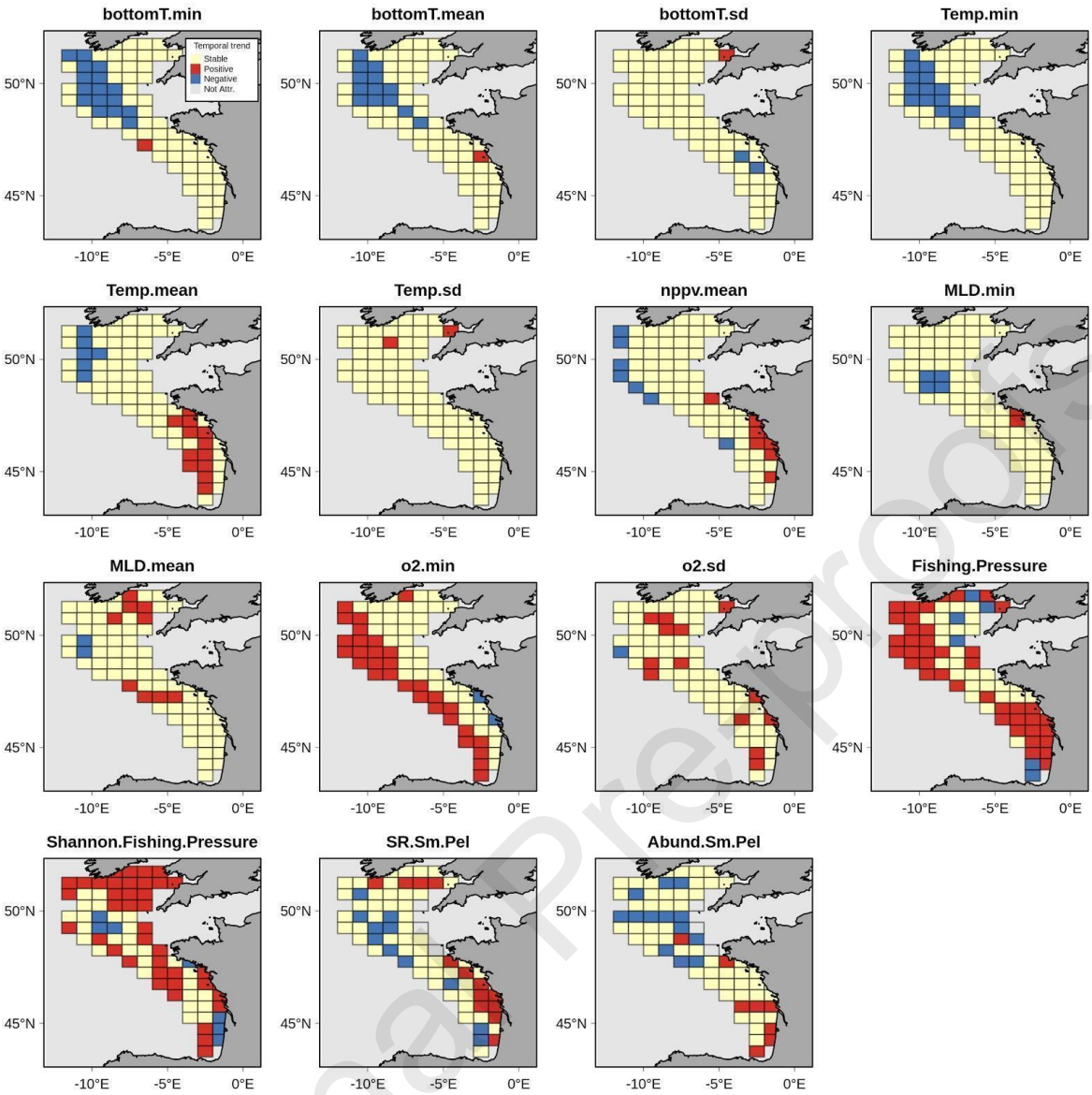


**Fig. S14:** Maps showing the temporal evolution of 15 dynamic environmental variables. bottomT.min: annual minimum bottom sea floor temperature, bottomT.mean: annual average of the bottom sea floor temperature, bottomT.sd: seasonality of the bottom sea floor temperature, Temp.min: annual minimum temperature integrated over depth, Temp.mean: average annual temperature integrated over depth, Temp.sd: seasonality of the temperature integrated over depth, nppv.mean: annual average of the net primary productivity, MLD.min: minimal annual thickness of the mixed layer depth, MLD.mean: average annual thickness of the mixed layer depth, o2.min: annual minimum oxygen concentration, o2.sd: seasonality of the oxygen concentration, Fishing.Pressure: sum of the fishing effort, Shannon.Fishing.Pressure: diversity of the fishing pressure based on the Shannon index of the fishing effort of the different fishing gears, SR.Sm.Pel: species richness of the small pelagic species, Abund.Sm.Pel: Abundance of the small pelagic species. Only 71 ICES rectangles sampled at least 5 times were retained for SR.Sm.Pel and Abund.Sm.Pel. The beige colour indicates a stable trend (slope not significantly different from 0 with a p.value > 0.1), while positive and negative trends are in red and blue, respectively.

## S4. Supplementary tables

**Table S1:** Variance partitioning based on linear model using the adjusted $R^2$ and considering the best set of spatial and temporal moran eigenvectors (MEM) in order to partition the variance attributed to space and time and their shared variance for each diversity index, for the demersal fish assemblages of the Bay of Biscay and the Celtic Sea. The full data set of 1242 rectangles by years was used to select the best spatial and temporal MEMs following the approach developed by Bauman et al. (2018). Values correspond to the percentage of explained variance.

| Metric | Explained | Space | Time | Shared.S.T. |
|---|---|---|---|---|
| SR | 10.4 | 6.3 | 4.5 | 0[a] |
| Abundance | 12.9 | 9.9 | 2.6 | 0.4 |
| Evenness | 11.4 | 9.3 | 1.7 | 0.4 |
| LBD.jac | 11 | 8.9 | 2.5 | 0[a] |
| LBD.jtu | 12.9 | 11.1 | 1.7 | 0.1 |
| LBD.jne | 8.5 | 2.7 | 5.7 | 0.1 |
| LBD.ruz | 8 | 5.6 | 2.3 | 0 |
| LBD.ruz.bal | 12.1 | 8.4 | 3.4 | 0.4 |
| LBD.ruz.gra | 12.9 | 8.6 | 4 | 0.3 |

[a]Negative values were converted to 0 (Legendre and Legendre, 1998), as such the sum of the variance of the individual categories might not add-up to the total explained variance.

**Table S2:** Variables and predictors (i.e. all linear and quadratic terms of the explanatory variables included in the model) selected for energy, habitat, and fishing pressure for all taxonomic alpha indices, for the contemporaneous variables. The 4 best predictors were retained per group of variables. To be retained, a predictor had to be selected in more than 20% of the iterations of the elastic-net GLM per year. bottomT.min: annual minimum bottom sea floor temperature, bottomT.mean: annual average of the bottom sea floor temperature, bottomT.sd: seasonality of the bottom sea floor temperature, Temp.min : annual minimum temperature integrated over depth, Temp.mean: average annual temperature integrated over depth, Temp.sd: seasonality of the temperature integrated over depth, nppv.mean: annual average of the net primary productivity, SR.Sm.Pel: species richness of the small pelagic species, Abund.Sm.Pel: Abundance of the small pelagic species, MLD.min: annual minimum thickness of the mixed layer depth, MLD.mean: average annual thickness of the mixed layer depth, o2.min : annual minimum oxygen concentration, o2.sd: seasonality of the oxygen concentration, Area_Km2: aera of the ICES rectangle, Bathy: average bathymetry of the ICES rectangle, Dist2coast: distance to the nearest coast, Substrate.Hab.Shannon: habitat diversity based on the Shannon index of 11 substrat classes, Fishing.Pressure: sum of the fishing effort, Shannon.Fishing.Pressure: diversity of the fishing pressure based on the Shannon index of the fishing effort of the different fishing gears.

| Variables.group | Metric | SR | Abundance | Evenness | LBD.jac | LBD.jtu | LBD.jne | LBD.ruz | LBD.ruz.bal | LBD.ruz.gra |
|---|---|---|---|---|---|---|---|---|---|---|
| Energy | bottomT.min | 1 | 1 | 1 | 0 | 0 | 0 | 0 | 1 | 1 |
| | bottomT.mean | 1 | 0 | 1 | 1 | 0 | 0 | 0 | 0 | 1 |
| | bottomT.sd | 0 | 0 | 0 | 0 | 0 | 0 | 0 | 0 | 0 |
| | Temp.min | 0 | 0 | 0 | 0 | 0 | 0 | 0 | 0 | 0 |
| | Temp.mean | 0 | 0 | 0 | 0 | 1 | 0 | 0 | 0 | 0 |
| | Temp.sd | 0 | 0 | 0 | 0 | 0 | 0 | 0 | 0 | 0 |
| | nppv.mean | 0 | 0 | 0 | 0 | 0 | 0 | 0 | 0 | 0 |
| | SR.Sm.Pel | 0 | 0 | 1 | 0 | 0 | 1 | 0 | 1 | 1 |
| | Abund.Sm.Pel | 1 | 1 | 0 | 1 | 1 | 0 | 1 | 0 | 0 |
| | bottomT.min^2 | 0 | 0 | 0 | 0 | 0 | 1 | 1 | 0 | 0 |
| | bottomT.mean^2 | 0 | 0 | 0 | 0 | 0 | 0 | 0 | 0 | 0 |
| | bottomT.sd^2 | 0 | 0 | 0 | 1 | 1 | 1 | 1 | 1 | 0 |
| | Temp.min^2 | 0 | 0 | 0 | 0 | 0 | 0 | 0 | 0 | 0 |
| | Temp.mean^2 | 0 | 0 | 0 | 0 | 0 | 0 | 0 | 0 | 0 |
| | Temp.sd^2 | 0 | 0 | 0 | 0 | 0 | 0 | 0 | 0 | 0 |
| | nppv.mean^2 | 0 | 0 | 0 | 0 | 0 | 0 | 0 | 0 | 0 |
| | SR.Sm.Pel^2 | 0 | 1 | 1 | 1 | 1 | 1 | 1 | 1 | 1 |
| | Abund.Sm.Pel^2 | 1 | 1 | 0 | 0 | 0 | 0 | 0 | 0 | 0 |
| Habitat | MLD.min | 1 | 1 | 1 | 1 | 1 | 0 | 0 | 0 | 1 |
| | MLD.mean | 0 | 0 | 0 | 1 | 1 | 0 | 1 | 1 | 1 |
| | o2.min | 0 | 0 | 0 | 0 | 0 | 1 | 0 | 0 | 0 |
| | o2.sd | 1 | 0 | 0 | 0 | 0 | 0 | 0 | 0 | 0 |
| | Area_Km2 | 0 | 0 | 0 | 0 | 0 | 0 | 1 | 0 | 0 |
| | Bathy | 0 | 0 | 0 | 0 | 0 | 0 | 0 | 0 | 0 |
| | Dist2coast | 1 | 0 | 1 | 0 | 0 | 0 | 1 | 1 | 1 |
| | Substrate.Hab.Shannon | 0 | 0 | 1 | 0 | 0 | 1 | 0 | 0 | 1 |
| | MLD.min^2 | 0 | 1 | 0 | 0 | 1 | 1 | 0 | 1 | 0 |
| | MLD.mean^2 | 0 | 1 | 0 | 1 | 0 | 0 | 0 | 0 | 0 |
| | o2.min^2 | 0 | 0 | 1 | 0 | 0 | 0 | 0 | 0 | 0 |
| | o2.sd^2 | 0 | 1 | 0 | 0 | 0 | 0 | 0 | 0 | 0 |

| | | | | | | | | | | |
|---|---|---|---|---|---|---|---|---|---|---|
| | Area_Km2^2 | 0 | 0 | 0 | 0 | 0 | 0 | 0 | 0 | 0 |
| | Bathy^2 | 1 | 0 | 0 | 1 | 1 | 0 | 1 | 1 | 0 |
| | Dist2coast^2 | 0 | 0 | 0 | 0 | 0 | 1 | 0 | 0 | 0 |
| | Substrate.Hab.Shannon^2 | 0 | 0 | 0 | 0 | 0 | 0 | 0 | 0 | 0 |
| FishingP | Fishing.Pressure | 1 | 1 | 1 | 1 | 1 | 1 | 1 | 1 | 1 |
| | Shannon.Fishing.Pressure | 1 | 1 | 1 | 1 | 1 | 1 | 1 | 1 | 1 |
| | Fishing.Pressure^2 | 1 | 1 | 1 | 1 | 1 | 1 | 1 | 0 | 1 |
| | Shannon.Fishing.Pressure^2 | 1 | 1 | 1 | 1 | 1 | 1 | 1 | 1 | 1 |

**Table S3:** Variance partitioning based on GAMM models including time (i.e. Year effect) as a random intercept, for species richness (SR, abundance (log10.abundance), Hurlbert's evenness, and all local beta diversity metrics, without the time lag for the explanatory variables. The adjusted R2 was used to estimate the proportion of explained variance by the fixed effects. E: energy, H: habitat, F: fishing pressure.

| Metric | Explained | E | H | F | Shared.E.F | Shared.E.H | Shared.H.F | Shared.E.H.F |
|---|---|---|---|---|---|---|---|---|
| SR | 12.3 | 6.2 | 3.5 | 0.7 | 0.8 | 0[a] | 0.1 | 3.1 |
| Log10.Abundance | 23.2 | 18.4 | 3 | 1 | 0[a] | 0[a] | 0.5 | 4.4 |
| Hurlbert.Evenness | 5.2 | 1.2 | 3.1 | 0.4 | 0[a] | 0[a] | 0 | 3.7 |
| LBD.jac | 26.9 | 18.1 | 2.1 | 0.8 | 1.1 | 0[a] | 0.4 | 4.5 |
| LBD.jtu | 28.6 | 18.8 | 1.3 | 1.9 | 0.7 | 1.4 | 0[a] | 4.8 |
| LBD.jne | 10.7 | 6.7 | 0.7 | 1.6 | 0[a] | 0.2 | 0[a] | 2.8 |
| LBD.ruz | 21.2 | 12.2 | 1.9 | 1.7 | 0[a] | 0[a] | 0[a] | 7.4 |
| LBD.ruz.bal | 21.5 | 7.9 | 4.2 | 3.5 | 0[a] | 0[a] | 0[a] | 12 |
| LBD.ruz.gra | 15.6 | 4 | 3.7 | 2.6 | 0[a] | 0[a] | 1.8 | 5.1 |

[a]Negative values were converted to 0 (Legendre & Legendre, 1998), as such the sum of the variance of the individual categories might not add-up to the total explained variance.

**Table S4:** Estimates and significance of the contemporaneous predictors (i.e. all linear and quadratic terms of the explanatory variables included in the model) retained in the most parsimonious steady-state and temporal models for SR, including models taking into account temporal and spatial autocorrelation in the residuals. Pred.: Predictors. Est: coefficient estimates based on a LMM with time as a random intercept, and a LM for the steady-state and temporal models respectively. Est.AR1: coefficient estimates for LMM and LM models including a temporal autocorrelation structure (AR1) in the residuals. Est.Exp: coefficient estimates for LMM and LM models including a spatial autocorrelation structure (exponential structure) in the residuals. Est.AR1.Exp: coefficient estimates for LMM and LM models including temporal and spatial autocorrelation structures in the residuals. Coefficient estimates with a significant p.value (lower than 0.05) are indicated in bold, and variables explaining at least 5% of the explained deviance are highlighted in grey. Part.Marg.R2.: express the semi-partial marginal $R^2$ (surrogate of the relative importance of each predictor based on the marginal $R^2$ [Nakagawa et al., 2017]) for each predictor in %. Psd.$R^2$ : corresponds to the Pseudo $R^2$, which is the $R^2$ from a linear model between the observed and the fitted values. Cond.$R^2$: it is the conditional $R^2$ including both the fixed and the random effects; it is available in the column Est. for the steady-state model only fitted with LMM including time as a random effect. Abund.Sm.Pel : Abundance of the small pelagic species. SR.Sm.Pel : Species richness of the small pelagic species.

| Metric | Model | Pred. | Est. | P.LMM | Part.Marg.R2 | Est.AR1 | P.LMM.AR1 | Est.Exp | P.LMM.Exp | Est.AR1.Exp | P.LMM.AR1.Exp |
|---|---|---|---|---|---|---|---|---|---|---|---|
| SR | Steady-state | Dist2coast | **-0.723** | 0 | 6.042 | **-0.699** | 0 | **-0.629** | 0 | **-0.641** | 0 |
| SR | Steady-state | Fishing.Pressure | **-0.287** | 0.002 | 1.005 | **-0.273** | 0.015 | **-0.257** | 0.008 | **-0.253** | 0.017 |
| SR | Steady-state | Abund.Sm.Pel | **-0.607** | 0 | 5.500 | **-0.57** | 0 | **-0.389** | 0 | **-0.394** | 0 |
| SR | Steady-state | **Psd.R2/Cond.R2** | 0.17 | - | 0.108 | 0.582 | - | 0.668 | - | 0.885 | - |
| SR | Temp. | Dist2coast | **-0.588** | 0 | 4.538 | **-0.573** | 0 | **-0.531** | 0 | **-0.541** | 0 |
| SR | Temp. | Abund.Sm.Pel | **-0.634** | 0 | 5.718 | **-0.606** | 0 | **-0.392** | 0 | **-0.398** | 0 |
| SR | Temp. | **Psd.R2/Cond.R2** | - | - | 0.103 | 0.507 | - | 0.671 | - | 0.881 | - |

**Table S5:** Estimates and significance of the contemporaneous predictors (i.e. all linear and quadratic terms of the explanatory variables included in the model) retained in the most parsimonious steady-state and temporal models for abundance, including models taking into account temporal and spatial autocorrelation in the residuals. Pred.: Predictors. Est: coefficient estimates based on a LMM with time as a random intercept, and a LM for the steady-state and temporal models respectively. Est.AR1: coefficient estimates for LMM and LM models including a temporal autocorrelation structure (AR1) in the residuals. Est.Exp: coefficient estimates for LMM and LM models including a spatial autocorrelation structure (exponential structure) in the residuals. Est.AR1.Exp: coefficient estimates for LMM and LM models including temporal and spatial autocorrelation structures in the residuals. Coefficient estimates with a significant p.value (lower than 0.05) are indicated in bold, and variables explaining at least 5% of the explained deviance are highlighted in grey. Part.Marg.$R^2$.: express the semi-partial marginal $R^2$ (surrogate of the relative importance of each predictor based on the marginal $R^2$ [Nakagawa et al., 2017]) for each predictor in %. Psd.$R^2$: corresponds to the Pseudo $R^2$ , which is the $R^2$ from a linear model between the observed and the fitted values. Cond.$R^2$: it is the conditional $R^2$ including both the fixed and the random effects; it is available in the column Est. for the steady-state model only fitted with LMM including time as a random effect. Abund.Sm.Pel: Abundance of the small pelagic species. SR.Sm.Pel: Species richness of the small pelagic species.

| Metric | Model | Pred. | Est. | P.LMM | Part.Marg.R2 | Est.AR1 | P.LMM.AR1 | Est.Exp | P.LMM.Exp | Est.AR1.Exp | P.LMM.AR1.Exp |
|---|---|---|---|---|---|---|---|---|---|---|---|
| Abund. | Steady-state | Abund.Sm.Pel | **0.134** | 0 | 5.775 | **0.134** | 0 | **0.14** | 0 | **0.138** | 0 |
| Abund. | Steady-state | MLD.min | **0.091** | 0 | 3.747 | **0.087** | 0 | **0.087** | 0 | **0.088** | 0 |
| Abund. | Steady-state | MLD.min^2 | **-0.029** | 0.002 | 0.909 | **-0.026** | 0.012 | **-0.027** | 0.012 | **-0.027** | 0.016 |
| Abund. | Steady-state | o2.sd^2 | **0.032** | 0.001 | 1.020 | **0.03** | 0.01 | **0.036** | 0 | **0.034** | 0.003 |
| Abund. | Steady-state | SR.Sm.Pel | **-0.101** | 0 | 2.790 | **-0.099** | 0 | **-0.099** | 0 | **-0.097** | 0 |
| Abund. | Steady-state | SR.Sm.Pel ^2 | **-0.046** | 0 | 2.799 | **-0.042** | 0 | **-0.044** | 0 | **-0.043** | 0 |
| Abund. | Steady-state | **Psd.R2/Cond.R2** | 0.216 | - | 0.195 | 0.463 | - | 0.599 | - | 0.693 | - |
| Abund. | Temp. | Abund.Sm.Pel | **0.132** | 0 | 3.578 | **0.133** | 0 | **0.14** | 0 | **0.138** | 0 |
| Abund. | Temp. | MLD.min | **0.093** | 0 | 4.017 | **0.09** | 0 | **0.087** | 0 | **0.088** | 0 |

| | | | | | | | | | | | |
|---|---|---|---|---|---|---|---|---|---|---|---|
| Abund. | Temp. | MLD.min^2 | **-0.028** | 0.003 | 0.624 | **-0.026** | 0.01 | **-0.026** | 0.014 | **-0.026** | 0.019 |
| Abund. | Temp. | o2.sd^2 | **0.033** | 0.001 | 0.517 | **0.031** | 0.007 | **0.036** | 0 | **0.034** | 0.003 |
| Abund. | Temp. | SR.Sm.Pel | **-0.1** | 0 | 8.743 | **-0.098** | 0 | **-0.099** | 0 | **-0.097** | 0 |
| Abund. | Temp. | SR.Sm.Pel ^2 | **-0.046** | 0 | 2.363 | **-0.042** | 0 | **-0.044** | 0 | **-0.043** | 0 |
| Abund. | Temp. | Time | **-0.037** | 0.003 | 0.69 | **-0.042** | 0.003 | -0.032 | 0.101 | -0.035 | 0.074 |
| Abund. | Temp. | **Psd.R2/Cond.R2** | - | - | 0.205 | 0.443 | - | 0.608 | - | 0.719 | - |

**Table S6:** Estimates and significance of the contemporaneous predictors (i.e. all linear and quadratic terms of the explanatory variables included in the model) retained in the most parsimonious steady-state and temporal models for Hurlbert's evenness, including models taking into account temporal and spatial autocorrelation in the residuals. Pred.: Predictors. Est: coefficient estimates based on a LMM with time as a random intercept, and a LM for the steady-state and temporal models respectively. Est.AR1: coefficient estimates for LMM and LM models including a temporal autocorrelation structure (AR1) in the residuals. Est.Exp: coefficient estimates for LMM and LM models including a spatial autocorrelation structure (exponential structure) in the residuals. Est.AR1.Exp: coefficient estimates for LMM and LM models including temporal and spatial autocorrelation structures in the residuals. Coefficient estimates with a significant p.value (lower than 0.05) are indicated in bold, and variables explaining at least 5% of the explained deviance are highlighted in grey. Part.Marg.$R^2$.: express the semi-partial marginal $R^2$ (surrogate of the relative importance of each predictor based on the marginal $R^2$ [Nakagawa et al., 2017]) for each predictor in %. Psd.$R^2$: corresponds to the Pseudo $R^2$ , which is the $R^2$ from a linear model between the observed and the fitted values. Cond.$R^2$: it is the conditional $R^2$ including both the fixed and the random effects; it is available in the column Est. for the steady-state model only fitted with LMM including time as a random effect. Abund.Sm.Pel: Abundance of the small pelagic species. SR.Sm.Pel: Species richness of the small pelagic species.

| Metric | Model | Pred. | Est. | P.LMM | Part.Marg.R2 | Est.AR1 | P.LMM.AR1 | Est.Exp | P.LMM.Exp | Est.AR1.Exp | P.LMM.AR1.Exp |
|---|---|---|---|---|---|---|---|---|---|---|---|
| Hurlbert.Evenness | Steady-state | Dist2coast | **-0.013** | 0 | 1.377 | **-0.012** | 0.005 | **-0.01** | 0.018 | **-0.011** | 0.023 |
| Hurlbert.Evenness | Steady-state | SR.Sm.Pel ^2 | **0.006** | 0.001 | 1.140 | **0.006** | 0.001 | **0.006** | 0.001 | **0.006** | 0.001 |
| Hurlbert.Evenness | Steady-state | **Psd.R2/Cond.R2** | 0.056 | - | 0.026 | 0.352 | - | 0.459 | - | 0.561 | - |
| Hurlbert.Evenness | Temp. | Dist2coast | **-0.013** | 0 | 1.437 | **-0.012** | 0.005 | **-0.01** | 0.017 | **-0.01** | 0.018 |
| Hurlbert.Evenness | Temp. | SR.Sm.Pel ^2 | **0.007** | 0 | 1.351 | **0.007** | 0 | **0.006** | 0.001 | **0.006** | 0.001 |
| Hurlbert.Evenness | Temp. | **Psd.R2/Cond.R2** | - | - | 0.028 | 0.29 | - | 0.463 | - | 1 | - |

**Table S7:** Estimates and significance of the contemporaneous predictors (i.e. all linear and quadratic terms of the explanatory variables included in the model) retained in the most parsimonious steady-state and temporal models for LBD.jac, including models taking into account temporal and spatial autocorrelation in the residuals. Pred.: Predictors. Est: coefficient estimates based on a LMM with time as a random intercept, and a LM for the steady-state and temporal models respectively. Est.AR1: coefficient estimates for LMM and LM models including a temporal autocorrelation structure (AR1) in the residuals. Est.Exp: coefficient estimates for LMM and LM models including a spatial autocorrelation structure (exponential structure) in the residuals. Est.AR1.Exp: coefficient estimates for LMM and LM models including temporal and spatial autocorrelation structures in the residuals. Coefficient estimates with a significant p.value (lower than 0.05) are indicated in bold, and variables explaining at least 5% of the explained deviance are highlighted in grey. Part.Marg.$R^2$.: express the semi-partial marginal $R^2$ (surrogate of the relative importance of each predictor based on the marginal $R^2$ [Nakagawa et al., 2017]) for each predictor in %. Psd.$R^2$: corresponds to the Pseudo $R^2$ , which is the $R^2$ from a linear model between the observed and the fitted values. Cond.$R^2$: it is the conditional $R^2$ including both the fixed and the random effects; it is available in the column Est. for the steady-state model only fitted with LMM including time as a random effect. Abund.Sm.Pel: Abundance of the small pelagic species. SR.Sm.Pel: Species richness of the small pelagic species.

| Metric | Model | Pred. | Est. | P.LMM | Part.Marg.R2 | Est.AR1 | P.LMM.AR1 | Est.Exp | P.LMM.Exp | Est.AR1.Exp | P.LMM.AR1.Exp |
|---|---|---|---|---|---|---|---|---|---|---|---|
| LBD.jac | Steady-state | Bathy_mean^2 | **0.01** | 0 | 3.938 | **0.01** | 0 | **0.008** | 0 | **0.008** | 0 |
| LBD.jac | Steady-state | Fishing.Pressure | **0.009** | 0 | 1.511 | **0.009** | 0.012 | 0.005 | 0.056 | **0.006** | 0.049 |
| LBD.jac | Steady-state | Fishing.Pressure^2 | **0.006** | 0 | 1.610 | **0.006** | 0.001 | 0.001 | 0.559 | 0.002 | 0.348 |
| LBD.jac | Steady-state | Abund.Sm.Pel | **0.025** | 0 | 10.804 | **0.022** | 0 | **0.014** | 0 | **0.015** | 0 |
| LBD.jac | Steady-state | SR.Sm.Pel ^2 | **0.012** | 0 | 7.950 | **0.011** | 0 | **0.009** | 0 | **0.009** | 0 |
| LBD.jac | Steady-state | **Psd.R2/Cond.R2** | 0.265 | - | 0.227 | 0.776 | - | 0.86 | - | 0.92 | - |
| LBD.jac | Temp. | Bathy_mean^2 | **0.01** | 0 | 3.714 | **0.01** | 0 | **0.008** | 0 | **0.008** | 0 |
| LBD.jac | Temp. | Fishing.Pressure | **0.011** | 0 | 1.655 | **0.01** | 0.002 | **0.006** | 0.03 | **0.006** | 0.032 |
| LBD.jac | Temp. | Fishing.Pressure^2 | **0.006** | 0 | 2.886 | **0.006** | 0.002 | 0.001 | 0.431 | 0.002 | 0.3 |

| | | | | | | | | | | | |
|---|---|---|---|---|---|---|---|---|---|---|---|
| LBD.jac | Temp. | Abund.Sm.Pel | **0.024** | 0 | 8.019 | **0.022** | 0 | **0.015** | 0 | **0.015** | 0 |
| LBD.jac | Temp. | SR.Sm.Pel ^2 | **0.011** | 0 | 6.332 | **0.01** | 0 | **0.009** | 0 | **0.009** | 0 |
| LBD.jac | Temp. | Time | **-0.015** | 0 | 0.633 | **-0.014** | 0 | 0 | 0.969 | -0.001 | 0.878 |
| LBD.jac | Temp. | Bathy_mean^2:Time | **0.009** | 0 | 2.4 | **0.008** | 0 | **0.005** | 0 | **0.005** | 0 |
| LBD.jac | Temp. | **Psd.R2/Cond.R2** | - | - | 0.256 | 0.773 | - | 0.856 | - | 0.914 | - |

**Table S8:** Estimates and significance of the contemporaneous predictors (i.e. all linear and quadratic terms of the explanatory variables included in the model) retained in the most parsimonious steady-state and temporal models for LBD.jtu, including models taking into account temporal and spatial autocorrelation in the residuals. Pred.: Predictors. Est: coefficient estimates based on a LMM with time as a random intercept, and a LM for the steady-state and temporal models respectively. Est.AR1: coefficient estimates for LMM and LM models including a temporal autocorrelation structure (AR1) in the residuals. Est.Exp: coefficient estimates for LMM and LM models including a spatial autocorrelation structure (exponential structure) in the residuals. Est.AR1.Exp: coefficient estimates for LMM and LM models including temporal and spatial autocorrelation structures in the residuals. Coefficient estimates with a significant p.value (lower than 0.05) are indicated in bold, and variables explaining at least 5% of the explained deviance are highlighted in grey. Part.Marg.$R^2$.: express the semi-partial marginal $R^2$ (surrogate of the relative importance of each predictor based on the marginal $R^2$ [Nakagawa et al. 2017]) for each predictor in %. Psd.$R^2$: corresponds to the Pseudo $R^2$ , which is the $R^2$ from a linear model between the observed and the fitted values. Cond.$R^2$: it is the conditional $R^2$ including both the fixed and the random effects; it is available in the column Est. for the steady-state model only fitted with LMM including time as a random effect. Abund.Sm.Pel : Abundance of the small pelagic species. SR.Sm.Pel : Species richness of the small pelagic species.

| Metric | Model | Pred. | Est. | P.LMM | Part.Marg.R2 | Est.AR1 | P.LMM.AR1 | Est.Exp | P.LMM.Exp | Est.AR1.Exp | P.LMM.AR1.Exp |
|---|---|---|---|---|---|---|---|---|---|---|---|
| LBD.jtu | Steady-state | Bathy_mean^2 | **0.009** | 0 | 2.083 | **0.01** | 0.001 | **0.009** | 0 | **0.009** | 0 |
| LBD.jtu | Steady-state | Fishing.Pressure^2 | **0.006** | 0.001 | 1.083 | **0.006** | 0.008 | 0.001 | 0.593 | 0.001 | 0.443 |
| LBD.jtu | Steady-state | Abund.Sm.Pel | **0.028** | 0 | 9.683 | **0.024** | 0 | **0.014** | 0 | **0.015** | 0 |
| LBD.jtu | Steady-state | MLD.min | **-0.013** | 0 | 1.574 | -0.005 | 0.258 | -0.006 | 0.343 | -0.006 | 0.344 |
| LBD.jtu | Steady-state | MLD.min^2 | **0.009** | 0 | 2.083 | **0.007** | 0.003 | **0.007** | 0.005 | **0.007** | 0.007 |
| LBD.jtu | Steady-state | SR.Sm.Pel ^2 | **0.016** | 0 | 10.546 | **0.015** | 0 | **0.012** | 0 | **0.013** | 0 |
| LBD.jtu | Steady-state | **Psd.R2/Cond.R2** | 0.263 | - | 0.243 | 0.821 | - | 0.858 | - | 0.924 | - |
| LBD.jtu | Temp. | Bathy_mean^2 | **0.01** | 0 | 4.298 | **0.011** | 0 | **0.009** | 0 | **0.009** | 0 |
| LBD.jtu | Temp. | Abund.Sm.Pel | **0.024** | 0 | 7.168 | **0.022** | 0 | **0.015** | 0 | **0.015** | 0 |

| | | | | | | | | | | | |
|---|---|---|---|---|---|---|---|---|---|---|---|
| LBD.jtu | Temp. | MLD.min | **-0.015** | 0 | 0.688 | -0.006 | 0.116 | -0.005 | 0.356 | -0.006 | 0.335 |
| LBD.jtu | Temp. | MLD.min^2 | **0.008** | 0 | 1.937 | **0.005** | 0.036 | 0.004 | 0.112 | 0.004 | 0.116 |
| LBD.jtu | Temp. | SR.Sm.Pel ^2 | **0.015** | 0 | 9.48 | **0.014** | 0 | **0.012** | 0 | **0.012** | 0 |
| LBD.jtu | Temp. | Time | **-0.024** | 0 | 0.38 | **-0.021** | 0 | -0.012 | 0.214 | -0.012 | 0.203 |
| LBD.jtu | Temp. | Bathy_mean^2:Time | **0.007** | 0.001 | 2.467 | **0.005** | 0.037 | **0.005** | 0.001 | **0.005** | 0.004 |
| LBD.jtu | Temp. | MLD.min:Time | **-0.017** | 0 | 0.812 | **-0.018** | 0 | **-0.017** | 0.004 | **-0.017** | 0.003 |
| LBD.jtu | Temp. | MLD.min^2:Time | **0.012** | 0 | 1.821 | **0.012** | 0 | **0.009** | 0.001 | **0.009** | 0.001 |
| LBD.jtu | Temp. | Psd.R2/Cond.R2 | - | - | 0.291 | 0.828 | - | 0.857 | - | 0.923 | - |

**Table S9:** Estimates and significance of the contemporaneous predictors (i.e. all linear and quadratic terms of the explanatory variables included in the model) retained in the most parsimonious steady-state and temporal models for LBD.jne, including models taking into account temporal and spatial autocorrelation in the residuals. Pred.: Predictors. Est: coefficient estimates based on a LMM with time as a random intercept, and a LM for the steady-state and temporal models respectively. Est.AR1: coefficient estimates for LMM and LM models including a temporal autocorrelation structure (AR1) in the residuals. Est.Exp: coefficient estimates for LMM and LM models including a spatial autocorrelation structure (exponential structure) in the residuals. Est.AR1.Exp: coefficient estimates for LMM and LM models including temporal and spatial autocorrelation structures in the residuals. Coefficient estimates with a significant p.value (lower than 0.05) are indicated in bold, and variables explaining at least 5% of the explained deviance are highlighted in grey. Part.Marg.$R^2$.: express the semi-partial marginal $R^2$ (surrogate of the relative importance of each predictor based on the marginal $R^2$ [Nakagawa et al. 2017]) for each predictor in %. Psd.$R^2$: corresponds to the Pseudo $R^2$ , which is the $R^2$ from a linear model between the observed and the fitted values. Cond.$R^2$: it is the conditional $R^2$ including both the fixed and the random effects; it is available in the column Est. for the steady-state model only fitted with LMM including time as a random effect. Abund.Sm.Pel: Abundance of the small pelagic species. SR.Sm.Pel: Species richness of the small pelagic species.

| Metric | Model | Pred. | Est. | P.LMM | Part.Marg.R2 | Est.AR1 | P.LMM.AR1 | Est.Exp | P.LMM.Exp | Est.AR1.Exp | P.LMM.AR1.Exp |
|---|---|---|---|---|---|---|---|---|---|---|---|
| LBD.jne | Steady-state | Fishing.Pressure^2 | **-0.002** | 0.003 | 0.837 | **-0.002** | 0.009 | -0.001 | 0.102 | -[a] | -[a] |
| LBD.jne | Steady-state | Shannon.Fishing.Pressure | **-0.003** | 0 | 1.282 | **-0.003** | 0.002 | -0.002 | 0.159 | -[a] | -[a] |
| LBD.jne | Steady-state | SR.Sm.Pel ^2 | **-0.004** | 0 | 5.237 | **-0.004** | 0 | **-0.003** | 0 | -[a] | -[a] |
| LBD.jne | Steady-state | **Psd.R2/Cond.R2** | 0.202 | - | 0.089 | 0.917 | - | 0.705 | - | -[a] | - |
| LBD.jne | Temp. | Shannon.Fishing.Pressure | **-0.004** | 0 | 2.845 | **-0.004** | 0 | -0.002 | 0.071 | -0.002 | 0.058 |
| LBD.jne | Temp. | SR.Sm.Pel ^2 | **-0.004** | 0 | 5.998 | **-0.004** | 0 | **-0.003** | 0 | **-0.003** | 0 |
| LBD.jne | Temp. | **Psd.R2/Cond.R2** | - | - | 0.088 | 0.892 | - | 0.706 | - | 1 | - |

[a] The model did not converge properly

**Table S10:** Estimates and significance of the contemporaneous predictors (i.e. all linear and quadratic terms of the explanatory variables included in the model) retained in the most parsimonious steady-state and temporal models for LBD.ruz, including models taking into account temporal and spatial autocorrelation in the residuals. Pred.: Predictors. Est: coefficient estimates based on a LMM with time as a random intercept, and a LM for the steady-state and temporal models respectively. Est.AR1: coefficient estimates for LMM and LM models including a temporal autocorrelation structure (AR1) in the residuals. Est.Exp: coefficient estimates for LMM and LM models including a spatial autocorrelation structure (exponential structure) in the residuals. Est.AR1.Exp: coefficient estimates for LMM and LM models including temporal and spatial autocorrelation structures in the residuals. Coefficient estimates with a significant p.value (lower than 0.05) are indicated in bold, and variables explaining at least 5% of the explained deviance are highlighted in grey. Part.Marg.$R^2$.: express the semi-partial marginal $R^2$ (surrogate of the relative importance of each predictor based on the marginal $R^2$ [Nakagawa et al. 2017]) for each predictor in %. Psd.$R^2$: corresponds to the Pseudo $R^2$ , which is the $R^2$ from a linear model between the observed and the fitted values. Cond.R2 : it is the conditional $R^2$ including both the fixed and the random effects, it is available in the column Est. for the steady-state model only fitted with LMM including time as a random effect. Abund.Sm.Pel: Abundance of the small pelagic species. SR.Sm.Pel: Species richness of the small pelagic species.

| Metric | Model | Pred. | Est. | P.LMM | Part.Marg.R2 | Est.AR1 | P.LMM.AR1 | Est.Exp | P.LMM.Exp | Est.AR1.Exp | P.LMM.AR1.Exp |
|---|---|---|---|---|---|---|---|---|---|---|---|
| LBD.ruz | Steady-state | Bathy_mean^2 | **0.005** | 0 | 4.799 | **0.005** | 0 | **0.005** | 0 | **0.005** | 0 |
| LBD.ruz | Steady-state | bottomT.min | **-0.005** | 0 | 2.275 | **-0.006** | 0 | **-0.005** | 0.003 | **-0.005** | 0.006 |
| LBD.ruz | Steady-state | Abund.Sm.Pel | **0.009** | 0 | 6.274 | **0.009** | 0 | **0.008** | 0 | **0.008** | 0 |
| LBD.ruz | Steady-state | SR.Sm.Pel ^2 | **0.003** | 0 | 1.753 | **0.003** | 0 | **0.003** | 0 | **0.003** | 0 |
| LBD.ruz | Steady-state | **Psd.R2/Cond.R2** | 0.164 | - | 0.128 | 0.648 | - | 0.783 | - | 0.859 | - |
| LBD.ruz | Temp. | Bathy_mean^2 | **0.005** | 0 | 4.103 | **0.005** | 0 | **0.005** | 0 | **0.005** | 0 |
| LBD.ruz | Temp. | bottomT.min | **-0.005** | 0 | 1.48 | **-0.005** | 0 | **-0.005** | 0.003 | **-0.005** | 0.006 |
| LBD.ruz | Temp. | Abund.Sm.Pel | **0.009** | 0 | 5.703 | **0.009** | 0 | **0.008** | 0 | **0.008** | 0 |
| LBD.ruz | Temp. | SR.Sm.Pel ^2 | **0.003** | 0 | 1.593 | **0.003** | 0 | **0.003** | 0 | **0.003** | 0 |
| LBD.ruz | Temp. | **Psd.R2/Cond.R2** | - | - | 0.129 | 0.617 | - | 0.785 | - | 0.86 | - |

**Table S11:** Estimates and significance of the contemporaneous predictors (i.e. all linear and quadratic terms of the explanatory variables included in the model) retained in the most parsimonious steady-state and temporal models for LBD.ruz.bal, including models taking into account temporal and spatial autocorrelation in the residuals. Pred.: Predictors. Est: coefficient estimates based on a LMM with time as a random intercept, and a LM for the steady-state and temporal models respectively. Est.AR1: coefficient estimates for LMM and LM models including a temporal autocorrelation structure (AR1) in the residuals. Est.Exp: coefficient estimates for LMM and LM models including a spatial autocorrelation structure (exponential structure) in the residuals. Est.AR1.Exp: coefficient estimates for LMM and LM models including temporal and spatial autocorrelation structures in the residuals. Coefficient estimates with a significant p.value (lower than 0.05) are indicated in bold, and variables explaining at least 5% of the explained deviance are highlighted in grey. Part.Marg.$R^2$.: express the semi-partial marginal $R^2$ (surrogate of the relative importance of each predictor based on the marginal $R^2$ [Nakagawa et al. 2017]) for each predictor in %. Psd.$R^2$: corresponds to the Pseudo $R^2$ , which is the $R^2$ from a linear model between the observed and the fitted values. Cond.$R^2$: it is the conditional $R^2$ including both the fixed and the random effects; it is available in the column Est. for the steady-state model only fitted with LMM including time as a random effect. Abund.Sm.Pel: Abundance of the small pelagic species. SR.Sm.Pel: Species richness of the small pelagic species.

| Metric | Model | Pred. | Est. | P.LMM | Part.Marg.R2 | Est.AR1 | P.LMM.AR1 | Est.Exp | P.LMM.Exp | Est.AR1.Exp | P.LMM.AR1.Exp |
|---|---|---|---|---|---|---|---|---|---|---|---|
| LBD.ruz.bal | Steady-state | Bathy_mean^2 | **0.01** | 0 | 2.803 | **0.01** | 0 | **0.009** | 0 | **0.009** | 0 |
| LBD.ruz.bal | Steady-state | bottomT.min | **-0.013** | 0 | 2.367 | **-0.013** | 0 | **-0.008** | 0.027 | **-0.008** | 0.03 |
| LBD.ruz.bal | Steady-state | MLD.min | **-0.016** | 0 | 2.674 | **-0.012** | 0.001 | -0.009 | 0.113 | -0.008 | 0.155 |
| LBD.ruz.bal | Steady-state | MLD.min^2 | **0.01** | 0 | 2.639 | **0.009** | 0 | **0.007** | 0.002 | **0.007** | 0.006 |
| LBD.ruz.bal | Steady-state | SR.Sm.Pel | **0.016** | 0 | 3.964 | **0.016** | 0 | **0.014** | 0 | **0.014** | 0 |
| LBD.ruz.bal | Steady-state | **Psd.R2/Cond.R2** | 0.203 | - | 0.147 | 0.736 | - | 0.774 | - | 0.865 | - |
| LBD.ruz.bal | Temp. | Bathy_mean^2 | **0.011** | 0 | 4.46 | **0.011** | 0 | **0.009** | 0 | **0.009** | 0 |
| LBD.ruz.bal | Temp. | bottomT.min | **-0.012** | 0 | 2.727 | **-0.012** | 0 | **-0.009** | 0.017 | **-0.009** | 0.02 |
| LBD.ruz.bal | Temp. | MLD.min | **-0.013** | 0 | 0.693 | **-0.008** | 0.025 | -0.009 | 0.112 | -0.008 | 0.15 |
| LBD.ruz.bal | Temp. | MLD.min^2 | **0.01** | 0 | 2.91 | **0.008** | 0 | **0.007** | 0.002 | **0.007** | 0.006 |

| | | | | | | | | | | | |
|---|---|---|---|---|---|---|---|---|---|---|---|
| LBD.ruz.bal | Temp. | SR.Sm.Pel | **0.017** | 0 | 3.899 | **0.017** | 0 | **0.014** | 0 | **0.014** | 0 |
| LBD.ruz.bal | Temp. | Time | **0.008** | 0.001 | 0.902 | **0.01** | 0.001 | 0.013 | 0.057 | 0.012 | 0.069 |
| LBD.ruz.bal | Temp. | **Psd.R2/Cond.R2** | - | - | 0.156 | 0.684 | - | 0.779 | - | 0.868 | - |

**Table S12:** Estimates and significance of the contemporaneous predictors (i.e. all linear and quadratic terms of the explanatory variables included in the model) retained in the most parsimonious steady-state and temporal models for LBD.ruz.gra, including models taking into account temporal and spatial autocorrelation in the residuals. Pred.: Predictors. Est: coefficient estimates based on a LMM with time as a random intercept, and a LM for the steady-state and temporal models respectively. Est.AR1: coefficient estimates for LMM and LM models including a temporal autocorrelation structure (AR1) in the residuals. Est.Exp: coefficient estimates for LMM and LM models including a spatial autocorrelation structure (exponential structure) in the residuals. Est.AR1.Exp: coefficient estimates for LMM and LM models including temporal and spatial autocorrelation structures in the residuals. Coefficient estimates with a significant p.value (lower than 0.05) are indicated in bold, and variables explaining at least 5% of the explained deviance are highlighted in grey. Part.Marg.$R^2$.: express the semi-partial marginal $R^2$ (surrogate of the relative importance of each predictor based on the marginal $R^2$ [Nakagawa et al. 2017]) for each predictor in %. Psd.$R^2$: corresponds to the Pseudo $R^2$ , which is the $R^2$ from a linear model between the observed and the fitted values. Cond.$R^2$: it is the conditional $R^2$ including both the fixed and the random effects; it is available in the column Est. for the steady-state model only fitted with LMM including time as a random effect. Abund.Sm.Pel: Abundance of the small pelagic species. SR.Sm.Pel: Species richness of the small pelagic species.

| Metric | Model | Pred. | Est. | P.LMM | Part.Marg.R2 | Est.AR1 | P.LMM.AR1 | Est.Exp | P.LMM.Exp | Est.AR1.Exp | P.LMM.AR1.Exp |
|---|---|---|---|---|---|---|---|---|---|---|---|
| LBD.ruz.gra | Steady-state | Dist2coast | **0.011** | 0 | 3.114 | **0.011** | 0 | **0.006** | 0.031 | **0.007** | 0.017 |
| LBD.ruz.gra | Steady-state | Shannon.Fishing.Pressure | **-0.012** | 0 | 3.439 | **-0.011** | 0 | **-0.006** | 0.011 | **-0.006** | 0.012 |
| LBD.ruz.gra | Steady-state | SR.Sm.Pel | **-0.007** | 0 | 1.517 | **-0.008** | 0 | **-0.007** | 0 | **-0.007** | 0 |
| LBD.ruz.gra | Steady-state | **Psd.R2/Cond.R2** | 0.182 | - | 0.11 | 0.659 | - | 0.75 | - | 0.843 | - |
| LBD.ruz.gra | Temp. | Dist2coast | **0.011** | 0 | 6.056 | **0.011** | 0 | **0.006** | 0.028 | **0.007** | 0.017 |
| LBD.ruz.gra | Temp. | Shannon.Fishing.Pressure | **-0.012** | 0 | 4.091 | **-0.012** | 0 | **-0.006** | 0.01 | **-0.006** | 0.012 |
| LBD.ruz.gra | Temp. | SR.Sm.Pel | **-0.008** | 0 | 1.507 | **-0.008** | 0 | **-0.007** | 0 | **-0.007** | 0 |
| LBD.ruz.gra | Temp. | **Psd.R2/Cond.R2** | - | - | 0.117 | 0.575 | - | 0.75 | - | 0.843 | - |

**Table S13:** Univariate selection of the explanatory variables fitted with a generalised additive mixed model (GAMM) with the best lag worth to be retained. The temporal effect was included as a random intercept in the GAMM model and the spatial autocorrelation in the residuals was accounted for by an exponential structure. To avoid overfitting, a maximum of 3 basis dimensions were used to represent the smooth term in the GAMM. We have also presented the outcomes of the multivariate selection procedure for energy, habitat and fishing pressure based on the GLM elastic net models including the best lag variables when the 4 best predictors were retained. Highlighted in grey are the variables with lag providing an improvement of the adjust.$R^2$ higher than 0.03 (3%) comparatively to the contemporaneous (absence of lag) variable. Best.lag: the lag retained by the selection procedure, GAM.adj.R2: The adjusted $R^2$ produced by the GAMM model, Improvement.R2.lag0: improvement of the adjusted $R^2$ provided by the best lag in comparison to the fit of the contemporaneous variable. Select.4best; when 1 the variable was retained by the Elastic-net GLM approach, when 0 the variable was not retained.

| Metric | Variable | Best.lag | GAM.adj.R2 | Improvement.R2.lag0 | Select.4best |
|---|---|---|---|---|---|
| SR | bottomT.min | 1 | 0.042 | 0.021 | 1 |
| | bottomT.mean | 1 | 0.022 | 0.02 | 0 |
| | Temp.min | 2 | 0.034 | 0.026 | 0 |
| | o2.sd | 2 | 0.045 | 0.022 | 1 |
| LBD.jac | MLD.min | 2 | 0.074 | 0.03 | 1 |
| LBD.jtu | MLD.min | 2 | 0.08 | 0.037 | 1 |
| LBD.jne | o2.min | 2 | 0.043 | 0.022 | 1 |
| LBD.ruz | MLD.min | 2 | 0.048 | 0.021 | 1 |
| LBD.ruz.bal | MLD.min | 2 | 0.116 | 0.045 | 1 |
| LBD.ruz.gra | Temp.sd | 2 | 0.064 | 0.021 | 0 |
| | MLD.min | 2 | 0.114 | 0.049 | 1 |
| | MLD.mean | 1 | 0.065 | 0.02 | 1 |

**Table S14:** Variables and predictors (i.e. all linear and quadratic terms of the explanatory variables included in the model) selected for energy, habitat, and fishing pressure for all taxonomic alpha indices, with the best time lag selected for the explanatory variables. The 4 best predictors were retained per group of variables. To be retained, a predictor had to be selected in more than 20% of the iterations of the elastic-net GLM per year. bottomT.min: annual minimum bottom sea floor temperature, bottomT.mean: annual average of the bottom sea floor temperature, bottomT.sd: seasonality of the bottom sea floor temperature, Temp.min: annual minimum temperature integrated over depth, Temp.mean: average annual temperature integrated over depth, Temp.sd: seasonality of the temperature integrated over depth, nppv.mean : annual average of the net primary productivity, SR.Sm.Pel: species richness of the small pelagic species, Abund.Sm.Pel: Abundance of the small pelagic species, MLD.min: annual minimum thickness of the mixed layer depth, MLD.mean: average annual thickness of the mixed layer depth, o2.min: annual minimum oxygen concentration, o2.sd: seasonality of the oxygen concentration, Area_Km2: aera of the ICES rectangle, Bathy: average bathymetry of the ICES rectangle, Dist2coast: distance to the nearest coast, Substrate.Hab.Shannon: habitat diversity based on the Shannon index of 11 substrat classes, Fishing.Pressure: sum of the fishing effort, Shannon.Fishing.Pressure: diversity of the fishing pressure based on the Shannon index of the fishing effort of the different fishing gears.

| Variables.group | Metric | SR | Abundance | Evenness | LBD.jac | LBD.jtu | LBD.jne | LBD.ruz | LBD.ruz.bal | LBD.ruz.gra |
|---|---|---|---|---|---|---|---|---|---|---|
| Energy | bottomT.min | 1 | 0 | 1 | 1 | 0 | 0 | 1 | 1 | 1 |
| | bottomT.mean | 0 | 0 | 1 | 0 | 0 | 0 | 0 | 0 | 1 |
| | bottomT.sd | 0 | 0 | 0 | 0 | 0 | 0 | 0 | 0 | 0 |
| | Temp.min | 0 | 0 | 1 | 0 | 0 | 0 | 0 | 0 | 0 |
| | Temp.mean | 0 | 0 | 1 | 0 | 1 | 0 | 0 | 0 | 0 |
| | Temp.sd | 0 | 0 | 0 | 0 | 0 | 0 | 0 | 0 | 0 |
| | nppv.mean | 0 | 0 | 0 | 0 | 0 | 0 | 0 | 0 | 0 |
| | SR.Sm.Pel | 0 | 1 | 0 | 0 | 0 | 1 | 1 | 1 | 1 |
| | Abund.Sm.Pel | 1 | 1 | 0 | 1 | 1 | 0 | 1 | 0 | 0 |
| | bottomT.min^2 | 1 | 0 | 0 | 0 | 0 | 1 | 0 | 0 | 0 |
| | bottomT.mean^2 | 0 | 0 | 0 | 0 | 0 | 0 | 0 | 0 | 0 |
| | bottomT.sd^2 | 0 | 0 | 0 | 1 | 1 | 1 | 1 | 1 | 0 |
| | Temp.min^2 | 0 | 0 | 0 | 0 | 0 | 0 | 0 | 0 | 0 |
| | Temp.mean^2 | 0 | 0 | 0 | 0 | 0 | 0 | 0 | 0 | 0 |
| | Temp.sd^2 | 0 | 0 | 0 | 0 | 0 | 0 | 0 | 0 | 0 |
| | nppv.mean^2 | 0 | 0 | 0 | 0 | 0 | 0 | 0 | 0 | 0 |

| | | | | | | | | | | |
|---|---|---|---|---|---|---|---|---|---|---|
| | SR.Sm.Pel^2 | 0 | 1 | 0 | 1 | 1 | 1 | 0 | 1 | 1 |
| | Abund.Sm.Pel^2 | 1 | 1 | 0 | 0 | 0 | 0 | 0 | 0 | 0 |
| Habitat | MLD.min | 1 | 1 | 1 | 1 | 1 | 1 | 0 | 0 | 1 |
| | MLD.mean | 0 | 0 | 0 | 1 | 1 | 0 | 0 | 1 | 1 |
| | o2.min | 0 | 0 | 0 | 0 | 0 | 1 | 0 | 0 | 0 |
| | o2.sd | 1 | 0 | 0 | 0 | 0 | 0 | 0 | 0 | 0 |
| | Area_Km2 | 0 | 1 | 0 | 0 | 0 | 0 | 1 | 0 | 0 |
| | Bathy | 0 | 0 | 0 | 0 | 0 | 0 | 0 | 0 | 0 |
| | Dist2coast | 1 | 0 | 1 | 0 | 0 | 0 | 1 | 1 | 1 |
| | Substrate.Hab.Shannon | 0 | 0 | 1 | 0 | 0 | 0 | 0 | 0 | 0 |
| | MLD.min^2 | 1 | 1 | 0 | 1 | 1 | 1 | 1 | 1 | 0 |
| | MLD.mean^2 | 0 | 0 | 0 | 0 | 0 | 0 | 0 | 0 | 1 |
| | o2.min^2 | 0 | 0 | 0 | 0 | 0 | 0 | 0 | 0 | 0 |
| | o2.sd^2 | 0 | 0 | 1 | 0 | 0 | 0 | 0 | 0 | 0 |
| | Area_Km2^2 | 0 | 0 | 0 | 0 | 0 | 0 | 0 | 0 | 0 |
| | Bathy^2 | 0 | 0 | 0 | 1 | 1 | 1 | 1 | 1 | 0 |
| | Dist2coast^2 | 0 | 0 | 0 | 0 | 0 | 0 | 0 | 0 | 0 |
| | Substrate.Hab.Shannon^2 | 0 | 1 | 0 | 0 | 0 | 0 | 0 | 0 | 0 |
| FishingP | Fishing.Pressure | 1 | 1 | 1 | 1 | 1 | 1 | 1 | 1 | 1 |
| | Shannon.Fishing.Pressure | 1 | 1 | 1 | 1 | 1 | 1 | 1 | 1 | 1 |
| | Fishing.Pressure^2 | 1 | 1 | 1 | 1 | 1 | 1 | 1 | 0 | 0 |
| | Shannon.Fishing.Pressure^2 | 1 | 1 | 1 | 1 | 1 | 0 | 1 | 1 | 0 |

**Table S15:** Variance partitioning based on LMM models including time (i.e. Year effect) as a random intercept, for species richness (SR), and all local beta diversity metrics, with the best time lag for the explanatory variables. The marginal $R^2$ (Nakagawa et al., 2017) was used to estimate the proportion of explained variance by the fixed effects for the LMMs. E: energy, H: habitat, F: fishing pressure.

| **Metric** | **Explained** | **E** | **H** | **F** | **Shared.E.F** | **Shared.E.H** | **Shared.H.F** | **Shared.E.H.F** |
|---|---|---|---|---|---|---|---|---|
| SR | 12.6 | 6.8 | 2 | 1.2 | 0.1 | 2.8 | 0.3 | 0[a] |
| Log10.Abundance | No lag retained | | | | | | | |
| Hurlbert.Evenness | No lag retained | | | | | | | |
| LBD.jac | 25.5 | 14.4 | 3.3 | 1 | 0.8 | 1.6 | 0.3 | 4.1 |
| LBD.jtu | 26.5 | 14.3 | 3.3 | 1.1 | 1.1 | 1.6 | 0.8 | 4.3 |
| LBD.jne | 11.1 | 5.7 | 0.9 | 1.1 | 0.6 | 0.6 | 0.5 | 1.7 |
| LBD.ruz | 14.7 | 7.1 | 3.1 | 0.3 | 0 | 1.5 | 0.3 | 2.4 |
| LBD.ruz.bal | 18.2 | 4.8 | 4.9 | 0.1 | 0 | 1.1 | 2.1 | 5.1 |
| LBD.ruz.gra | 12.3 | 1.4 | 1.7 | 1.9 | 0.1 | 1.9 | 2.1 | 3.1 |

[a]Negative values were converted to 0 (Legendre & Legendre, 1998), as such the sum of the variance of the individual categories might not add-up to the total explained variance.

**Table S16:** Estimates and significance of the predictors (i.e. all linear and quadratic terms of the explanatory variables included in the model) retained in the most parsimonious steady-state and temporal models for SR, including the best lag variables and models taking into account the temporal and spatial autocorrelation in the residuals. Pred.: Predictors. Est: coefficient estimates based on a LMM with time as a random intercept, and a LM for the steady-state and temporal models respectively. Est.AR1: coefficient estimates for LMM and LM models including a temporal autocorrelation structure (AR1) in the residuals. Est.Exp: coefficient estimates for LMM and LM models including a spatial autocorrelation structure (exponential structure) in the residuals. Est.AR1.Exp: coefficient estimates for LMM and LM models including temporal and spatial autocorrelation structures in the residuals. Coefficient estimates with a significant p.value (lower than 0.05) are indicated in bold, and variables explaining at least 5% of the explained deviance are highlighted in grey. Part.Marg.$R^2$.: express the semi-partial marginal $R^2$ (surrogate of the relative importance of each predictor based on the marginal $R^2$ [Nakagawa et al. 2017]) for each predictor in %. Psd.$R^2$: corresponds to the Pseudo $R^2$ , which is the $R^2$ from a linear model between the observed and the fitted values. Cond.$R^2$: it is the conditional $R^2$ including both the fixed and the random effects; it is available in the column Est. for the steady-state model only fitted with LMM including time as a random effect. Abund.Sm.Pel: Abundance of the small pelagic species. SR.Sm.Pel: Species richness of the small pelagic species.

| Metric | Model.Type | Parameters | Est. | P.LMM | Part.Marg.R2 | Est.AR1 | P.LMM.AR1 | Est.Exp | P.LMM.Exp | Est.AR1.Exp | P.LMM.AR1.Exp |
|---|---|---|---|---|---|---|---|---|---|---|---|
| SR | Steady-state | bottomT.min | -0.314 | 0.001 | 1.105 | -0.292 | 0.008 | -0.293 | 0.026 | -0.286 | 0.036 |
| SR | Steady-state | Dist2coast | -0.579 | 0 | 3.328 | -0.567 | 0 | -0.489 | 0 | -0.502 | 0 |
| SR | Steady-state | Fishing.Pressure | -0.333 | 0 | 1.322 | -0.313 | 0.005 | -0.302 | 0.002 | -0.298 | 0.006 |
| SR | Steady-state | Abund.Sm.Pel | -0.6 | 0 | 5.46 | -0.57 | 0 | -0.393 | 0 | -0.397 | 0 |
| SR | Steady-state | **Psd.R2/Cond.R2** | 0.175 | - | 0.117 | 0.567 | - | 0.663 | - | 0.876 | - |
| SR | Temp. | bottomT.min | -0.342 | 0 | 3.911 | -0.341 | 0.001 | -0.278 | 0.028 | -0.278 | 0.028 |
| SR | Temp. | Dist2coast | -0.564 | 0 | 1.653 | -0.551 | 0 | -0.489 | 0 | -0.489 | 0 |
| SR | Temp. | Fishing.Pressure | -0.318 | 0.001 | 1.213 | -0.312 | 0.002 | -0.288 | 0.003 | -0.288 | 0.003 |
| SR | Temp. | Abund.Sm.Pel | -0.614 | 0 | 5.48 | -0.598 | 0 | -0.403 | 0 | -0.403 | 0 |
| SR | Temp. | Time | 0.208 | 0.01 | 0.393 | 0.213 | 0.017 | 0.13 | 0.487 | 0.13 | 0.487 |
| SR | Temp. | bottomT.min:Time | -0.424 | 0 | 2.218 | -0.423 | 0 | -0.428 | 0 | -0.428 | 0 |
| SR | Temp. | **Psd.R2/Cond.R2** | - | - | 0.149 | 0.485 | - | 0.648 | - | 0.648 | - |

**Table S17:** Estimates and significance of the predictors (i.e. all linear and quadratic terms of the explanatory variables included in the model) retained in the most parsimonious steady-state and temporal models for LBD.jac, including the best lag variables and models taking into account the temporal and spatial autocorrelation in the residuals. Pred.: Predictors. Est: coefficient estimates based on a LMM with time as a random intercept, and a LM for the steady-state and temporal models respectively. Est.AR1: coefficient estimates for LMM and LM models including a temporal autocorrelation structure (AR1) in the residuals. Est.Exp: coefficient estimates for LMM and LM models including a spatial autocorrelation structure (exponential structure) in the residuals. Est.AR1.Exp: coefficient estimates for LMM and LM models including temporal and spatial autocorrelation structures in the residuals. Coefficient estimates with a significant p.value (lower than 0.05) are indicated in bold, and variables explaining at least 5% of the explained deviance are highlighted in grey. Part.Marg.$R^2$. : express the semi-partial marginal $R^2$ (surrogate of the relative importance of each predictor based on the marginal $R^2$ [Nakagawa et al. 2017]) for each predictor in %. Psd.$R^2$: corresponds to the Pseudo $R^2$ , which is the $R^2$ from a linear model between the observed and the fitted values. Cond.R2: it is the conditional $R^2$ including both the fixed and the random effects, it is available in the column Est. for the steady-state model only fitted with LMM including time as a random effect. Abund.Sm.Pel: Abundance of the small pelagic species. SR.Sm.Pel: Species richness of the small pelagic species.

| Metric | Model.Type | Parameters | Est. | P.LMM | Part.Marg.R2 | Est.AR1 | P.LMM.AR1 | Est.Exp | P.LMM.Exp | Est.AR1.Exp | P.LMM.AR1.Exp |
|---|---|---|---|---|---|---|---|---|---|---|---|
| LBD.jac | Steady-state | Bathy_mean^2 | **0.006** | 0 | 1.542 | **0.005** | 0.028 | **0.007** | 0 | **0.007** | 0 |
| LBD.jac | Steady-state | Abund.Sm.Pel | **0.025** | 0 | 11.461 | **0.021** | 0 | **0.014** | 0 | **0.015** | 0 |
| LBD.jac | Steady-state | MLD.min | **-0.017** | 0 | 3.658 | **-0.021** | 0 | **-0.013** | 0.008 | **-0.015** | 0.005 |
| LBD.jac | Steady-state | MLD.min^2 | **0.012** | 0 | 3.507 | **0.014** | 0 | **0.01** | 0 | **0.01** | 0 |
| LBD.jac | Steady-state | SR.Sm.Pel^2 | **0.012** | 0 | 8.276 | **0.011** | 0 | **0.009** | 0 | **0.009** | 0 |
| LBD.jac | Steady-state | **Psd.R2/Cond.R2** | 0.289 | - | 0.243 | 0.789 | - | 0.855 | - | 0.915 | - |
| LBD.jac | Temp. | Bathy_mean^2 | **0.006** | 0 | 3.714 | **0.007** | 0.003 | **0.007** | 0 | **0.007** | 0 |
| LBD.jac | Temp. | Abund.Sm.Pel | **0.021** | 0 | 8.773 | **0.019** | 0 | **0.014** | 0 | **0.014** | 0 |
| LBD.jac | Temp. | MLD.min | **-0.019** | 0 | 1.445 | **-0.016** | 0 | **-0.013** | 0.006 | **-0.014** | 0.004 |
| LBD.jac | Temp. | MLD.min^2 | **0.013** | 0 | 3.179 | **0.014** | 0 | **0.009** | 0 | **0.009** | 0 |
| LBD.jac | Temp. | SR.Sm.Pel^2 | **0.01** | 0 | 6.668 | **0.01** | 0 | **0.009** | 0 | **0.009** | 0 |
| LBD.jac | Temp. | Time | **-0.019** | 0 | 0.604 | **-0.013** | 0.002 | -0.009 | 0.28 | -0.009 | 0.287 |

| | | | | | | | | | | | |
|---|---|---|---|---|---|---|---|---|---|---|---|
| LBD.jac | Temp. | Bathy_mean^2:Time | **0.006** | 0 | 2.699 | **0.005** | 0.013 | **0.005** | 0 | **0.005** | 0.001 |
| LBD.jac | Temp. | MLD.min:Time | **-0.016** | 0 | 1.65 | **-0.016** | 0 | **-0.016** | 0.001 | **-0.015** | 0.003 |
| LBD.jac | Temp. | MLD.min^2:Time | **0.006** | 0.001 | 0.712 | 0.002 | 0.277 | 0.006 | 0.009 | **0.006** | 0.016 |
| LBD.jac | Temp. | **Psd.R2/Cond.R2** | - | - | 0.294 | 0.801 | - | 0.858 | - | 0.909 | - |

**Table S18:** Estimates and significance of the predictors (i.e. all linear and quadratic terms of the explanatory variables included in the model) retained in the most parsimonious steady-state and temporal models for LBD.jtu, including the best lag variables and models taking into account the temporal and spatial autocorrelation in the residuals. Pred.: Predictors. Est: coefficient estimates based on a LMM with time as a random intercept, and a LM for the steady-state and temporal models respectively. Est.AR1: coefficient estimates for LMM and LM models including a temporal autocorrelation structure (AR1) in the residuals. Est.Exp: coefficient estimates for LMM and LM models including a spatial autocorrelation structure (exponential structure) in the residuals. Est.AR1.Exp: coefficient estimates for LMM and LM models including temporal and spatial autocorrelation structures in the residuals. Coefficient estimates with a significant p.value (lower than 0.05) are indicated in bold, and variables explaining at least 5% of the explained deviance are highlighted in grey. Part.Marg.$R^2$.: express the semi-partial marginal $R^2$ (surrogate of the relative importance of each predictor based on the marginal $R^2$ [Nakagawa et al. 2017]) for each predictor in %. Psd.$R^2$: corresponds to the Pseudo $R^2$ , which is the $R^2$ from a linear model between the observed and the fitted values. Cond.R2: it is the conditional $R^2$ including both the fixed and the random effects, it is available in the column Est. for the steady-state model only fitted with LMM including time as a random effect. Abund.Sm.Pel: Abundance of the small pelagic species. SR.Sm.Pel: Species richness of the small pelagic species.

| Metric | Model.Type | Parameters | Est. | P.LMM | Part.Marg.R2 | Est.AR1 | P.LMM.AR1 | Est.Exp | P.LMM.Exp | Est.AR1.Exp | P.LMM.AR1.Exp |
|---|---|---|---|---|---|---|---|---|---|---|---|
| LBD.jtu | Steady-state | Bathy_mean^2 | **0.009** | 0 | 1.949 | **0.008** | 0.008 | **0.009** | 0 | **0.009** | 0 |
| LBD.jtu | Steady-state | Abund.Sm.Pel | **0.028** | 0 | 9.904 | **0.023** | 0 | **0.014** | 0 | **0.015** | 0 |
| LBD.jtu | Steady-state | MLD.min | **-0.02** | 0 | 3.640 | **-0.022** | 0 | **-0.016** | 0.009 | **-0.017** | 0.006 |
| LBD.jtu | Steady-state | MLD.min^2 | **0.015** | 0 | 3.580 | **0.016** | 0 | **0.011** | 0 | **0.011** | 0 |
| LBD.jtu | Steady-state | SR.Sm.Pel^2 | **0.016** | 0 | 10.181 | **0.014** | 0 | **0.012** | 0 | **0.012** | 0 |
| LBD.jtu | Steady-state | **Psd.R2/Cond.R2** | 0.272 | - | 0.252 | 0.837 | - | 0.855 | - | 0.923 | - |
| LBD.jtu | Temp. | Bathy_mean^2 | **0.008** | 0 | 4.298 | **0.008** | 0.002 | **0.008** | 0 | **0.009** | 0 |
| LBD.jtu | Temp. | Abund.Sm.Pel | **0.023** | 0 | 7.168 | **0.02** | 0 | **0.014** | 0 | **0.015** | 0 |
| LBD.jtu | Temp. | MLD.min | **-0.024** | 0 | 1.936 | **-0.021** | 0 | **-0.016** | 0.006 | **-0.017** | 0.004 |
| LBD.jtu | Temp. | MLD.min^2 | **0.015** | 0 | 3.16 | **0.016** | 0 | **0.01** | 0 | **0.01** | 0 |
| LBD.jtu | Temp. | SR.Sm.Pel^2 | **0.013** | 0 | 8.443 | **0.013** | 0 | **0.012** | 0 | **0.012** | 0 |
| LBD.jtu | Temp. | Time | **-0.023** | 0 | 0.322 | **-0.015** | 0.002 | -0.011 | 0.263 | -0.01 | 0.267 |
| LBD.jtu | Temp. | Bathy_mean^2:Time | **0.007** | 0 | 2.626 | **0.006** | 0.012 | **0.006** | 0 | **0.005** | 0.002 |
| LBD.jtu | Temp. | MLD.min:Time | **-0.02** | 0 | 1.27 | **-0.018** | 0 | **-0.018** | 0.003 | **-0.018** | 0.003 |

| | | | | | | | | | | | |
|---|---|---|---|---|---|---|---|---|---|---|---|
| LBD.jtu | Temp. | MLD.min^2:Time | **0.01** | 0 | 1.196 | 0.004 | 0.083 | **0.008** | 0.005 | **0.008** | 0.008 |
| LBD.jtu | Temp. | **Psd.R2/Cond.R2** | - | - | 0.304 | 0.852 | - | 0.857 | - | 0.924 | - |

**Table S19:** Estimates and significance of the predictors (i.e. all linear and quadratic terms of the explanatory variables included in the model) retained in the most parsimonious steady-state and temporal models for LBD.jne, including the best lag variables and models taking into account the temporal and spatial autocorrelation in the residuals. Pred.: Predictors. Est: coefficient estimates based on a LMM with time as a random intercept, and a LM for the steady-state and temporal models respectively. Est.AR1: coefficient estimates for LMM and LM models including a temporal autocorrelation structure (AR1) in the residuals. Est.Exp: coefficient estimates for LMM and LM models including a spatial autocorrelation structure (exponential structure) in the residuals. Est.AR1.Exp: coefficient estimates for LMM and LM models including temporal and spatial autocorrelation structures in the residuals. Coefficient estimates with a significant p.value (lower than 0.05) are indicated in bold, and variables explaining at least 5% of the explained deviance are highlighted in grey. Part.Marg.R2.: express the semi-partial marginal $R^2$ (surrogate of the relative importance of each predictor based on the marginal $R^2$ [Nakagawa et al. 2017]) for each predictor in %. Psd.R2: corresponds to the Pseudo $R^2$ , which is the $R^2$ from a linear model between the observed and the fitted values. Cond.R2: it is the conditional $R^2$ including both the fixed and the random effects; it is available in the column Est. for the steady-state model only fitted with LMM including time as a random effect. Abund.Sm.Pel: Abundance of the small pelagic species. SR.Sm.Pel: Species richness of the small pelagic species.

| Metric | Model.Type | Parameters | Est. | P.LMM | Part.Marg.R2 | Est.AR1 | P.LMM.AR1 | Est.Exp | P.LMM.Exp | Est.AR1.Exp | P.LMM.AR1.Exp |
|---|---|---|---|---|---|---|---|---|---|---|---|
| LBD.jne | Steady-state | Bathy_mean^2 | **-0.003** | 0 | 1.552 | **-0.003** | 0.001 | **-0.002** | 0.002 | -[a] | -[a] |
| LBD.jne | Steady-state | Fishing.Pressure^2 | **-0.002** | 0 | 1.133 | **-0.002** | 0.003 | -0.001 | 0.116 | -[a] | -[a] |
| LBD.jne | Steady-state | SR.Sm.Pel^2 | **-0.004** | 0 | 5.600 | **-0.004** | 0 | **-0.003** | 0 | -[a] | -[a] |
| LBD.jne | Steady-state | **Psd.R2/Cond.R2** | 0.207 | - | 0.092 | 0.921 | - | 0.711 | - | -[a] | - |
| LBD.jne | Temp. | Bathy_mean^2 | **-0.003** | 0 | 2.286 | **-0.003** | 0 | **-0.002** | 0.001 | **-0.002** | 0.002 |
| LBD.jne | Temp. | SR.Sm.Pel^2 | **-0.004** | 0 | 6.602 | **-0.004** | 0 | **-0.003** | 0 | **-0.003** | 0 |
| LBD.jne | Temp. | **Psd.R2/Cond.R2** | - | - | 0.089 | 0.883 | - | 0.715 | - | 1 | - |

[a] The model did not converge properly.

**Table S20:** Estimates and significance of the predictors (i.e. all linear and quadratic terms of the explanatory variables included in the model) retained in the most parsimonious steady-state and temporal models for LBD.ruz, including the best lag variables and models taking into account the temporal and spatial autocorrelation in the residuals. Pred.: Predictors. Est: coefficient estimates based on a LMM with time as a random intercept, and a LM for the steady-state and temporal models respectively. Est.AR1: coefficient estimates for LMM and LM models including a temporal autocorrelation structure (AR1) in the residuals. Est.Exp: coefficient estimates for LMM and LM models including a spatial autocorrelation structure (exponential structure) in the residuals. Est.AR1.Exp: coefficient estimates for LMM and LM models including temporal and spatial autocorrelation structures in the residuals. Coefficient estimates with a significant p.value (lower than 0.05) are indicated in bold, and variables explaining at least 5% of the explained deviance are highlighted in grey. Part.Marg.R2.: express the semi-partial marginal $R^2$ (surrogate of the relative importance of each predictor based on the marginal $R^2$ [Nakagawa et al. 2017]) for each predictor in %. Psd.R: corresponds to the Pseudo $R^2$, which is the $R^2$ from a linear model between the observed and the fitted values. Cond.R2: it is the conditional $R^2$ including both the fixed and the random effects; it is available in the column Est. for the steady-state model only fitted with LMM including time as a random effect. Abund.Sm.Pel: Abundance of the small pelagic species. SR.Sm.Pel: Species richness of the small pelagic species.

| Metric | Model.Type | Parameters | Est. | P.LMM | Part.Marg.R2 | Est.AR1 | P.LMM.AR1 | Est.Exp | P.LMM.Exp | Est.AR1.Exp | P.LMM.AR1.Exp |
|---|---|---|---|---|---|---|---|---|---|---|---|
| LBD.ruz | Steady-state | Bathy_mean^2 | **0.005** | 0 | 3.065 | **0.004** | 0 | **0.005** | 0 | **0.005** | 0 |
| LBD.ruz | Steady-state | bottomT.min | **-0.004** | 0 | 1.358 | **-0.004** | 0.002 | **-0.004** | 0.023 | **-0.004** | 0.025 |
| LBD.ruz | Steady-state | Abund.Sm.Pel | **0.009** | 0 | 5.670 | **0.008** | 0 | **0.007** | 0 | **0.007** | 0 |
| LBD.ruz | Steady-state | MLD.min | **-0.004** | 0.002 | 0.967 | **-0.004** | 0.012 | **-0.005** | 0.027 | -0.005 | 0.051 |
| LBD.ruz | Steady-state | MLD.min^2 | **0.005** | 0 | 2.225 | **0.005** | 0 | **0.004** | 0.001 | **0.004** | 0.003 |
| LBD.ruz | Steady-state | **Psd.R2/Cond.R2** | 0.169 | - | 0.132 | 0.608 | - | 0.797 | - | 0.851 | - |
| LBD.ruz | Temp. | Bathy_mean^2 | **0.004** | 0 | 4.103 | **0.004** | 0 | **0.005** | 0 | **0.005** | 0 |
| LBD.ruz | Temp. | bottomT.min | **-0.004** | 0 | 1.48 | **-0.004** | 0.002 | **-0.003** | 0.027 | **-0.004** | 0.025 |
| LBD.ruz | Temp. | Abund.Sm.Pel | **0.009** | 0 | 5.703 | **0.008** | 0 | **0.007** | 0 | **0.007** | 0 |
| LBD.ruz | Temp. | MLD.min | **-0.005** | 0 | 0.198 | **-0.005** | 0.002 | **-0.005** | 0.027 | **-0.004** | 0.049 |
| LBD.ruz | Temp. | MLD.min^2 | **0.004** | 0 | 1.774 | **0.005** | 0 | **0.004** | 0.001 | **0.004** | 0.003 |
| LBD.ruz | Temp. | Time | 0.001 | 0.642 | 0.609 | 0.001 | 0.418 | 0.001 | 0.588 | 0.002 | 0.546 |

| | | | | | | | | | | | |
|---|---|---|---|---|---|---|---|---|---|---|---|
| LBD.ruz | Temp. | Bathy_mean^2:Time | **0.002** | 0.002 | 0.822 | **0.002** | 0.018 | **0.003** | 0 | **0.003** | 0.002 |
| LBD.ruz | Temp. | **Psd.R2/Cond.R2** | - | - | 0.147 | 0.554 | - | 0.799 | - | 0.847 | - |

**Table S21:** Estimates and significance of the predictors (i.e. all linear and quadratic terms of the explanatory variables included in the model) retained in the most parsimonious steady-state and temporal models for LBD.ruz.bal, including the best lag variables and models taking into account the temporal and spatial autocorrelation in the residuals. Pred.: Predictors. Est: coefficient estimates based on a LMM with time as a random intercept, and a LM for the steady-state and temporal models respectively. Est.AR1: coefficient estimates for LMM and LM models including a temporal autocorrelation structure (AR1) in the residuals. Est.Exp: coefficient estimates for LMM and LM models including a spatial autocorrelation structure (exponential structure) in the residuals. Est.AR1.Exp: coefficient estimates for LMM and LM models including temporal and spatial autocorrelation structures in the residuals. Coefficient estimates with a significant p.value (lower than 0.05) are indicated in bold, and variables explaining at least 5% of the explained deviance are highlighted in grey. Part.Marg.R2.: express the semi-partial marginal $R^2$ (surrogate of the relative importance of each predictor based on the marginal $R^2$ [Nakagawa et al. 2017]) for each predictor in %. Psd.R2: corresponds to the Pseudo $R^2$ , which is the $R^2$ from a linear model between the observed and the fitted values. Cond.R2: it is the conditional $R^2$ including both the fixed and the random effects; it is available in the column Est. for the steady-state model only fitted with LMM including time as a random effect. Abund.Sm.Pel: Abundance of the small pelagic species. SR.Sm.Pel: Species richness of the small pelagic species.

| Metric | Model.Type | Parameters | Est. | P.LMM | Part.Marg.R2 | Est.AR1 | P.LMM.AR1 | Est.Exp | P.LMM.Exp | Est.AR1.Exp | P.LMM.AR1.Exp |
|---|---|---|---|---|---|---|---|---|---|---|---|
| LBD.ruz.bal | Steady-state | Bathy_mean | **0.017** | 0 | 2.523 | **0.015** | 0 | **0.013** | 0 | **0.013** | 0.002 |
| LBD.ruz.bal | Steady-state | bottomT.min | **-0.022** | 0 | 4.226 | **-0.021** | 0 | **-0.017** | 0 | **-0.016** | 0.001 |
| LBD.ruz.bal | Steady-state | MLD.min | **-0.03** | 0 | 11.128 | **-0.029** | 0 | **-0.024** | 0 | **-0.025** | 0 |
| LBD.ruz.bal | Steady-state | MLD.min^2 | **0.019** | 0 | 7.092 | **0.018** | 0 | **0.015** | 0 | **0.014** | 0 |
| LBD.ruz.bal | Steady-state | SR.Sm.Pel | **0.017** | 0 | 4.315 | **0.016** | 0 | **0.014** | 0 | **0.014** | 0 |
| LBD.ruz.bal | Steady-state | **Psd.R2/Cond.R2** | 0.222 | - | 0.177 | 0.754 | - | 0.769 | - | 0.865 | - |
| LBD.ruz.bal | Temp. | Bathy_mean | 0.018 | **0** | 0.631 | **0.016** | 0 | **0.014** | 0 | **0.013** | 0.001 |
| LBD.ruz.bal | Temp. | bottomT.min | -0.023 | **0** | 1.45 | **-0.021** | 0 | **-0.018** | 0 | **-0.017** | 0 |
| LBD.ruz.bal | Temp. | MLD.min | -0.032 | **0** | 5.552 | **-0.031** | 0 | **-0.025** | 0 | **-0.025** | 0 |
| LBD.ruz.bal | Temp. | MLD.min^2 | 0.02 | **0** | 6.585 | **0.019** | 0 | **0.015** | 0 | **0.015** | 0 |
| LBD.ruz.bal | Temp. | SR.Sm.Pel | 0.015 | **0** | 3.729 | **0.015** | 0 | **0.014** | 0 | **0.014** | 0 |
| LBD.ruz.bal | Temp. | Time | 0.009 | **0** | 1.111 | **0.011** | 0 | **0.013** | 0.022 | **0.013** | 0.03 |

| | | | | | | | | | | | |
|---|---|---|---|---|---|---|---|---|---|---|---|
| LBD.ruz.bal | Temp. | MLD.min:Time | -0.009 | **0** | 1.201 | **-0.01** | 0 | -0.007 | 0.058 | -0.007 | 0.087 |
| LBD.ruz.bal | Temp. | **Psd.R2/Cond.R2** | - | - | 0.203 | 0.745 | - | 0.777 | - | 0.871 | - |

**Table S22:** Estimates and significance of the predictors (i.e. all linear and quadratic terms of the explanatory variables included in the model) retained in the most parsimonious steady-state and temporal models for LBD.ruz.gra, including the best lag variables and models taking into account the temporal and spatial autocorrelation in the residuals. Pred.: Predictors. Est: coefficient estimates based on a LMM with time as a random intercept, and a LM for the steady-state and temporal models respectively. Est.AR1: coefficient estimates for LMM and LM models including a temporal autocorrelation structure (AR1) in the residuals. Est.Exp: coefficient estimates for LMM and LM models including a spatial autocorrelation structure (exponential structure) in the residuals. Est.AR1.Exp: coefficient estimates for LMM and LM models including temporal and spatial autocorrelation structures in the residuals. Coefficient estimates with a significant p.value (lower than 0.05) are indicated in bold, and variables explaining at least 5% of the explained deviance are highlighted in grey. Part.Marg.$R^2$.: express the semi-partial marginal $R^2$ (surrogate of the relative importance of each predictor based on the marginal $R^2$ [Nakagawa et al. 2017]) for each predictor in %. Psd.$R^2$: corresponds to the Pseudo $R^2$ , which is the $R^2$ from a linear model between the observed and the fitted values. Cond.$R^2$: it is the conditional $R^2$ including both the fixed and the random effects; it is available in the column Est. for the steady-state model only fitted with LMM including time as a random effect. Abund.Sm.Pel: Abundance of the small pelagic species. SR.Sm.Pel: Species richness of the small pelagic species.

| Metric | Model.Type | Parameters | Est. | P.LMM | Part.Marg.R2 | Est.AR1 | P.LMM.AR1 | Est.Exp | P.LMM.Exp | Est.AR1.Exp | P.LMM.AR1.Exp |
|---|---|---|---|---|---|---|---|---|---|---|---|
| LBD.ruz.gra | Steady-state | Dist2coast | **0.011** | 0 | 3.114 | **0.011** | 0 | **0.006** | 0.031 | **0.007** | 0.017 |
| LBD.ruz.gra | Steady-state | Shannon.Fishing.Pressure | **-0.012** | 0 | 3.439 | **-0.011** | 0 | **-0.006** | 0.011 | **-0.006** | 0.012 |
| LBD.ruz.gra | Steady-state | SR.Sm.Pel | **-0.007** | 0 | 1.517 | **-0.008** | 0 | **-0.007** | 0 | **-0.007** | 0 |
| LBD.ruz.gra | Steady-state | **Psd.R2/Cond.R2** | 0.182 | - | 0.11 | 0.659 | - | 0.75 | - | 0.843 | - |
| LBD.ruz.gra | Temp. | Dist2coast | **0.011** | 0 | 6.056 | **0.011** | 0 | **0.006** | 0.028 | **0.007** | 0.017 |
| LBD.ruz.gra | Temp. | Shannon.Fishing.Pressure | **-0.012** | 0 | 4.091 | **-0.012** | 0 | **-0.006** | 0.01 | **-0.006** | 0.012 |
| LBD.ruz.gra | Temp. | SR.Sm.Pel | **-0.008** | 0 | 1.507 | **-0.008** | 0 | **-0.007** | 0 | **-0.007** | 0 |
| LBD.ruz.gra | Temp. | **Psd.R2/Cond.R2** | - | - | 0.117 | 0.575 | - | 0.75 | - | 0.843 | - |

**Table S23**: Results of the modelling of the temporal evolution of each biodiversity metric in relation to the temporal evolution of each dynamic environnemental variable using generalised additive mixed models, taking into account for spatial autocorrelation in the residual with an exponential structure. We used the slope of the linear model between a response variable (Biodiversity metric and environmental variables) and time as surrogate of the temporal evolution of the metric over the time series. Temporal evolution for each biodiversity metric and environnemental variable was estimated for each of the 71 ICES rectangles visited at least 5 times by the biodiversity survey between 1997 and 2018 (without 2017) but for fishing pressure and Shannon of the fishing pressure (2000-2016). To avoid overfitting of the GAMMs, we used a maximum of 3 basis dimensions to represent the smooth term. For each biodiversity we considered a Gaussian error and identity link. The prefix « Slope. » for both biodiversity metrics and environmental variables is a reminder that the slope had been used as a proxy of temporal evolution of the variables. bottomT.min: annual minimum bottom sea floor temperature, bottomT.mean: annual average of the bottom sea floor temperature, bottomT.sd: seasonality of the bottom sea floor temperature, Temp.min: annual minimum temperature integrated over depth, Temp.mean: average annual temperature integrated over depth, Temp.sd: seasonality of the temperature integrated over depth, nppv.mean: annual average of the net primary productivity, SR.Sm.Pel: species richness of the small pelagic species, Abund.Sm.Pel: Abundance of the small pelagic species, MLD.min: annual minimum thickness of the mixed layer depth, MLD.mean: average annual thickness of the mixed layer depth, o2.min: annual minimum oxygen concentration, o2.sd: seasonality of the oxygen concentration, Fishing.Pressure: sum of the fishing effort, Shannon.Fishing.Pressure: diversity of the fishing pressure based on the Shannon index of the fishing effort of the different fishing gears. Edf: Estimated degrees of freedom, reference degrees of freedom, F: F statistic, Adj.R.sq: Adjusted R squared, AICc: Akaike's Information criterion corrected for small sample size. Variables highlighted in grey were retained for the multi-model inference approach; they had to have a significant p.value and adjusted.$R^2$ above 0.05.

| Metric | Explar.Var | edf | Ref.df | F | p.value | Adj.R.sq | AICc |
|---|---|---|---|---|---|---|---|
| Slope.SR | Slope.Fishing.Pressure | 1 | 1 | 4.476 | 0.038 | 0.041 | -111.825 |
| Slope.SR | Slope.o2.min | 1 | 1 | 4.133 | 0.046 | 0.084 | -111.466 |
| Slope.SR | Slope.bottomT.sd | 1 | 1 | 3.163 | 0.08 | -0.204 | -110.179 |
| Slope.SR | Slope.nppv.mean | 1.63 | 1.63 | 0.762 | 0.293 | 0.054 | -109.101 |
| Slope.SR | Slope.Temp.sd | 1.623 | 1.623 | 0.821 | 0.464 | 0.003 | -108.137 |
| Slope.SR | Slope.Temp.mean | 1.568 | 1.568 | 0.762 | 0.542 | 0.057 | -107.928 |
| Slope.SR | Slope.Abund.Sm.Pel | 1 | 1 | 0.411 | 0.523 | 0.016 | -107.853 |
| Slope.SR | Slope.MLD.mean | 1.495 | 1.495 | 0.599 | 0.612 | -0.059 | -107.838 |
| Slope.SR | Slope.bottomT.min | 1 | 1 | 0.1 | 0.753 | -0.04 | -107.532 |

| | | | | | | | |
|---|---|---|---|---|---|---|---|
| Slope.SR | Slope.MLD.min | 1 | 1 | 0.065 | 0.8 | 0.01 | -107.501 |
| Slope.SR | Slope.bottomT.mean | 1 | 1 | 0.061 | 0.806 | -0.001 | -107.501 |
| Slope.SR | Slope.o2.sd | 1 | 1 | 0.055 | 0.815 | -0.016 | -107.497 |
| Slope.SR | Slope.SR.Sm.Pel | 1 | 1 | 0.044 | 0.835 | -0.013 | -107.486 |
| Slope.SR | Slope.Temp.min | 1 | 1 | 0.046 | 0.831 | 0.008 | -107.479 |
| Slope.SR | Slope.Shannon.Fishing.Pressure | 1 | 1 | 0.012 | 0.915 | -0.02 | -107.452 |
| Slope.Abundance | Slope.nppv.mean | 1.906 | 1.906 | 8.954 | 0.003 | 0.206 | -350.679 |
| Slope.Abundance | Slope.SR.Sm.Pel | 1 | 1 | 9.337 | 0.003 | 0.145 | -348.372 |
| Slope.Abundance | Slope.Temp.min | 1.865 | 1.865 | 3.88 | 0.016 | 0.132 | -348.364 |
| Slope.Abundance | Slope.o2.min | 1.852 | 1.852 | 6.713 | 0.016 | 0.12 | -348.221 |
| Slope.Abundance | Slope.o2.sd | 1 | 1 | 5.37 | 0.023 | 0.021 | -345.618 |
| Slope.Abundance | Slope.Temp.sd | 1.645 | 1.645 | 4.724 | 0.065 | 0.094 | -345.528 |
| Slope.Abundance | Slope.MLD.mean | 1.862 | 1.862 | 3.19 | 0.03 | 0.137 | -345.452 |
| Slope.Abundance | Slope.Temp.mean | 1.812 | 1.812 | 1.944 | 0.097 | 0.088 | -344.187 |
| Slope.Abundance | Slope.bottomT.min | 1.578 | 1.578 | 1.326 | 0.161 | 0.066 | -343.362 |
| Slope.Abundance | Slope.bottomT.mean | 1.743 | 1.743 | 1.241 | 0.188 | 0.069 | -342.868 |
| Slope.Abundance | Slope.Fishing.Pressure | 1.647 | 1.647 | 0.797 | 0.284 | 0.035 | -342.234 |
| Slope.Abundance | Slope.Shannon.Fishing.Pressure | 1 | 1 | 1.688 | 0.198 | 0.014 | -342.079 |
| Slope.Abundance | Slope.MLD.min | 1 | 1 | 1.142 | 0.289 | -0.008 | -341.521 |
| Slope.Abundance | Slope.Abund.Sm.Pel | 1.191 | 1.191 | 0.841 | 0.449 | -0.026 | -341.08 |
| Slope.Abundance | Slope.bottomT.sd | 1 | 1 | 0.279 | 0.599 | -0.002 | -340.674 |
| Slope.Evenness | Slope.o2.sd | 1 | 1 | 2.68 | 0.106 | 0.024 | -356.527 |
| Slope.Evenness | Slope.SR.Sm.Pel | 1 | 1 | 2.242 | 0.139 | 0.018 | -356.071 |
| Slope.Evenness | Slope.Temp.min | 1.751 | 1.751 | 1.172 | 0.216 | 0.029 | -355.907 |
| Slope.Evenness | Slope.Fishing.Pressure | 1 | 1 | 1.381 | 0.244 | 0.005 | -355.276 |
| Slope.Evenness | Slope.o2.min | 1 | 1 | 1.241 | 0.269 | 0.003 | -354.938 |
| Slope.Evenness | Slope.bottomT.mean | 1.143 | 1.143 | 0.607 | 0.393 | 0.001 | -354.77 |
| Slope.Evenness | Slope.nppv.mean | 1.595 | 1.595 | 1.001 | 0.468 | 0.01 | -354.722 |
| Slope.Evenness | Slope.bottomT.min | 1.501 | 1.501 | 0.321 | 0.515 | 0.006 | -354.627 |
| Slope.Evenness | Slope.Temp.sd | 1.115 | 1.115 | 0.697 | 0.466 | -0.004 | -354.517 |
| Slope.Evenness | Slope.Temp.mean | 1.471 | 1.471 | 0.244 | 0.576 | 0.003 | -354.455 |

| | | | | | | | |
|---|---|---|---|---|---|---|---|
| Slope.Evenness | Slope.bottomT.sd | 1.043 | 1.043 | 0.456 | 0.529 | -0.008 | -354.329 |
| Slope.Evenness | Slope.MLD.mean | 1.231 | 1.231 | 0.045 | 0.796 | -0.008 | -353.995 |
| Slope.Evenness | Slope.Shannon.Fishing.Pressure | 1 | 1 | 0.069 | 0.793 | -0.014 | -353.958 |
| Slope.Evenness | Slope.MLD.min | 1 | 1 | 0.03 | 0.863 | -0.014 | -353.919 |
| Slope.Evenness | Slope.Abund.Sm.Pel | 1 | 1 | 0.001 | 0.973 | -0.014 | -353.89 |
| Slope.LBD.jac | Slope.Temp.sd | 1.823 | 1.823 | 3.846 | 0.075 | 0.125 | -392.845 |
| Slope.LBD.jac | Slope.SR.Sm.Pel | 1.648 | 1.648 | 0.996 | 0.225 | 0.099 | -390.922 |
| Slope.LBD.jac | Slope.Fishing.Pressure | 1.78 | 1.78 | 1.916 | 0.203 | 0.005 | -390.746 |
| Slope.LBD.jac | Slope.bottomT.sd | 1.037 | 1.037 | 2.095 | 0.158 | -0.12 | -390.649 |
| Slope.LBD.jac | Slope.bottomT.mean | 1.284 | 1.284 | 1.102 | 0.227 | 0.132 | -390.456 |
| Slope.LBD.jac | Slope.Temp.mean | 1 | 1 | 0.971 | 0.328 | 0.108 | -389.474 |
| Slope.LBD.jac | Slope.MLD.min | 1 | 1 | 0.612 | 0.437 | 0.057 | -389.196 |
| Slope.LBD.jac | Slope.Temp.min | 1 | 1 | 0.558 | 0.458 | 0.057 | -389.163 |
| Slope.LBD.jac | Slope.Abund.Sm.Pel | 1 | 1 | 0.26 | 0.612 | 0.016 | -388.867 |
| Slope.LBD.jac | Slope.o2.min | 1 | 1 | 0.185 | 0.669 | -0.027 | -388.794 |
| Slope.LBD.jac | Slope.MLD.mean | 1.337 | 1.337 | 0.087 | 0.763 | 0.003 | -388.759 |
| Slope.LBD.jac | Slope.Shannon.Fishing.Pressure | 1 | 1 | 0.022 | 0.883 | -0.014 | -388.636 |
| Slope.LBD.jac | Slope.o2.sd | 1 | 1 | 0.008 | 0.93 | -0.013 | -388.621 |
| Slope.LBD.jac | Slope.bottomT.min | 1 | 1 | 0.001 | 0.971 | -0.011 | -388.615 |
| Slope.LBD.jac | Slope.nppv.mean | 1 | 1 | 0 | 0.985 | -0.016 | -388.614 |
| Slope.LBD.jtu | Slope.Temp.sd | 1.847 | 1.847 | 4.679 | 0.044 | 0.129 | -387.737 |
| Slope.LBD.jtu | Slope.Fishing.Pressure | 1.792 | 1.792 | 1.998 | 0.184 | 0.007 | -384.671 |
| Slope.LBD.jtu | Slope.SR.Sm.Pel | 1.684 | 1.684 | 0.959 | 0.241 | 0.082 | -384.516 |
| Slope.LBD.jtu | Slope.bottomT.mean | 1.462 | 1.462 | 0.952 | 0.237 | 0.121 | -384.488 |
| Slope.LBD.jtu | Slope.bottomT.sd | 1.298 | 1.298 | 1.775 | 0.259 | -0.099 | -384.065 |
| Slope.LBD.jtu | Slope.Temp.min | 1 | 1 | 0.621 | 0.433 | 0.058 | -383 |
| Slope.LBD.jtu | Slope.Temp.mean | 1 | 1 | 0.665 | 0.418 | 0.088 | -382.996 |
| Slope.LBD.jtu | Slope.Abund.Sm.Pel | 1 | 1 | 0.296 | 0.588 | 0.017 | -382.673 |
| Slope.LBD.jtu | Slope.o2.sd | 1 | 1 | 0.212 | 0.646 | -0.009 | -382.595 |
| Slope.LBD.jtu | Slope.o2.min | 1 | 1 | 0.075 | 0.785 | -0.022 | -382.454 |
| Slope.LBD.jtu | Slope.MLD.min | 1 | 1 | 0.058 | 0.811 | 0.009 | -382.436 |

| | | | | | | | |
|---|---|---|---|---|---|---|---|
| Slope.LBD.jtu | Slope.bottomT.min | 1 | 1 | 0.031 | 0.862 | 0.002 | -382.411 |
| Slope.LBD.jtu | Slope.nppv.mean | 1 | 1 | 0.022 | 0.884 | -0.023 | -382.401 |
| Slope.LBD.jtu | Slope.Shannon.Fishing.Pressure | 1 | 1 | 0.012 | 0.915 | -0.014 | -382.392 |
| Slope.LBD.jtu | Slope.MLD.mean | 1 | 1 | 0.002 | 0.962 | -0.013 | -382.382 |
| Slope.LBD.jne | Slope.MLD.mean | 1.873 | 1.873 | 3.01 | 0.048 | -0.077 | -464.053 |
| Slope.LBD.jne | Slope.Temp.sd | 1.698 | 1.698 | 3.524 | 0.124 | 0.105 | -463.298 |
| Slope.LBD.jne | Slope.o2.sd | 1.622 | 1.622 | 1.151 | 0.19 | -0.009 | -462.412 |
| Slope.LBD.jne | Slope.bottomT.mean | 1.173 | 1.173 | 1.579 | 0.171 | 0.113 | -461.85 |
| Slope.LBD.jne | Slope.bottomT.min | 1.326 | 1.326 | 0.655 | 0.34 | 0.071 | -461.015 |
| Slope.LBD.jne | Slope.Temp.min | 1 | 1 | 1.143 | 0.289 | 0.075 | -460.841 |
| Slope.LBD.jne | Slope.Shannon.Fishing.Pressure | 1.245 | 1.245 | 1.009 | 0.418 | -0.01 | -460.613 |
| Slope.LBD.jne | Slope.MLD.min | 1 | 1 | 0.544 | 0.463 | -0.084 | -460.227 |
| Slope.LBD.jne | Slope.o2.min | 1 | 1 | 0.527 | 0.471 | 0.002 | -460.226 |
| Slope.LBD.jne | Slope.SR.Sm.Pel | 1.514 | 1.514 | 0.285 | 0.626 | 0.018 | -460.082 |
| Slope.LBD.jne | Slope.Temp.mean | 1.018 | 1.018 | 0.314 | 0.572 | 0.054 | -460.01 |
| Slope.LBD.jne | Slope.Fishing.Pressure | 1.383 | 1.383 | 0.123 | 0.7 | -0.009 | -459.973 |
| Slope.LBD.jne | Slope.bottomT.sd | 1.188 | 1.188 | 0.111 | 0.699 | 0.006 | -459.943 |
| Slope.LBD.jne | Slope.nppv.mean | 1 | 1 | 0.07 | 0.792 | 0 | -459.774 |
| Slope.LBD.jne | Slope.Abund.Sm.Pel | 1 | 1 | 0.053 | 0.819 | -0.027 | -459.76 |
| Slope.LBD.ruz | Slope.Fishing.Pressure | 1.89 | 1.89 | 3.539 | 0.027 | 0.061 | -400.659 |
| Slope.LBD.ruz | Slope.Temp.sd | 1.748 | 1.748 | 5.037 | 0.054 | 0.098 | -400.45 |
| Slope.LBD.ruz | Slope.SR.Sm.Pel | 1.64 | 1.64 | 1.264 | 0.17 | 0.075 | -397.737 |
| Slope.LBD.ruz | Slope.bottomT.mean | 1.461 | 1.461 | 1.214 | 0.185 | 0.055 | -397.361 |
| Slope.LBD.ruz | Slope.MLD.min | 1.76 | 1.76 | 1.22 | 0.215 | 0.018 | -396.861 |
| Slope.LBD.ruz | Slope.bottomT.min | 1 | 1 | 0.794 | 0.376 | 0.018 | -395.584 |
| Slope.LBD.ruz | Slope.MLD.mean | 1 | 1 | 0.621 | 0.433 | -0.001 | -395.448 |
| Slope.LBD.ruz | Slope.Abund.Sm.Pel | 1 | 1 | 0.583 | 0.448 | 0.012 | -395.362 |
| Slope.LBD.ruz | Slope.bottomT.sd | 1.371 | 1.371 | 0.562 | 0.639 | 0.006 | -395.216 |
| Slope.LBD.ruz | Slope.Temp.min | 1 | 1 | 0.362 | 0.549 | 0.005 | -395.17 |
| Slope.LBD.ruz | Slope.nppv.mean | 1 | 1 | 0.401 | 0.529 | 0.02 | -395.142 |
| Slope.LBD.ruz | Slope.Temp.mean | 1 | 1 | 0.278 | 0.6 | 0.008 | -395.058 |

| | | | | | | | |
|---|---|---|---|---|---|---|---|
| Slope.LBD.ruz | Slope.o2.min | 1 | 1 | 0.207 | 0.651 | -0.027 | -395.017 |
| Slope.LBD.ruz | Slope.o2.sd | 1 | 1 | 0.101 | 0.751 | -0.006 | -394.918 |
| Slope.LBD.ruz | Slope.Shannon.Fishing.Pressure | 1 | 1 | 0 | 0.987 | -0.014 | -394.821 |
| Slope.LBD.ruz.bal | Slope.Temp.sd | 1.834 | 1.834 | 6.093 | 0.025 | 0.119 | -380.634 |
| Slope.LBD.ruz.bal | Slope.SR.Sm.Pel | 1.594 | 1.594 | 3.275 | 0.031 | 0.148 | -379.367 |
| Slope.LBD.ruz.bal | Slope.bottomT.mean | 1.762 | 1.762 | 2.183 | 0.071 | 0.094 | -378.337 |
| Slope.LBD.ruz.bal | Slope.MLD.mean | 1.57 | 1.57 | 1.236 | 0.175 | 0.057 | -376.27 |
| Slope.LBD.ruz.bal | Slope.nppv.mean | 1 | 1 | 3.069 | 0.084 | 0.076 | -376.138 |
| Slope.LBD.ruz.bal | Slope.Abund.Sm.Pel | 1 | 1 | 1.353 | 0.249 | 0.031 | -374.719 |
| Slope.LBD.ruz.bal | Slope.Fishing.Pressure | 1.724 | 1.724 | 1.11 | 0.322 | -0.009 | -374.717 |
| Slope.LBD.ruz.bal | Slope.Temp.min | 1.443 | 1.443 | 0.362 | 0.469 | 0.022 | -374.344 |
| Slope.LBD.ruz.bal | Slope.bottomT.min | 1.139 | 1.139 | 0.636 | 0.386 | 0.026 | -374.318 |
| Slope.LBD.ruz.bal | Slope.Temp.mean | 1 | 1 | 0.908 | 0.344 | 0.021 | -374.308 |
| Slope.LBD.ruz.bal | Slope.o2.min | 1 | 1 | 0.879 | 0.352 | 0.031 | -374.198 |
| Slope.LBD.ruz.bal | Slope.o2.sd | 1.533 | 1.533 | 0.525 | 0.607 | 0.013 | -373.855 |
| Slope.LBD.ruz.bal | Slope.MLD.min | 1.478 | 1.478 | 0.227 | 0.653 | 0.002 | -373.79 |
| Slope.LBD.ruz.bal | Slope.bottomT.sd | 1.071 | 1.071 | 0.017 | 0.876 | -0.017 | -373.498 |
| Slope.LBD.ruz.bal | Slope.Shannon.Fishing.Pressure | 1 | 1 | 0.001 | 0.976 | -0.015 | -373.467 |
| Slope.LBD.ruz.gra | Slope.SR.Sm.Pel | 1 | 1 | 16.953 | 0 | 0.196 | -408.928 |
| Slope.LBD.ruz.gra | Slope.bottomT.mean | 1.789 | 1.789 | 2.516 | 0.053 | 0.107 | -404.43 |
| Slope.LBD.ruz.gra | Slope.Temp.sd | 1.812 | 1.812 | 4.756 | 0.053 | 0.096 | -404.399 |
| Slope.LBD.ruz.gra | Slope.MLD.mean | 1.817 | 1.817 | 2.438 | 0.058 | 0.113 | -403.613 |
| Slope.LBD.ruz.gra | Slope.nppv.mean | 1 | 1 | 4.639 | 0.035 | 0.084 | -403.257 |
| Slope.LBD.ruz.gra | Slope.o2.min | 1.325 | 1.325 | 5.07 | 0.04 | 0.11 | -403.203 |
| Slope.LBD.ruz.gra | Slope.Temp.min | 1.688 | 1.688 | 0.873 | 0.272 | 0.047 | -400.797 |
| Slope.LBD.ruz.gra | Slope.o2.sd | 1.739 | 1.739 | 1.779 | 0.256 | 0.054 | -400.579 |
| Slope.LBD.ruz.gra | Slope.Abund.Sm.Pel | 1 | 1 | 1.636 | 0.205 | 0.031 | -400.527 |
| Slope.LBD.ruz.gra | Slope.bottomT.min | 1.57 | 1.57 | 0.664 | 0.322 | 0.046 | -400.504 |
| Slope.LBD.ruz.gra | Slope.Temp.mean | 1.415 | 1.415 | 0.619 | 0.342 | 0.032 | -400.345 |
| Slope.LBD.ruz.gra | Slope.bottomT.sd | 1 | 1 | 0.179 | 0.673 | -0.022 | -399.165 |
| Slope.LBD.ruz.gra | Slope.Fishing.Pressure | 1 | 1 | 0.054 | 0.818 | -0.018 | -399.046 |

| | | | | | | | |
|---|---|---|---|---|---|---|---|
| Slope.LBD.ruz.gra | Slope.MLD.min | 1 | 1 | 0.039 | 0.844 | -0.011 | -399.032 |
| Slope.LBD.ruz.gra | Slope.Shannon.Fishing.Pressure | 1 | 1 | 0.002 | 0.966 | -0.015 | -398.996 |

**Table S24**: Estimate and significance of the multi-model inference approach between the temporal evolution of the biodiversity metric and the best set of explanatory variables (temporal evolution). The selection procedure was performed using generalised least square models (GLS) taking into account spatial autocorrelation using an exponential structure in the residuals. We presented only the results of the multi-model averaging performed on the best set of models with a delta AICc lower than 2 with the best model. var.Weight: sum of AICc weights of models in which the predictor occurred (it provides the relative importance of the predictor). Highlighted in bold were the predictors with a significant p.value and AICc weight of 1 (retained in all the best models).

| **Metric** | **Variables** | **Estimate** | **Std.Error** | **Adjusted.SE** | **z.value** | **P.value** | **var.Weight** |
|---|---|---|---|---|---|---|---|
| Slope.SR | Intercept | 0.013 | 0.025 | 0.025 | 0.501 | 0.617 | NA |
| Slope.SR | Slope.o2.min^2 | -7.681 | 41.828 | 42.585 | 0.18 | 0.857 | 1 |
| Slope.SR | Slope.o2.min | -2.736 | 1.285 | 1.308 | 2.091 | 0.036 | 1 |
| Slope.Abundance | Intercept | -0.011 | 0.004 | 0.004 | 2.432 | 0.015 | NA |
| Slope.Abundance | Slope.MLD.mean^2 | 18.203 | 10.377 | 10.567 | 1.723 | 0.085 | 1 |
| Slope.Abundance | Slope.nppv.mean^2 | -138.491 | 46.215 | 46.989 | 2.947 | 0.003 | 1 |
| Slope.Abundance | Slope.o2.min^2 | 15.137 | 6.125 | 6.239 | 2.426 | 0.015 | 1 |
| Slope.Abundance | Slope.SR.Sm.Pel^2 | -0.507 | 0.43 | 0.438 | 1.159 | 0.246 | 0.309 |
| Slope.Abundance | Slope.Temp.min^2 | -6.415 | 12.594 | 12.801 | 0.501 | 0.616 | 1 |
| Slope.Abundance | Slope.nppv.mean | -0.634 | 0.468 | 0.477 | 1.329 | 0.184 | 0.372 |
| Slope.Abundance | Slope.Temp.min | -0.334 | 0.194 | 0.197 | 1.694 | 0.09 | 0.167 |
| SlopeLBD.jtu | Intercept | -0.005 | 0.004 | 0.004 | 1.086 | 0.277 | NA |
| Slope.LBD.jtu | Slope.Temp.sd^2 | 41.627 | 15.444 | 15.701 | 2.651 | 0.008 | 1 |
| Slope.LBD.jtu | Slope.Temp.sd | -0.662 | 0.338 | 0.344 | 1.926 | 0.054 | 0.599 |
| Slope.LBD.ruz | Intercept | 0.003 | 0.003 | 0.003 | 1.126 | 0.26 | NA |
| Slope.LBD.ruz | Slope.Fishing.Pressure^2 | 0.766 | 0.528 | 0.533 | 1.438 | 0.15 | 0.523 |
| Slope.LBD.ruz | Slope.Fishing.Pressure | -0.13 | 0.051 | 0.052 | 2.487 | 0.013 | 0.237 |
| Slope.LBD.ruz.bal | Intercept | 0.004 | 0.004 | 0.004 | 1.087 | 0.277 | NA |
| Slope.LBD.ruz.bal | Slope.SR.Sm.Pel^2 | 0.645 | 0.423 | 0.43 | 1.499 | 0.134 | 0.561 |

| | | | | | | | |
|---|---|---|---|---|---|---|---|
| Slope.LBD.ruz.bal | Slope.Temp.sd^2 | 26.714 | 13.912 | 14.12 | 1.892 | 0.059 | 1 |
| Slope.LBD.ruz.bal | Slope.Temp.sd | -0.606 | 0.308 | 0.314 | 1.932 | 0.053 | 0.687 |
| Slope.LBD.ruz.gra | Intercept | -0.008 | 0.002 | 0.002 | 3.594 | 0 | NA |
| Slope.LBD.ruz.gra | Slope.nppv.mean^2 | 28.865 | 27.602 | 28.11 | 1.027 | 0.304 | 1 |
| Slope.LBD.ruz.gra | Slope.o2.min^2 | 6.294 | 3.485 | 3.549 | 1.773 | 0.076 | 1 |
| Slope.LBD.ruz.gra | Slope.SR.Sm.Pel | -0.101 | 0.025 | 0.026 | 3.883 | 0 | 1 |

**Table S25:** For the 147 species where we could evaluate the temporal trend of abundance over more than 5 years, we classified the species as increasing, decreasing or stable based on the slope and p.value of linear models. Slope.lm.Log10Abund : slope of the linear model, P.val.slope: p.value of the slope of the linear model, we considered significant trends for p.values >=0.1.

| Trends | Species.names | Slope.lm.Log10Abund | P.val.slope |
|---|---|---|---|
| Increasing | Aphanopus carbo | 0.0053 | 0.0196 |
| Increasing | Arctozenus risso | 0.0301 | 0.0024 |
| Increasing | Belone belone | 0.0113 | 5e-04 |
| Increasing | Buenia jeffreysii | 0.0073 | 0.0022 |
| Increasing | Callionymus reticulatus | 0.0443 | 0.0018 |
| Increasing | Chelidonichthys lucerna | 0.0167 | 0.024 |
| Increasing | Chelon labrosus | 0.0127 | 0.0218 |
| Increasing | Eutrigla gurnardus | 0.0285 | 0.0201 |
| Increasing | Lampanyctus crocodilus | 0.0261 | 0.0312 |
| Increasing | Macroramphosus scolopax | 0.0185 | 0.0272 |
| Increasing | Microstomus kitt | 0.0125 | 0.0186 |
| Increasing | Myctophum punctatum | 0.0207 | 0.0768 |
| Increasing | Notacanthus bonaparte | 0.0161 | 0.0069 |
| Increasing | Pagellus erythrinus | 0.0141 | 0.048 |
| Increasing | Pleuronectes platessa | 0.0647 | 2e-04 |
| Increasing | Pollachius virens | 0.0091 | 0.0225 |
| Increasing | Solea senegalensis | 0.009 | 0.0674 |
| Increasing | Trigla lyra | 0.0122 | 0.0084 |
| Increasing | Trisopterus esmarkii | 0.0396 | 0.0143 |
| Increasing | Umbrina canariensis | 0.0387 | 0.0024 |
| Increasing | Zeugopterus punctatus | 0.0141 | 0.0132 |
| Decreasing | Arnoglossus | -0.0184 | 0.0012 |
| Decreasing | Atherina boyeri | -0.0014 | 0.0493 |
| Decreasing | Beryx decadactylus | -0.0092 | 0.0011 |
| Decreasing | Callionymus maculatus | -0.0133 | 0.0303 |
| Decreasing | Crystallogobius linearis | -0.0551 | 0.0939 |
| Decreasing | Cyttopsis rosea | -0.0039 | 0.0571 |
| Decreasing | Echiichthys vipera | -0.0211 | 0.0121 |
| Decreasing | Lophius piscatorius | -0.0134 | 0.0087 |
| Decreasing | Macrourus berglax | -0.0351 | 0.0519 |
| Decreasing | Microchirus variegatus | -0.008 | 0.0245 |
| Decreasing | Mola mola | -0.0106 | 0.0649 |
| Decreasing | Mullus surmuletus | -0.0247 | 0.0196 |
| Decreasing | Neoscopelus macrolepidotus | -0.0012 | 0.0237 |
| Decreasing | Pollachius pollachius | -0.0064 | 0.0901 |
| Decreasing | Polymetme thaeocoryla | -0.0285 | 0.0403 |
| Decreasing | Polyprion americanus | -3e-04 | 0.0867 |
| Decreasing | Scorpaena scrofa | -0.0158 | 0.0129 |
| Decreasing | Serranus cabrilla | -0.0046 | 0.0289 |
| Decreasing | Stomias boa boa | -0.0499 | 0.0396 |

| | | | |
|---|---|---|---|
| Decreasing | Trisopterus luscus | -0.0169 | 0.0253 |
| Stable | Acantholabrus palloni | -0.0012 | 0.8233 |
| Stable | Agonus cataphractus | 0.0028 | 0.3026 |
| Stable | Anguilla anguilla | -0.0013 | 0.104 |
| Stable | Aphia minuta | -0.0069 | 0.7419 |
| Stable | Argentina | -0.0045 | 0.4345 |
| Stable | Argyropelecus | 0.0054 | 0.3413 |
| Stable | Argyrosomus regius | 0.0021 | 0.8866 |
| Stable | Balistes | 0.0034 | 0.7128 |
| Stable | Bathysolea profundicola | -0.0064 | 0.2554 |
| Stable | Beryx splendens | 0.0109 | 0.1804 |
| Stable | Blennius ocellaris | 0.0026 | 0.643 |
| Stable | Boops boops | 0.0131 | 0.2637 |
| Stable | Brama brama | 0.001 | 0.9052 |
| Stable | Buglossidium luteum | 0.0134 | 0.3154 |
| Stable | Coelorinchus caelorhincus | -0.0224 | 0.2074 |
| Stable | Callionymus lyra | -0.0052 | 0.2951 |
| Stable | Capros aper | 0.0017 | 0.8705 |
| Stable | Cepola macrophthalma | -0.0118 | 0.212 |
| Stable | Ceratoscopelus maderensis | 0.0065 | 0.2589 |
| Stable | Chelidonichthys cuculus | -0.0054 | 0.2171 |
| Stable | Chelidonichthys obscurus | 0.003 | 0.5776 |
| Stable | Chirolophis ascanii | -7e-04 | 0.156 |
| Stable | Ciliata mustela | 0.0036 | 0.755 |
| Stable | Chlorophthalmus agassizi | -9e-04 | 0.167 |
| Stable | Clupea harengus | -0.0018 | 0.9434 |
| Stable | Conger conger | 0.0015 | 0.7384 |
| Stable | Coryphaenoides rupestris | 0.0288 | 0.3147 |
| Stable | Ctenolabrus rupestris | -0.0018 | 0.4216 |
| Stable | Dicentrarchus labrax | 4e-04 | 0.9605 |
| Stable | Dicentrarchus punctatus | -0.0034 | 0.3776 |
| Stable | Dicologlossa cuneata | -0.0044 | 0.6787 |
| Stable | Diplodus sargus | 0.0095 | 0.2203 |
| Stable | Diplodus vulgaris | 0.007 | 0.4811 |
| Stable | Echiodon drummondii | -8e-04 | 0.787 |
| Stable | Enchelyopus cimbrius | -0.0108 | 0.2613 |
| Stable | Entelurus aequoreus | -6e-04 | 0.9739 |
| Stable | Ammodytidae | -0.009 | 0.5872 |
| Stable | Gadiculus argenteus | -0.0103 | 0.1608 |
| Stable | Gadus morhua | 0.0123 | 0.1573 |
| Stable | Gaidropsarus | -0.0061 | 0.3846 |
| Stable | Glyptocephalus cynoglossus | 0.0159 | 0.1729 |
| Stable | Gobius paganellus | -0.0509 | 0.1858 |
| Stable | Gymnammodytes semisquamatus | 0.0215 | 0.3088 |
| Stable | Halargyreus johnsonii | 0.0156 | 0.1976 |
| Stable | Helicolenus dactylopterus | 0.0089 | 0.3176 |
| Stable | Hippoglossoides platessoides | 0.0097 | 0.3589 |

| | | | |
|---|---|---|---|
| Stable | Hippocampus | 0.0051 | 0.2801 |
| Stable | Hoplostethus mediterraneus mediterraneus | -0.0073 | 0.6741 |
| Stable | Labrus | 2e-04 | 0.9668 |
| Stable | Lampanyctus intricarius | -3e-04 | 0.2302 |
| Stable | Lepidion eques | 0.0015 | 0.5432 |
| Stable | Lepidorhombus boscii | -1e-04 | 0.9743 |
| Stable | Lepidorhombus whiffiagonis | 0.0035 | 0.2189 |
| Stable | Lepidopus caudatus | 0.0038 | 0.2394 |
| Stable | Lepidotrigla dieuzeidei | -0.1994 | 0.1265 |
| Stable | Lesueurigobius friesii | -0.0149 | 0.2207 |
| Stable | Limanda limanda | 0.0105 | 0.4067 |
| Stable | Lithognathus mormyrus | 0.0145 | 0.373 |
| Stable | Liza aurata | 0.0102 | 0.4793 |
| Stable | Liza ramada | 0.0206 | 0.1068 |
| Stable | Lophius budegassa | 0.0043 | 0.4977 |
| Stable | Malacocephalus laevis | -0.0072 | 0.371 |
| Stable | Maurolicus muelleri | 0.0224 | 0.1674 |
| Stable | Melanogrammus aeglefinus | 0.0098 | 0.3866 |
| Stable | Merluccius merluccius | 9e-04 | 0.8903 |
| Stable | Merlangius merlangus | 0.0085 | 0.3383 |
| Stable | Micromesistius poutassou | -0.0135 | 0.1997 |
| Stable | Molva macrophthalma | -0.014 | 0.232 |
| Stable | Molva molva | 0.0026 | 0.5744 |
| Stable | Mora moro | -0.0048 | 0.5525 |
| Stable | Nerophis lumbriciformis | -2e-04 | 0.1232 |
| Stable | Notoscopelus | -5e-04 | 0.959 |
| Stable | Pagellus acarne | 0.0246 | 0.1337 |
| Stable | Pagellus bogaraveo | 0.0098 | 0.5869 |
| Stable | Pagrus pagrus | -0.0036 | 0.413 |
| Stable | Pegusa lascaris | 0.0014 | 0.811 |
| Stable | Phrynorhombus norvegicus | -4e-04 | 0.9577 |
| Stable | Phycis blennoides | 0.0082 | 0.1454 |
| Stable | Platichthys flesus | 3e-04 | 0.6768 |
| Stable | Polymetme corythaeola | -0.0114 | 0.168 |
| Stable | Pomatoschistus | 0.0279 | 0.1545 |
| Stable | Raniceps raninus | -0.0018 | 0.6055 |
| Stable | Sarda sarda | -0.0202 | 0.1664 |
| Stable | Scomberesox saurus saurus | -2e-04 | 0.1456 |
| Stable | Scomber colias | -0.0207 | 0.3758 |
| Stable | Scophthalmus maximus | 0.0037 | 0.3252 |
| Stable | Scophthalmus rhombus | 0.0033 | 0.4336 |
| Stable | Scorpaena loppei | -0.0121 | 0.1215 |
| Stable | Scorpaena notata | 0.0115 | 0.1733 |
| Stable | Scorpaena porcus | 0 | 0.9972 |
| Stable | Serranus scriba | -5e-04 | 0.152 |
| Stable | Solea solea | -0.0011 | 0.8769 |

| | | | |
|---|---|---|---|
| Stable | Sparus aurata | 0.0049 | 0.438 |
| Stable | Spondyliosoma cantharus | -0.0063 | 0.5712 |
| Stable | Symphodus bailloni | 2e-04 | 0.1756 |
| Stable | Symphodus roissali | -6e-04 | 0.1514 |
| Stable | Synaphobranchus kaupii | 0.0096 | 0.2107 |
| Stable | Syngnathus | -0.0073 | 0.3408 |
| Stable | Trachinus draco | -0.0029 | 0.7831 |
| Stable | Trachyrincus scabrus | -0.0013 | 0.1117 |
| Stable | Trachyscorpia cristulata echinata | -0.0036 | 0.1299 |
| Stable | Trigloporus lastoviza | 1e-04 | 0.981 |
| Stable | Trisopterus minutus | -0.0033 | 0.4707 |
| Stable | Xenodermichthys copei | 0.0107 | 0.292 |
| Stable | Xiphias gladius | 0.0022 | 0.6069 |
| Stable | Zeus faber | 0.0061 | 0.1351 |

**References:**

Baselga, A., Orme, D., Villeger, S., De Bortoli, J. & Leprieur, F. (2018). betapart: Partitioning Beta Diversity into Turnover and Nestedness Components. R package version 1.5.1. https://CRAN.R-project.org/package=betapart

Bates, D., Mächler, M., Bolker, B. & Walker, S. (2015). Fitting Linear Mixed-Effects Models Using lme4. J. Stat. Software; Vol 1, Issue 1. https://doi.org/10.18637/jss.v067.i01
Bartoń, K. (2019). MuMIn: Multi-Model Inference. R package version 1.43.15. https://CRAN.R-project.org/package=MuMIn

Bauman, D., Drouet, T., Fortin, M.-J. & Dray, S. (2018). Optimizing the choice of a spatial weighting matrix in eigenvector-based methods. *Ecology,* **99**, 2159–2166. https://doi.org/https://doi.org/10.1002/ecy.2469

Bivand, R.S., Pebesma, E. & Gomez-Rubio, V. (2013). Applied spatial data analysis with R, Second edition. Springer, New York, http://www.asdar-book.org/

Brooks, M.E., Kristensen, K., van Benthem, K.J., Magnusson, A., Berg, C.W., Nielsen, A., Skaug, H.J., Mächler M. & Bolker. B.M. (2017). glmmTMB Balances Speed and Flexibility Among Packages for Zero-inflated Generalized Linear Mixed Modeling. *The R Journal,* **9**, 378-400. https://doi.org/10.32614/RJ-2017-066

Burnham, K.P. & Anderson, D.R. (2002). Model Selection and Multimodel Inference: A Practical Information-Theoretic Approach. 2nd Edition. Springer-Verlag, New York.

Dray, S., Pélissier, R., Couteron, P., Fortin, M.-J., Legendre, P., Peres-Neto, P.R., Bellier, E., Bivand, R., Blanchet, F.G., De Cáceres, M., Dufour, A.-B., Heegaard, E., Jombart, T., Munoz, F., Oksanen, J., Thioulouse, J. & Wagner, H.H. (2012). Community ecology in the age of multivariate multiscale spatial analysis. *Ecological Monographs*, **82**, 257–275. https://doi.org/https://doi.org/10.1890/11-1183.1

Dray, S., Legendre, P. & Peres-Neto, P.R. (2006). Spatial modelling: a comprehensive framework for principal coordinate analysis of neighbour matrices (PCNM). *Ecological Modelling*, **196**, 483–493. https://doi.org/https://doi.org/10.1016/j.ecolmodel.2006.02.015

Dray, S., Bauman, D., Blanchet, G., Borcard, D., Clappe, S., Guenard, G., Jombart, T., Larocque, G., Legendre, P., Madi, N. & Wagner, H.H. (2019). adespatial: Multivariate Multiscale Spatial Analysis. R package version 0.3-7. https://CRAN.R-project.org/package=adespatial

Efron, B. (1978). Regression and ANOVA with zero-one data: Measures of residual variation. *Journal of the American Statistical Association*, **73**, 113-121.

Friedman, J., Hastie, T. & Tibshirani, R. (2010). Regularization Paths for Generalized Linear Models via Coordinate Descent. *Journal of Statistical Software*, **33**, 1–22.

Grueber, C.E., Nakagawa, S., Laws, R.J., Jamieson, I.G., 2011. Multimodel inference in ecology and evolution: Challenges and solutions. Journal of Evolutionary Biology, **24**, 699–711. https://doi.org/10.1111/j.1420-9101.2010.02210.x

Huret, M., Bourriau, P., Doray, M., Gohin, F. & Petitgas, P. (2018). Survey timing vs. ecosystem scheduling: Degree-days to underpin observed interannual variability in marine ecosystems. *Progress in Oceanography,* **166**, 30–40. https://doi.org/https://doi.org/10.1016/j.pocean.2017.07.007

Jaeger, B.C. (2017). r2glmm: Computes R Squared for Mixed (Multilevel) Models. R package version 0.1.2. https://CRAN.R-project.org/package=r2glmm

Jaeger, B.C., Edwards, L.J., Das, K., Sen, P.K., 2017. An R2 statistic for fixed effects in the generalized linear mixed model. *Journal of Applied Statistics,* **44**, 1086–1105. https://doi.org/10.1080/02664763.2016.1193725

Legendre, P. & Gauthier, O. (2014). Statistical methods for temporal and space–time analysis of community composition data. *Proceedings of the Royal Society B Biological Sciences*, **281**, 20132728. https://doi.org/10.1098/rspb.2013.2728

Legendre, P. & Legendre, L. (1998). Numerical Ecology, 2nd Edition. Elsevier, Amsterdam.

Nakagawa, S., Johnson, P.C.D. & Schielzeth, H. (2017). The coefficient of determination R(2) and intra-class correlation coefficient from generalized linear mixed-effects models revisited and expanded. *Journal of the Royal Society Interface*, **14**. https://doi.org/10.1098/rsif.2017.0213

Oksanen, J., Blanchet, G.F., Friendly, M., Kindt, R., Legendre, P., McGlinn, D., Minchin, P.R., O'Hara, B.R., Simpson, G.L., Solymos, P., Stevens, M.H.H., Szoecs, E. & Wagner, H. (2019). vegan: Community Ecology Package. R package version 2.5-6. https://CRAN.R-project.org/package=vegan

Pinheiro J, Bates D, DebRoy S, Sarkar D, R Core Team (2019). nlme: Linear and Nonlinear Mixed Effects Models. R package version 3.1-142,<URL: https://CRAN.R-project.org/package=nlme>

Wood, S.N. (2004). Stable and Efficient Multiple Smoothing Parameter Estimation for Generalized

Additive Models. *Journal of the American Statistical Association*, **99**, 673–686. https://doi.org/10.1198/016214504000000980

Zou, H. & Hastie, T. (2005). Regularization and variable selection via the elastic net. *Journal of the Royal Statistical Society Series B*, **67**, 301–320. https://doi.org/https://doi.org/10.1111/j.1467-9868.2005.00503.x

Zuur, A., Ieno, E.N. & Smith, G.M. (2007). Analysing ecological data. Springer-Verlag, New York

Zuur, A., Ieno, E.N., Walker, N., Saveliev, A.A. & Smith, G.M. (2009). Mixed Effects Models and Extensions in Ecology with R. Springer-Verlag, New York

## DECLARATION OF COMPETING INTERESTS

The authors declare that they have no conflict of interest.

## HIGHLIGHTS

1) The spatiotemporal dynamics of demersal fish communities were investigated in the Bay of Biscay (BoB) and Celtic Sea (CS).
2) The role of two decades of changes in temperature, trophic resources, habitat and fishing pressure on community dynamics were assessed.
3) Diversity patterns showed greater variability in space than in time and species richness and abundance weakly changed overall.
4) Communities are becoming more spatially similar (homogeneous) in the CS and differentiated in the BoB.
5) Such patterns are best explained by the dynamics of trophic resources mediated by small pelagic species rather than changes in temperature or fishing.